UNIVERSITY OF CALIFORNIA, MERCED

cDNA microarray-based studies of thermal stress-induced bleaching in the Caribbean corals *Montastraea faveolata* and *Acropora palmata*

A dissertation submitted in partial satisfaction of the requirements for the degree Doctor of Philosophy

in

Quantitative and Systems Biology

by

Michael Kenneth DeSalvo

Committee in charge:

University of California, Merced

Professor Mónica Medina, Chair
Professor David Ojcius
Professor Michael Dawson

California State University, San Francisco

Professor Jonathon Stillman

2010

DEDICATION

This dissertation is dedicated to all my family and friends. The way I see it, a person is 50% genetics and 50% environment. For my genes, I thank my parents, grand parents, and ancestors. For my environment, I thank my entire family and the many friends and teachers along the way that have helped me achieve my goals.

EPIGRAPH

How far you go in life depends on your being tender with the young, compassionate with the aged, sympathetic with the striving and tolerant of the weak and strong. Because someday in your life you will have been all of these.

-- *George Washington Carver*

We do not inherit the Earth from our ancestors; we borrow it from our children.

-- *Native American Proverb*

TABLE OF CONTENTS

ACKNOWLEDGEMENTS

I would like to acknowledge Professor Mónica Medina for her support as the chair of my committee. Through many field trips, spawning seasons, microarray hybridizations, PCRs, and stressful times, her guidance and mentorship helped me persevere and find success. I would also like to acknowledge all past and present members of the Medina Lab, without whom my research would have not only taken a lot longer but also would not have been nearly as high quality.

I would also like to thank Julissa Gonzalez for her love and support over the last 5 years. I must also recognize my parents, Kathy Kerns and George DeSalvo, who have always encouraged my education, and for this, I am eternally thankful. You both unwittingly cultivated a marine scientist – thank you so much for steering me in this direction.

Chapter 1, in full, is a reprint of the material as it appears in DeSalvo MK, Voolstra CR, Sunagawa S, Schwarz JA, Stillman JH, Coffroth MA, Szmant AM, Medina M (2008) Differential gene expression during thermal stress and bleaching in the Caribbean coral *Montastraea faveolata*. *Molecular Ecology*, volume 17, pages 3952–3971. The dissertation author was the primary investigator and author of this paper.

Chapter 2, in full, is a reprint of the material as it appears in DeSalvo MK, Sunagawa S, Voolstra CR, Medina M (2010) Transcriptomic responses to heat stress and bleaching in the Elkhorn coral *Acropora palmata*. *Marine Ecology Progress*

Series, volume 402, pages 97-113. The dissertation author was the primary investigator and author of this paper.

Chapter 3, in full, is a reprint of the material as it appears in DeSalvo MK, Sunagawa S, Fisher PL, Voolstra CR, Iglesias-Prieto R, Medina M (2010) Coral host transcriptomic states are correlated with *Symbiodinium* genotypes. *Molecular Ecology*, volume 19, pages 1174-1186. The dissertation author and Shinichi Sunagawa equally contributed to the completion of this paper.

VITA

Bachelor of Arts, University of California, Berkeley, December 2002.

PUBLICATIONS

DeSalvo, MK*, S Sunagawa*, PL Fisher, CR Voolstra, R Iglesias-Prieto, and M Medina (2010) Coral host transcriptomic states are correlated with *Symbiodinium* genotypes. *Molecular Ecology* 19: 1174-1186. * these authors contributed equally.

DeSalvo, MK, S Sunagawa, CR Voolstra, and M Medina (2010) Transcriptomic responses to heat stress and bleaching in the Elkhorn coral *Acropora palmata*. *Marine Ecology Progress Series* 402: 97-113.

Reyes-Bermudez, A*, MK DeSalvo*, CR Voolstra, S Sunagawa, AM Szmant, R Iglesias-Prieto, and M Medina (2009) Gene expression microarray analysis encompassing metamorphosis and the onset of calcification in the scleractinian coral *Montastraea faveolata. Marine Genomics* 2: 149-159. * these authors contributed equally.

Sunagawa, S, MK DeSalvo, CR Voolstra, A Reyes-Bermudez, M Medina (2009) Identification and Gene Expression Analysis of a Taxonomically Restricted Cysteine-Rich Protein Family in Reef-Building Corals. *PLoS ONE* 4(3): e4865.

Voolstra, CR, JA Schwarz, J Schnetzer, S Sunagawa, MK DeSalvo, AM Szmant, MA Coffroth, M Medina (2009) The host transcriptome remains unaltered during the establishment of coral-algal symbioses. *Molecular Ecology* 18: 1823-33.

Sunagawa, S, TZ DeSantis, YM Piceno, EL Brodie, MK DeSalvo, CR Voolstra, E Weil, GL Andersen, M Medina (2009) Bacterial Diversity and White Plague Disease-Associated Community Changes in the Caribbean Coral *Montastraea faveolata*. *The ISME Journal* 3: 512-21.

DeSalvo, MK, CR Voolstra, S Sunagawa, JA Schwarz, JH Stillman, MA Coffroth, AM Szmant, and M Medina (2008) Differential gene expression during thermal stress and bleaching in the Caribbean coral *Montastraea faveolata*. *Molecular Ecology* 17: 3952-71.

Bainton, RJ, LT-Y Tsai, T Schwabe, M DeSalvo, U Gaul, and U Heberlein (2005) moody encodes two GPCRs that regulate cocaine behaviors and blood-brain barrier permeability in *Drosophila*. *Cell* 123(1): 145-156.

HONORS & AWARDS

Graduate

NSF Doctoral Dissertation Enhancement Project, Office of International Science and Engineering. Title: “Heterologous and comparative genomic hybridizations to *Acropora palmata* and *Montastraea faveolata* coral microarrays”.

New England Biolabs Travel Award, International Coral Reef Symposium, July 2008.

Sigma Xi Grant-In-Aid of Research, December 2007. Amount: $1,000.

UCMEXUS Dissertation Grant. Title: "A genomic and physiological approach to the study of coral bleaching resistance".

Pre-doctoral Visiting Scientist, Bocas del Toro Research Station, Smithsonian Tropical Research Institute, Sep to Nov 2006.

Tuition and Travel Scholarship, Microarray Data Analysis Module, Summer Institute in Statistical Genetics, Department of Biostatistics, Univ. of Washington, June 14-16, 2006.

Undergraduate
Departmental Citation, Integrative Biology Commencement Ceremony, May 2003.

Gompertz Summer Undergraduate Research Grant, Dept of Integrative Biology, Summer 2002.

Travel Grant for Undergraduate Research, College of Letters and Science, Summer 2002.

PROFESSIONAL SERVICES

Memberships
Sigma Xi, The Scientific Research Society, Inducted December 2007.

Golden Key International Honour Society, Inducted Apr 2002.

National Society of Collegiate Scholars, Inducted Apr 2000.

Reviewer for the following journals and funding bodies
Molecular Ecology

Molecular Ecology Resources

Insect Molecular Biology

National Sea Grant College Program

ABSTRACT OF THE DISSERTATION

cDNA microarray-based studies of thermal stress-induced bleaching in the Caribbean corals *Montastraea faveolata* and *Acropora palmata*

by

Michael Kenneth DeSalvo

Doctor of Philosophy in Quantitative and Systems Biology

University of California, Merced

Professor Mónica Medina, Chair

The reef-building coral species of tropical seas worldwide, together with their algal endosymbionts, drive the productivity of coral reef ecosystems by forming the three-dimensional structure of reefs and by functioning as primary producers. The photosynthetic endosymbionts (of the genus *Symbiodinium*) are key to the role of primary production. This mutualism is under intense investigation because high temperature anomalies in coastal seas trigger a breakdown in the symbiosis known as coral bleaching. As sea surface temperatures rise due to global climate change, understanding the physiological, cellular, and molecular mechanisms underlying coral bleaching is imperative to predict whether corals will survive this age of human-

induced environmental degradation. Operating under this impetus, genomic approaches to studying the coral-algal symbiosis and its breakdown, such as cDNA microarrays, offer great promise. Microarrays allow for the rapid quantification of gene expression for thousands of genes in a single snapshot. In focusing on thermal stress and bleaching microarray experiments in the Caribbean corals *Acropora palmata* and *Montastraea faveolata*, I have found that the following cellular processes/components are affected during bleaching: oxidative stress, chaperone activity, the glyoxylate cycle, DNA repair, calcium homeostasis, cell death, the extracellular matrix, cell cycle progression, the actin cytoskeleton, nitric oxide signaling, and metabolite transfer between host and symbiont. Specific differentially expressed genes represent subjects of further investigation that are likely involved in coral-specific processes such as calcification, symbiosis maintenance, and bleaching. Furthermore, my experiments have revealed the striking effects that both stress and different symbiont genotypes can have on the host transcriptome. It is hypothesized that the host transcriptome is shaped by the competing effects of stress and the symbionts, and that this balance depends on both technical parameters (e.g. acclimation time, thermal treatment) and biological factors (e.g. species-specific stress sensitivities).

INTRODUCTION

The importance of coral reefs and the coral holobiont

Existing on tropical coastlines worldwide, coral reefs are geological structures built by calcifying marine organisms, principally the corals of the class Anthozoa (Hexacorallia: Scleractinia). The economic importance of the world's coral ecosystems has been estimated at $375 billion per year due to their immense ecosystem services such as fisheries, tourism, recreation, shoreline protection, construction materials, and cultural values (Spurgeon 1992, Costanza et al. 1997). While local populations worldwide rely heavily upon coral reefs, the reefs themselves are currently threatened by disease outbreaks (Harvell et al. 1999, Weil et al. 2006), overfishing and eutrophication (Hughes 1994, Jackson et al. 2001, Pandolfi et al. 2003), mass bleaching events (Hoegh-Guldberg 1999), and ocean acidification (Hoegh-Guldberg et al. 2007).

Acropora palmata and *Montastraea faveolata* are two highly important species of scleractinian coral existing in the Caribbean. Both species are major reef builders and provide essential habitat for a multitude of coral reef organisms (Gladfelter et al. 1978, Lirman 1999, Levitan et al. 2004). *A. palmata* populations are in a depressed state due to the many factors mentioned above (Bruckner 2002). Populations of *M. faveolata* are also in a state of decline and suffering from depressed recruitment (Hughes & Tanner 2000).

The evolutionary success of reef-building corals as structural and energetic keystone species is attributed to their symbiotic algae (*Symbiodinium* spp., commonly

referred to as zooxanthellae). The energy generated by algal photosynthesis offers nutrition to the coral host thereby enhancing the continued deposition of their calcium carbonate skeleton. However, recent research has also exposed a multitude of other microorganisms that associate with corals. The term "coral holobiont" refers to the coral host and its associated protists, bacteria, archaea, endolithic algae, and fungi (Shashar & Stambler 1992, Bentis et al. 2000, Rohwer et al. 2002, Baker 2003, Kellogg 2004, Wegley et al. 2004, Rosenberg et al. 2007, Harel et al. 2008).

The molecular biology of coral-algal symbiosis

Despite the importance of coral-algal symbioses in the marine environment, the molecular mechanisms underlying the interactions of the two main players in the symbiosis are poorly understood. These interactions include the initial recognition, uptake, maintenance, and termination of the relationship.

The initial recognition between the coral and its symbiont is thought to be mediated by lectins and glycans, which are cell-surface carbohydrate binding proteins. Initial discoveries revealed that *Hydra* binds to its *Chlorella* symbionts via lectin binding. Treatment of cultured *Chlorella* with Con A, or injection of Con A into the stomach of *Hydra* inhibit infection via neutralization of the cell surface carbohydrates necessary for recognition (Meints & Pardy 1980). More recently, a D-galactose binding lectin, SLL-2, was isolated from the octocoral *Sinularia lochmodes*. SLL-2 binds to glycoproteins on the surface of the zooxanthellae (Jimbo et al. 2000). This lectin was further shown to arrest symbionts in a non-motile stage while cell division

was unaffected (Koike et al. 2004). Using flow cytometry, Wood-Charlson *et al.,* (2006) found that lectins on the coral cell surface were interacting with glycan ligands, such as α-mannose/α-glucose and α-galactose on the algal cell surface. Furthermore, a transcriptomic study of development in *Acropora millepora* revealed a gene with a lectin domain that has an expression profile consistent with a role in symbiont uptake (Grasso et al. 2008).

Given the difficulty of studying the recognition of symbionts by coral larvae, the paucity of information regarding this critical symbiotic event is perhaps not surprising. However, the molecular mechanisms regulating the maintenance of a healthy symbiosis are even more poorly understood than those surrounding recognition and uptake. The study by Koike *et al.* (2004) mentioned above touched upon an important event – a host-derived molecule (SLL-2) that arrests symbionts in a non-motile stage. These types of signaling events are required to maintain coral-algal symbioses since symbiotic *Symbiodinium* have different ultrastructural features than free-living *Symbiodinium* (Trench 1979). Furthermore, the cell division of host and symbiont cells must be concerted (Muscatine & Pool 1979), and/or the host must be able to regulate symbiont density by degrading symbionts at the same rate that the symbionts are dividing (Titlyanov et al. 1996). Despite both the theoretical and observed processes underlying symbiosis maintenance, no molecular signals have been identified to further elucidate these interactions. The transfer of metabolites between host and symbiont may indeed act as a molecular signal regulating symbiont density. Nutrient translocation has been heavily studied – the coral host provides the

Symbiodinium with glycine, ammonium, nitrate, sulfate, and guanine; the *Symbiodinium* provide the coral host with glycolic acid, glycerol, glucose, alanine, lipids, and CO_2; and both partners shuttle cystine, methionine, and cystathione back and forth (e.g. Muscatine 1967, Patton et al. 1977, Trench 1979, Papina et al. 2003). However, how these metabolites may act as signal transducers affecting host and symbiont cell death/division has yet to be investigated.

Molecular mechanisms of coral bleaching

Coral bleaching marks the breakdown in symbiosis between the coral host and its algal endosymbiont. The major symptom of bleaching is the loss of the coral's color. Since the coral's color is due to photosynthetic pigments of the endosymbionts, losing these symbionts translates to a complete loss of colony color. Many conditions are thought to induce bleaching, including temperature extremes, solar irradiation, pathogens, darkness, and heavy metals (Douglas 2003). Color loss occurs as a result of a decline in the intracellular density of symbiotic algae, a decline in the pigment concentration within the algae, or both (Hoegh-Guldberg & Smith 1989). Bleaching due to heat and light stress can occur on regional scales causing widespread devastation. The 1998 and 2005 bleaching events caused extensive reef degradation across large areas in all of the world's coral reef provinces (Hoegh-Guldberg 1999, Hoegh-Guldberg et al. 2007).

Exploring the molecular mechanisms underlying coral bleaching has been a burgeoning area of research in the last two decades. The events leading to bleaching

are thought to begin with heat- and/or light-induced photoinactivation of photosystem II in the zooxanthellae (reviewed in Smith et al. 2005). The inactivation of photosystem II results from either damage to the D1 protein of photosystem II (Warner et al. 1999, Lesser & Farrell 2004) or impairment of CO_2 fixation (Lesser 1996, Jones et al. 1998). The net result of either of these scenarios is the production of reactive oxygen species (ROS) by transport chain electrons (Hoegh-Guldberg 1999, Lesser 2006). Rampant ROS production is known to be cytotoxic, and thus the leakage of ROS from photo-damaged zooxanthellae to the coral host provides a physiologically coherent mechanism by which stress leads to the breakdown of the coral-algal symbiosis.

Despite a logical link between environmental stress and cytotoxicity, the exact molecular signaling processes leading to bleaching are unknown. It is reasonable to expect numerous mechanisms given that bleaching can occur from a reduction in algal cell densities and/or a decrease in algal pigment concentration (e.g. Hoegh-Guldberg & Smith 1989, Fitt & Warner 1995). Furthermore, a reduction in algal cell density might result from detachment of host gastrodermal cells containing symbionts (Gates et al. 1992), necrosis and apoptosis of both host and symbiont cells (Dunn et al. 2002, Dunn et al. 2004, Strychar et al. 2004, Richier et al. 2006, Dunn et al. 2007), digestion of zooxanthellae by the coral host (Brown et al. 1995), which has since been termed 'symbiophagy' (Downs et al. 2009), and exocytosis of zooxanthellae (Steen & Muscatine 1987, Brown et al. 1995).

Even though the cellular signaling cascade remains unknown, protein-level studies have provided a link between environment stress and the cellular physiology of corals. Heat shock protein (HSP) expression in stressed corals has been studied extensively; the majority of studies quantifying stress protein expression in corals have found an induction of HSP expression during thermal stress (Black et al. 1995, Hayes & King 1995, Fang et al. 1997, Sharp et al. 1997, Gates & Edmunds 1999, Downs et al. 2000, Downs et al. 2002, Downs et al. 2005). While HSPs may be potent biomarkers for assessing coral health in the field, their activities do not point to a mechanism for bleaching. As mentioned above, oxidative stress in both the coral and symbiont represents a cellular basis for bleaching, and indeed, antioxidant enzymes and other molecules involved in the oxidative stress response have proven to be effective biomarkers: (Downs et al. 2000) – Cu/ZnSOD, MnSOD, LPO, GSH; (Downs et al. 2002) – same proteins plus protein carbonyl; (Brown et al. 2002) – HNE, GPx, MnSOD; (Lesser & Farrell 2004) – Cu/ZnSOD; (Downs et al. 2005) – same as previous 2 papers plus GST. Additional cellular markers of coral stress that have been assessed include: ubiquitin – increased levels suggest increased protein degradation (Downs et al. 2000, Downs et al. 2002, Downs et al. 2005); MDR – a P-glycoprotein that acts in the detoxification of xenobiotics (Downs et al. 2005); CPD – cyclobutane pyrimidine dimer – increased formation is indicative of DNA damage (Lesser & Farrell 2004); and p53 – a cell cycle protein – increased expression is indicative of DNA damage, apoptosis, and necrosis (Lesser & Farrell 2004).

Nitric oxide signaling (Perez & Weis 2006) also represents a candidate cellular pathway responsible for bleaching. Furthermore, a recent paper implicates another protein-level response to thermal stress; a GFP homolog in *Acropora millepora* is consistently down-regulated in response to thermal stress (Smith-Keune & Dove 2007). This result is interesting as GFP down-regulation took place prior to photoinhibition and bleaching, which suggests that GFP expression may be related to the cellular basis of events leading to bleaching. In synthesizing the available evidence, we can conclude that: 1) thermal stress results in HSP expression, GFP down-regulation, and oxidative stress; 2) oxidative stress results in increased antioxidant protein expression and damage to DNA, lipids, and proteins; and 3) oxidative stress and nitric oxide signaling are likely involved in the cellular basis of bleaching.

Microarrays and marine genomics

Microarrays are literally glass microscope slides with thousands of microscopic "DNA spots" precisely deposited in a grid pattern. After isolation of RNA from a tissue and/or condition of interest, one can probe the microarray by allowing the RNA to hybridize with the DNA printed on the microscope slide. Tissues and/or physiological conditions can be compared by competitively hybridizing two RNA samples to a microarray in which the two RNA samples are labeled with two different color dyes. For example, in experiments described in this dissertation, an RNA sample from a control, non-stressed coral fragment is labeled with green dye, and an RNA

sample from a bleached sample is labeled with red dye. Following competitive hybridization to the microarray, gene expression can be quantified because a gene expressed higher in the control sample will appear green, a gene expressed higher in the stressed sample will appear red, and gene equally expressed in both conditions will appear yellow.

Microarray analysis is a powerful approach to examine the expression of thousands of genes simultaneously, thereby expediting the discovery of candidate genes and pathways involved in particular cellular processes. However, it is worthy to note that microarrays measure gene expression at the transcriptomic level, i.e. at the level of mRNA molecules. Whether this directly translates to the protein level has been a subject of investigation. In the goby *Gillichthys mirabilis*, microarray estimated increases in mRNA were mirrored by increases at the protein-level, however the timing and magnitude of the increase in protein was not always consistent (Buckley et al. 2006). To make matters more complicated, protein function does not only depend on simple translation of mRNA molecules to proteins. Subcellular localization and post-translational modifications such as phosphorylation, ubiquitination, and homo- and heterodimerization with other proteins are critical factors in protein function. Taking these caveats into account, the results of microarray analyses, while powerful and incisive, require follow-up studies to definitively pinpoint protein function during conditions of interest.

The recent development of DNA microarrays for the study of coral symbiosis holds immense promise to elucidate the cellular underpinnings of processes that are

important on an ecological scale, e.g. coral bleaching. Small-scale cDNA microarray approaches (32 genes) have been carried out with *Montastraea faveolata* exposed to environmental stress (Edge et al. 2005, Morgan et al. 2005). Large-scale microarray studies on marine organisms such as porcelain crabs (Teranishi & Stillman 2007, Stillman & Tagmount 2009), damselfish (Kassahn et al. 2007), and gobies (Gracey et al. 2001, Buckley et al. 2006) have provided immense transcriptomic information in relation to thermal physiology. The studies described in this dissertation utilize microarrays that contain over 1,000 genes of *M. faveolata* and *A. palmata*, and they represent the first large-scale microarray studies of scleractinian coral biology.

Motivation for and overview of the dissertation

At a time when coral reefs worldwide are threatened by myriad human-induced stressors, it is imperative to understand the molecular basis of the symbiotic relationship that allows these diverse ecosystems to thrive. By understanding the collapse of symbiosis, i.e. coral bleaching, novel insights into the onset, maintenance, and breakdown of the symbiosis will be established. The dissertation presented here attempts to bridge our gaps in knowledge concerning the molecular mechanisms of coral bleaching by using powerful genomic technique that, up until now, have not been amenable to non-model organisms such as reef-building corals. By taking an evolutionary comparative approach and measuring the transcriptomic response to heat stress and bleaching in both *M. faveolata* (Chapter 1) and *A. palmata* (Chapter 2), we will gain an increased understanding of both conserved and species-specific molecular

events surrounding the coral stress response and subsequent bleaching. Furthermore, adding an endosymbiont-centric view to coral bleaching mechanisms, by measuring the transcriptomic responses to stress and bleaching in fragments of *M. faveolata* that contain different genotypes of *Symbiodinium* (Chapter 3), will integrate another level of complexity into our conceptual framework of coral bleaching physiology.

This dissertation contains three chapters and a conclusion following this section. Chapter 1 describes the results of laboratory thermal stress experiments performed with *M. faveolata* at the Smithsonian Tropical Research Institute in Bocas del Toro, Panama. RNA samples from stressed and non-stressed fragments were used to interrogate the *M. faveolata* microarray containing approximately 1,300 genes isolated from cDNA libraries described in (Schwarz et al. 2008). Two primary experiments will be described: 1) a single host genotype experiment where one colony was split and the fragments divided evenly into control and experimental tanks (samples were frozen for microarray analysis at one timepoint – nine days after the initiation of thermal stress); and 2) a multiple colony experiment where fragments were collected from four different colonies and samples were collected for microarray analysis at four timepoints during a nine-day period. Results from both experiments suggested that thermal stress and bleaching in *M. faveolata* affect the following processes: oxidative stress, Ca^{2+} homeostasis, cytoskeletal organization, cell death, calcification, metabolism, protein synthesis, heat shock protein activity, and transposon activity. Chapter 1, in full, is a reprint of the material as it appears in (DeSalvo et al. 2008).

Chapter 2 describes the results of laboratory thermal stress experiments performed with *A. palmata* at the Smithsonian Tropical Research Institute in Bocas del Toro, Panama. RNA samples from stressed and non-stressed fragments were used to interrogate the *A. palmata* microarray containing approximately 2,050 genes (Schwarz et al. 2008). Similar to the multiple colony experiment described above for *M. faveolata* in Chapter 1, the experiment described in Chapter 2 is derived from four colonies of which samples were collected for microarray analysis at three timepoints over a two-day period. Results from this experiment indicate a cellular stress response in *A. palmata* involving: (1) growth arrest; (2) chaperone activity; (3) nucleic acid stabilization and repair; and (4) the removal of damaged macromolecules. Other differentially expressed processes include sensory perception, metabolite transfer between host and endosymbiont, nitric oxide signaling, and modifications to the actin cytoskeleton and extracellular matrix. When comparing these results with those obtained in experiments described in Chapter 1, a picture of stress-responsive cellular processes evolutionarily conserved across scleractinian corals begins to emerge. Chapter 2, in full, is a reprint of the material as it appears in (DeSalvo et al. 2010b).

Chapter 3 describes the results of laboratory thermal stress experiments performed with *M. faveolata* at the UNAM - Instituto de Ciencias del Mar y Limnología field station in Puerto Morelos, Mexico. RNA samples from control, stressed, and recovered fragments were used to interrogate the *M. faveolata* microarray containing approximately 1,300 genes. Two primary experiments will be described: 1) a multiple colony experiment where fragments were collected from five

different colonies and samples were collected for microarray analysis at three timepoints during a 60 day period; and 2) a single host genotype experiment where fragments were collected from one host colony along a depth gradient and samples were collected for microarray analysis at one timepoint – six days following the initiation of thermal stress. Both experiments also benefited from collecting algal physiology, algal genotyping, and host genotyping data. Interestingly, in both experiments, gene expression was more similar among samples with the same *Symbiodinium* content rather than the same experimental condition. This was highly unexpected and revealed a striking correlation between coral host transcriptomic states and the genotype of their resident algal symbionts. Chapter 3, in full, is a reprint of the material as it appears in (DeSalvo et al. 2010a).

CHAPTER 1

DIFFERENTIAL GENE EXPRESSION DURING THERMAL STRESS AND BLEACHING IN THE CARIBBEAN CORAL *MONTASTRAEA FAVEOLATA*

ABSTRACT

The declining health of coral reefs worldwide is likely to intensify in response to continued anthropogenic disturbance from coastal development, pollution, and climate change. In response to these stresses, reef-building corals may exhibit bleaching, which marks the breakdown in symbiosis between coral and zooxanthellae. Mass coral bleaching due to elevated water temperature can devastate coral reefs on a large geographic scale. In order to understand the molecular and cellular basis of bleaching in corals, we have measured gene expression changes associated with thermal stress and bleaching using a cDNA microarray containing 1,310 genes of the Caribbean coral *Montastraea faveolata*. In a first experiment, we identified differentially expressed genes by comparing experimentally bleached *M. faveolata* fragments to control non-heat-stressed fragments. In a second experiment, we identified differentially expressed genes during a time course experiment with four time points across nine days. Results suggest that thermal stress and bleaching in *M. faveolata* affect the following processes: oxidative stress, Ca^{2+} homeostasis, cytoskeletal organization, cell death, calcification, metabolism, protein synthesis, heat shock protein activity, and transposon activity. These results represent the first medium-scale transcriptomic study focused on revealing the cellular foundation of thermal stress-induced coral bleaching. We postulate that oxidative stress in thermal-

stressed corals causes a disruption of Ca^{2+} homeostasis, which in turn leads to cytoskeletal and cell adhesion changes, decreased calcification, and the initiation of cell death via apoptosis and necrosis.

INTRODUCTION

Coral reefs are important tropical marine ecosystems currently threatened by disease outbreaks (Harvell et al. 1999, Weil et al. 2006), overfishing and eutrophication (Hughes 1994, Jackson et al. 2001, Pandolfi et al. 2003), and mass bleaching events (Hoegh-Guldberg 1999). These factors will be exacerbated by future climate change (Hughes et al. 2003), and predictions of ocean acidification represent yet another threat to coral vitality (Hoegh-Guldberg et al. 2007). Coral bleaching describes the morphological changes that occur during the breakdown in symbiosis between the coral host and its dinoflagellate endosymbiont (*Symbiodinium* sp. or zooxanthellae). Upon bleaching, the coral host loses its coloration via the loss of its photosynthetic pigment-containing endosymbionts. The bleaching response can result from exposure to abnormal water temperature (e.g. Glynn 1993), pathogens (e.g. Kushmaro et al. 1996), high light and ultraviolet radiation (e.g. Gleason & Wellington 1993), a synergistic combination of multiple factors (e.g. Lesser & Farrell 2004), herbicides (Jones 2005), and other known stressors (reviewed in Douglas 2003). Of utmost importance is thermal stress-induced coral bleaching, which is predicted to increase in intensity and frequency due to global warming (Hoegh-Guldberg 1999). Bleaching due to anomalously high seawater temperature can occur over a large

geographic range (e.g. Berkelmans & Oliver 1999) and can lead to widespread coral mortality across the globe (Goreau et al. 2000).

A detailed description of the molecular and cellular events leading to bleaching is incomplete. It is possible that multiple mechanisms exist given that bleaching can result from a reduction in algal cell densities and/or a decrease in algal pigment concentration (e.g. Hoegh-Guldberg & Smith 1989, Fitt & Warner 1995). A decrease in algal density can occur via the detachment of host cells containing symbionts (Gates et al. 1992), necrosis and apoptosis of both host and symbiont cells (Dunn et al. 2002, Dunn et al. 2004, Strychar et al. 2004, Richier et al. 2006, Dunn et al. 2007), digestion of zooxanthellae by the coral host (Brown et al. 1995), and exocytosis of zooxanthellae (Steen & Muscatine 1987, Brown et al. 1995).

The events leading to a decrease in density of zooxanthellae is thought to begin with heat- and/or light-induced photoinactivation of photosystem II in the zooxanthellae (reviewed in Smith et al. 2005). Briefly, decreased photosynthesis in cultured zooxanthellae (e.g. Iglesias-Prieto et al. 1992) and zooxanthellae *in hospite* (e.g. Fitt & Warner 1995, Warner et al. 1996) in response to elevated temperatures is thought to result from damage to the D1 protein of photosystem II (Warner et al. 1999, Lesser 2004), or impairment of CO_2 fixation (Lesser 1996, Jones et al. 1998). The net result of either of these scenarios is the production of reactive oxygen species (ROS) by transport chain electrons (Hoegh-Guldberg 1999, Lesser 2006). Rampant ROS production is known to result in apoptosis/necrosis (e.g. Tiwari et al. 2002), and thus

the production of ROS by photo-damaged zooxanthellae provides a mechanism by which environmental stressors can lead to degradation of the coral-algal symbiosis.

The use of molecular tools to assess the cellular basis of coral health has recently intensified. Investigated protein biomarkers consist mainly of heat shock proteins (HSPs) and proteins involved in the oxidative stress response (see Table 2 in van Oppen and Gates (2006) for a comprehensive list of protein biomarkers). While HSPs may be potent biomarkers for assessing coral health in the field, their activities do not point to a mechanism of bleaching. However, both oxidative stress and nitric oxide signaling (Perez & Weis 2006) represent cellular pathways responsible for bleaching. Green fluorescent protein (GFP) homologs may also be involved in bleaching mechanisms. Although GFPs are thought to be photoprotective (Salih et al. 2000), and have also been shown to quench superoxide radicals (Bou-Abdallah et al. 2006), their expression appears to decrease during thermal stress (Dove et al. 2006, Smith-Keune & Dove 2007). In summarizing the available evidence, we can conclude that: 1) thermal stress results in HSP expression, GFP down-regulation, and oxidative stress; 2) oxidative stress results in increased antioxidant protein expression and damage to DNA, lipids, and proteins; and 3) oxidative stress and nitric oxide signaling are likely involved in the cellular basis of bleaching.

The emergence of cDNA microarrays for non-model organisms, which can assay the expression of thousands of genes simultaneously, has accelerated the discovery of stress responsive genes and mechanisms in recent years (Gibson 2002, Gracey & Cossins 2003, Hofmann et al. 2005). Small-scale cDNA microarray

approaches (32 genes) have been carried out with the scleractinian coral, *Montastraea faveolata*, exposed to environmental stress (Edge et al. 2005, Morgan et al. 2005). Large-scale microarray studies on marine organisms such as porcelain crabs (Teranishi & Stillman 2007), damselfish (Kassahn et al. 2007), mussels (Place et al. 2008), and gobies (Gracey et al. 2001, Buckley et al. 2006) have provided immense transcriptomic information in relation to thermal physiology. In this study, we report the first medium-scale cDNA microarray study on *M. faveolata* exposed to thermal stress and bleaching in a controlled laboratory setting. Differential gene expression was assessed during early stage thermal stress and partial bleaching. The results confirm HSP expression, GFP down-regulation and oxidative stress during bleaching; and also suggest that Ca^{2+} homeostasis, cytoskeletal dynamics, calcification, metabolism, and protein synthesis are affected by thermal stress and symbiosis breakdown.

MATERIALS AND METHODS

Field experiments

Two experiments were performed at the Smithsonian Tropical Research Institute's Bocas del Toro field station in Panamá during September and October 2006. The following apply to both experiments: 1) aquaria were exposed to shaded ambient light; 2) aquaria were placed in large fiberglass ponds with continuous water flow to buffer temperature fluctuations; 3) aquaria did not have running seawater but each contained a pump to generate continuous water flow; and 4) heaters were used to raise the temperature in heated aquaria.

A single time point, single genotype thermal stress experiment ("Experiment 1") was performed first. A large colony of *Montastraea faveolata* was collected near Isla Solarte (9°19'56.78" N and 82°12'54.65" W). A single colony was targeted in order to eliminate sources of variation from coral and zooxanthellae genotypes and thermal/light history (e.g. Rowan et al. 1997, Glynn et al. 2001, Brown et al. 2002). Ten coral "plugs" were taken from the top of the colony using a 2.5cm diameter punch tool. The fragments were divided evenly between two identical 75-liter aquaria, ca. 25cm deep, and kept at ambient temperature (29.23±0.48°C) for three days. After the acclimation period, two 200-Watt aquarium heaters were turned on in the experimental aquarium, which subsequently increased to 31.5°C over three hours. The average temperature of the experimental aquarium during the entire experiment was 32.23±0.48°C. HOBO Pendant Temperature/Light Data Loggers (Onset Corp UA-002-64) recorded temperature and light data every three minutes. These data loggers are not designed to measure photosynthetically active radiation (PAR – 400-700nm), as only ~30% of the measured light is in the range of PAR. For this reason, relative light levels in the aquaria are reported (expressed as the percentage of the average 10am to 2pm light intensity measured on a reef ~4m deep in Bocas del Toro (9°22'68.4" N and 82°18'24.6" W) during September and October 2007). The control aquarium received slightly more light (37%) than the heated aquarium (28% of reef light). The experiment lasted 10 days and 17 hours, after which all fragments were frozen in liquid nitrogen for molecular analysis. Immediately prior to freezing, a

polyp-size tissue scraping (~12.6mm^2) was preserved in 1mL of 3.7% formaldehyde for zooxanthellae cell density analysis.

A time course experiment ("Experiment 2") was conducted with four colonies of *M. faveolata* sampled from two separate reefs 21 km apart (two colonies from Isla Solarte – 9^{o}19'56.78" N and 82^{o}12'54.65" W, and two colonies from Cayos Zapatillas – 9^{o}15'08.79" N and 82^{o}02'24.63" W). Each colony was broken into eight fragments using a hammer and chisel. For each colony, four fragments were placed in a control aquarium, and four fragments were placed in an experimental aquarium fitted with two heaters, such that each colony was represented by a pair of aquaria (total of four control and four heated aquaria, all 75-liter). After an acclimation period of four days at the natural temperature of the seawater system (mean temperature = 30.29±0.07^{o}C), a fragment from each control and experimental aquaria was sampled as described above (time zero). After time zero sampling, the heaters in each of the experimental aquaria were turned on, and the rate of temperature increase was similar to Experiment 1. The mean temperature of the control aquaria during the entire experiment was 29.74±0.03^{o}C, and the mean temperature of the heated aquaria was 32.72±0.32^{o}C. Control and experimental fragments were sampled again one day after turning on the heaters, at the first signs of slight bleaching (two to four days after heating began, depending on coral genotype), and lastly, when all experimental fragments were partially bleached (nine days after heating began). All samples were taken at night. Light intensity differed slightly between the four aquaria fitted with HOBOs (control

aquaria 1 – 43%; control aquaria 2 – 46%; heated aquaria 1 – 35%; and heated aquaria 2 – 34% of reef light).

Zooxanthellae cell counts and 18S RFLP analysis

The formaldehyde-fixed tissue scrapings were homogenized by maceration with a dissecting needle and vortexed. Cell counts were performed with a hemocytometer. For Experiment 1, four replicate cell counts were performed per sample, averaged, and values adjusted to the number of cells per cm^2. An Independent Samples t-test was performed to determine statistical significance between the two groups. For Experiment 2, eight replicate cell counts were averaged for each coral genotype at each time point. After testing for normality and equal variances within time points, significance between time points was assessed using a One Way Repeated Measures ANOVA and Tukey post-hoc testing. All statistical tests were performed using SigmaStat 3.11.

Genomic DNA was isolated from frozen coral powder (see below) using the PowerPlant DNA Isolation kit (MoBio). The *Symbiodinium* 18S ribosomal subunit DNA was amplified using a universal forward primer (5' - GGTTGATCCTGCCAGTAGTCATATGCTTG - 3') and a zooxanthellae-specific reverse primer (5' – AGCACTGCGTCAGTCCGAATAATTCACCGG – 3') following the protocols of (Rowan & Powers 1991). The resulting 1.5kb fragment was digested with *Taq1* restriction enzyme, and the resulting fragments were compared to zooxanthellae clade standards (Rowan & Powers 1991).

RNA extraction and microarray hybridization

Total RNA from all frozen coral fragments was isolated using Qiazol lysis reagent (QIAGEN). Live tissue was chiseled off each coral fragment and homogenized using a pre-chilled mortar and pestle. Frozen coral powder was transferred directly to Qiazol. Two chloroform extractions were performed, followed by isopropanol precipitation and two washes in 80% ethanol. RNA pellets were re-dissolved in nuclease-free water and cleaned further with RNeasy Mini columns (QIAGEN). RNA quantity and integrity were assessed with a NanoDrop ND-1000 spectrophotometer and an Agilent 2100 Bioanalyzer, respectively.

Microarray protocols followed those established by the Center for Advanced Technology at the University of California, San Francisco (http://cat.ucsf.edu/). 1,310 PCR amplified cDNAs from *M. faveolata* were spotted in duplicate on poly-lysine-coated slides yielding a microarray with 2,620 total features. cDNAs were chosen from EST libraries described in Schwarz *et al*. (2008). To annotate the cDNAs, we performed a BLASTX analysis (E-value cut-off $1e^{-5}$) against the GenBank non-redundant DNA and protein database (nr). Prior to hybridization, microarrays were post-processed by: 1) UV crosslinking at 60 mJ; 2) a "shampoo" treatment (3x SSC, 0.2% SDS at 65^{o}C); 3) blocking with 5.5g succinic anhydride dissolved in 335mL 1-methyl-2-pyrrilidinone and 15mL sodium borate; and 4) drying via centrifugation.

For Experiment 1, 1µg of total RNA was amplified using the MessageAmp II aRNA kit (Ambion), and 3µg of aRNA per sample were primed with 5µg/µL random nonamer for 10min at 70^{o}C. Reverse transcription (RT) lasted for 2hr at 42^{o}C using a master mix containing a 3:2 ratio of aminoallyl-dUTP to TTP. Following RT, single-

stranded RNA was hydrolyzed by incubating the RT reactions in 10µL 0.5M EDTA and 10µL 1M NaOH for 15min at 65°C. After hydrolysis, RT reactions were cleaned using Zymo Clean and Concentrator columns. Cy3 and Cy5 dyes (GE Healthcare) were dissolved in 17µL DMSO, and the coupling reactions lasted for 2hr at room temperature in the dark. Dye-coupled cDNAs were cleaned (Zymo), and appropriate Cy3 and Cy5 labeled cDNAs were mixed together in a hybridization buffer containing 0.25% SDS, 25mM HEPES, and 3x SSC. The hybridization mixtures were boiled for 2min at 99°C then allowed to cool at room temperature for 5min. The cooled hybridization mixtures were pipetted under an mSeries Lifterslip (Erie Scientific), and hybridization took place in Corning hybridization chambers overnight at 63°C. Microarrays were washed twice in 0.6x SSC and 0.01% SDS followed by a rinse in 0.06x SSC and dried via centrifugation. Slides were immediately scanned using an Axon 4000B scanner. All aforementioned techniques were also conducted with coral fragments from Experiment 2, omitting the initial RNA amplification, as total RNA quantity was adequate to prime 10µg of total RNA with 5µg/µL of Oligo-dT primer prior to RT.

Microarray data analysis

Experiment 1 followed a dye-swap design where each of the five control fragments was randomly paired to one of the five heat-stressed fragments. Each hybridization was performed twice with dye swapping between technical replicates, which allows for the control of dye labeling bias (Kerr 2003). Data analysis was performed using J/MAANOVA (Wu et al. 2003, Wu & Churchill 2005). Background-

subtracted mean intensity values were $\log_2$ transformed and normalized using the spatial-intensity joint lowess algorithm. Following $\log_2$ transformation and lowess normalization, in-slide duplicate spots were collapsed by taking the mean. A fixed-effect MAANOVA model was fit to the intensity data with array, sample, and dye terms. Differentially expressed genes were identified by testing the sample term according to the Empirical-Bayes Fs statistic (Cui et al. 2005). P-values for each gene were generated by shuffling the residuals over 500 permutations. FDR adjustments were applied to the p-values using a step-down FDR control method (Westfall & Young 1993), and genes were chosen at an adjusted alpha = 0.05.

Experiment 2 followed a reference design in which all heat-stressed RNA samples (four per time point) were compared to a pooled reference RNA sample composed of RNA from all control (untreated) coral fragments over all time points. Since all experimental RNA samples were compared to the reference sample, direct comparisons of gene expression across all time points can be performed. Background-subtracted mean intensity values were transformed and normalized as described above using J/MAANOVA. A MAANOVA fixed-effects model was fit to the intensity data with array and sample terms. Differentially expressed genes were identified using the same statistical methods described above. To visualize the temporal expression of differentially expressed genes, K-means clustering was performed using TIGR TMEV 4.0 software (Saeed et al. 2003). Microarray data from both Experiments 1 and 2 have been deposited in Gene Expression Omnibus (GSE10680).

Quantitative real-time PCR (qPCR)

In order to validate microarray gene expression estimates, qPCR was performed for seven genes chosen based on biological interest and to represent three classes of microarray data: 1) down-regulated > 2-fold; 2) down-regulated < 2-fold; and 3) up-regulated. SCRiP2, SCRiP8, and PXDN were > 2-fold down-regulated; EF-hand and C/EBPβ were < 2-fold down-regulated; MMP and AOSF722 were up-regulated. cDNAs from Experiment 1 (five non-bleached and five partially bleached) were synthesized from 1μg of aRNA and diluted to a final volume of 200μL. qPCR primers (Table S1) were designed using Primer Express 3.0 (Applied Biosystems), and test-PCRs confirmed specific amplification of the desired amplicons (70-100bp). Two μL of cDNA were used in triplicate 12.5μL qPCR reactions with 0.2μM primers and Power SYBR Green PCR Master Mix (Applied Biosystems) for 40 cycles. Delta Ct (dCt) values were calculated by subtracting the Ct of a housekeeping gene (HKG) (CAON1295 – a myosin) from the Ct's of the genes of interest. CAON1295 was the best-performing HKG from a group of candidates chosen from the microarray expression data. The quantitative methods used to identify candidate HKGs were identical to those reported by (Rodriguez-Lanetty et al. 2008). Delta delta Ct (ddCt) values were calculated by subtracting the dCt's from non-bleached and bleached samples, and fold changes were calculated using the $2^{-\Delta\Delta Ct}$ method (Livak & Schmittgen 2001). Statistical significance between the two groups was assessed at the dCt level using a two-tailed t-test.

RESULTS

Experiment 1: single colony, bleached versus non-bleached

Thermal-stressed fragments at 32.2^{o}C were visibly paled after three days and continued to lose color over the course of the experiment; however, they did not reach a fully bleached state. Algal cell density counts revealed that after nearly 11 days of thermal stress, experimental fragments contained an average of $1.44x10^{6}$ ($\pm$ $5.02x10^{5}$) cells/cm^{2} compared to an average of $2.5x10^{6}$ ($\pm$ $3.64x10^{5}$) cells/cm^{2} for controls (t-test, $p<0.001$; Figure 1). All control and heat-stressed fragments contained clade A zooxanthellae (data not shown).

Microarray analysis revealed large shifts in gene expression coincident with thermal stress and partial bleaching. MAANOVA identified 309 differentially expressed genes between untreated and thermal stressed coral fragments (24% of all assayed genes). Of these 309 genes, 191 were up-regulated (higher expression during thermal stress), and 118 were down-regulated (lower expression during thermal stress) (Table S2). Fold change magnitudes ranged from +1.9 to -4. Of the differentially expressed genes, only 21 up-regulated genes (11% of 191) and 47 down-regulated genes (39% of 118) had BLASTX hits ($E \leq 1x10^{-5}$). Six members of a newly discovered scleractinian cysteine-rich, putatively secreted peptide family (SCRiPs) (Sunagawa *et al*. in preparation) were among the most highly down-regulated transcripts. Therefore, the function of 74 genes, or 24% of all genes identified as differentially expressed, were used to guide discussion on the transcriptomic response to thermal stress and bleaching (Table 1).

Differentially expressed genes presented in Table 1 are grouped according to Gene Ontology (GO) biological processes, cellular components, or manually defined

categories. In addition, the putative functional roles are based on GO molecular functions, or manual definitions determined through literature searches and perusal of protein databases (e.g. PFAM and InterPro). Based on the molecular and cellular functions of the annotated genes, the following processes seem to be affected by thermal stress-induced bleaching: 1) extracellular matrix deposition; 2) secretion of cysteine-rich peptides; 3) oxidative stress; 4) heat shock protein expression; 5) transposon activity; 6) protein synthesis; 7) organization of the actin cytoskeleton and cell adhesion; 8) cell signaling; 9) Ca^{2+} homeostasis; 10) nucleosome organization; and 11) metabolism.

Experiment 2: multiple colonies, time course

Heat-treated corals at 32.72±0.32°C did not show any visible signs of bleaching after one day of elevated temperature. Slight bleaching of the four colonies did not occur simultaneously; one colony was slightly bleached after two days, two colonies after three days, and the fourth colony after four days. All thermal-stressed corals were partially bleached nine days after beginning the experiment. Algal cell densities had declined by the slightly and partially bleached time points (Figure 1). Cell densities of all later time points were statistically lower (ANOVA, $p<0.001$) than time zero and 1-day, but there was no difference between time zero and 1-day cell densities. Algal cell densities in the control fragments also decreased during the experiment, albeit less than the heat-treated fragments. At slight bleaching (two to four days), control fragments had 11% less zooxanthellae relative to the time zero baseline (heat-stressed fragments had 31% less zooxanthellae). At partial bleaching

(nine days), control fragments had 29% less zooxanthellae relative to time zero (heat-stressed fragments had 64% less zooxanthellae). The loss of zooxanthellae in the control fragments was likely due to the low light levels present during the experiments. All control and heat-treated fragments for two of the colonies contained only clade A *Symbiodinium*. The two other colonies displayed high RFLP clade diversity ranging from only clade C to multiple clade mixes (data not shown).

Microarray analysis of Experiment 2 was primarily focused on the temporal dynamics of genes that were differentially expressed upon heat treatment, i.e. do the same genes identified in Experiment 1 show temporal dynamics, or are they up-/down-regulated over all time points in a similar magnitude? Since all time zero and heat-stressed coral fragments were compared to the identical pooled reference RNA sample, we could directly compare levels of gene expression across time points. Using this approach, MAANOVA identified 280 differentially expressed genes, or 21% of all the genes on the microarray (Table S3). 29% of the 280 genes, or 81 total genes, were annotated by BLASTX.

Clustering of the differentially expressed genes grouped those behaving similarly over the time course. K-means clustering sorted the differentially expressed genes into eight clusters containing between four and 98 genes (Table S3). Figure 2 contains heat maps for the annotated genes within the 8 clusters; however, since the majority of genes within clusters 5 and 6 are stably expressed across time points, only those annotated genes that show changes in gene expression are included in Figure 2.

Genes within cluster 1 show large fold changes across the entire time course (mean expression profile = -1.4, -0.4, -0.2, -2.1); their expression at 1-day and slightly bleached is around two-fold higher than time zero, and expression at partially bleached is around two-fold less than time zero. These genes include the scleractinian cysteine-rich peptides (SCRiPs) and the ECM component peroxidasin (PXDN); they represent the most down-regulated genes during bleaching. Genes within cluster 2 exhibit the same temporal pattern to cluster 1 but on a smaller scale (mean expression profile = -0.5, +0.1, +0.1, -0.7). Cluster 8 (mean expression profile = +0.2, -0.3, -0.2, +0.1) contains genes that show expression patterns opposite to those of clusters 1 and 2; expression at 1-day and slightly bleached is lower than time zero, and expression at partially bleached is slightly lower than time zero. Genes within cluster 3 show gene expression changes on the same scale as cluster 1, but in the opposite direction (mean expression profile = +0.3, +0.6, +1.7, +1.6). These genes are the most up-regulated during bleaching – their expression ramps up during early stage thermal stress but then levels off between slight and partial bleaching. Genes in cluster 7 are also among the most up-regulated during bleaching (mean expression profile = -0.5, +0.1, +0.2, +0.1). This cluster contains cell signaling proteins (cylindromatosis protein (CYLD), a rhodopsin-like GPCR, and protein-tyrosine phosphatase 4A1), and a heat-shock protein (TCP-1). Opposite to cluster 7 is cluster 4 (mean expression profile = +0.2, 0, 0, -0.4) – these genes decrease in expression from time zero to 1-day and then decrease further from slight to partial bleaching. This cluster includes ribosomal proteins and two calcium-binding proteins (calmodulin (CaM) and an unknown EF-

hand protein). Lastly, cluster 5 genes (mean expression profile = +0.1, +0.1, +0.2, +0.2) tend to increase during thermal stress, and cluster 6 genes tend to do the opposite (-0.1, -0.2, -0.2, and -0.1); although most genes in clusters 5 and 6 were remarkably stable across the time course.

Overlap between Experiments 1 and 2

In response to thermal stress for 10 and nine days, respectively, corals in Experiments 1 and 2 became partially bleached. Given the similar endpoint in both experiments, a comparison was made of the differentially expressed genes. In total, 88 genes were differentially expressed in both Experiments 1 and 2. Of these 88 genes, 57 genes show directionally consistent patterns of expression; 23 genes are consistently up-regulated, and 34 genes are consistently down-regulated (Table S4). Annotated genes that were differentially expressed in Experiments 1 and 2 showed both consistent patterns of gene expression (**, Figure 2), and opposite patterns of gene expression (*, Figure 2). In total, there are 19 annotated genes that yield similar results and five genes that yield opposite results between both experiments. Notable genes consistently down-regulated at partial bleaching are five SCRiPs, CaM, an unknown EF-hand protein, three ribosomal proteins, CCAAT/enhancer binding protein β (C/EBPβ), and a cobalamin-binding protein. Notable genes that are consistently up-regulated include glutathione S-transferase sigma (GST-S), TCP-1, tachylectin-2, and two reverse transcriptases.

qPCR validation

The qPCR-estimated fold changes of the seven tested genes were in the same direction as the microarray estimates, and dCt's of the non-bleached samples were statistically different from dCt's of the bleached samples (t-test, $p<0.05$). For the six annotated genes, the qPCR estimates were inflated compared to the microarray results (Table 1). One non-annotated gene was tested (AOSF722), which had an array fold change = +1.7; its qPCR result was deflated compared to the microarray (+1.4). At the ddCt level, we could assess the variation in qPCR expression. Three genes greater than two-fold down-regulated, SCRiP8 (mean ddCt 4.47 ± 1.3 SD), SCRiP2 (mean ddCt = 2.71 ± 0.65), and PXDN (mean ddCt = 3.37 ± 1.09), showed large variation in expression. Two genes less than two-fold down-regulated, EF-hand (mean ddCt = 1.37 ± 0.64) and C/EBPβ (mean ddCt = 1.35 ± 0.91), and two genes up-regulated, MMP (mean ddCt = -1.46 ± 1.13) and AOSF722 (mean ddCt = -0.45 ± 0.45), also exhibited large variation in expression. Variation in qPCR data was consistent with microarray estimates of variation (Table S5). Overall, qPCR results confirmed statistically significant differential expression of the seven genes tested and tended to yield expression estimates greater than those measured using the microarray.

DISCUSSION

Using a cDNA microarray platform, we identified differentially expressed genes during thermal stress and bleaching. While thermal stress likely affects all cells, transcriptomic changes associated with the loss of symbionts may be confined to the gastrodermal cells – the primary zooxanthellae-harboring cells. Low fold changes in some genes may reflect dilution of mRNA abundances for processes occurring only in

symbiotic cells (Rodriguez-Lanetty et al. 2006), while larger fold changes may reflect processes occurring in both symbiotic and non-symbiotic cells (e.g. cells of the epithelium and calicoblastic epithelium). It is likely, also, that both control and thermally stressed coral fragments experienced stress involved in transplantation from the reef and changes associated with aquarium conditions (e.g. low light levels). As a result, it is likely that a stress response was present in both control and experimental corals, perhaps masking the degree of gene expression changes due to thermal stress alone. However, there were clear expression patterns associated with the thermal stress conditions that speak to the biology of corals that are subjected to conditions that cause bleaching.

qPCR validation of six genes yielded fold change values on average three times greater than the microarray fold change estimates. Compression of microarray-estimated fold changes relative to qPCR estimates are reported repeatedly in both technique-driven (e.g. Rajeevan et al. 2001, Yuen et al. 2002, Dallas et al. 2005, Wang et al. 2006) and functional genomics literature (e.g. Covarrubias et al. 205, Hawkins et al. 2007). Reasons for microarray-based fold change compression include the level of gene expression (i.e. reduced agreement occurs in genes with very high or very low levels of gene expression), and location of qPCR primers (i.e. reduced agreement when there is large separation between the location of the primers and microarray probes) (Etienne et al. 2004). Furthermore, the normalization method can have an effect on the agreement between microarray and qPCR data. For example, Wang *et al.*

(2006) found that fold change compression was more evident when LOWESS normalization was used (i.e. the normalization method utilized in the present study).

A striking observation from Experiment 1 is that even though more genes were up-regulated (191) than down-regulated (118), only 10% of the up-regulated genes are annotated, whereas 40% of the down-regulated genes are annotated by BLASTX. While this may be due to chance, it could be suggestive of coral-specific genes and processes being up-regulated during bleaching, and evolutionarily conserved cellular processes being down-regulated during bleaching. Many non-annotated (NA) genes displayed large fold changes (Tables S2 and S3). NA genes may represent ESTs that contain mainly untranslated regions, or they may be coral-specific genes. The sequencing of the *Nematostella vectensis* genome (Putnam et al. 2007) has been beneficial to coral genomics; however, given the future growth of coral functional genomic analyses, our ability to formulate meaningful conclusions will be greatly enhanced by a coral genome project.

While 57 genes show consistent patterns of gene expression at a partially bleached state, it is notable that there is not higher overlap between the results of Experiments 1 and 2. Given the differing designs of the two experiments (i.e. single colony, single time point versus multi-colony, time course), we did not expect to see high overlap. Additionally, the four colonies in Experiment 2 were not uniform in their symbiont genotype. Although never shown before, the clade of *Symbiodinium* within the coral host may strongly influence host gene expression. This factor is likely another reason why we see different stress-induced gene expression in both

experiments. Nevertheless, the activities of the genes listed in Table S4 and the annotated genes with a double-asterisk in Figure 2 reveal stunning, consistent heat stress-induced gene expression patterns. Genes such as CaM, the SCRiPs, EF-hand, C/EBPβ and PXDN are prime candidates for future work on protein function and localization.

A transcriptome-based bleaching model

Heat shock proteins (HSPs). Figure 3 illustrates a putative model of bleaching based on past studies and the present findings. The induction of HSPs is a hallmark of the heat shock response (reviewed in Lindquist 1986). As expected, transcriptomic data suggest increased HSP activity in heat-stressed *M. faveolata*. Both HSP90 and a TCP-1 chaperonin homolog show increased expression in Experiment 1 (Table 1). The same TCP-1 gene is differentially expressed in Experiment 2 – as a member of cluster 7 (Figure 2), its expression at all later time points is greater than its expression at time zero. The expression level of TCP-1 at slight bleaching is nearly two-fold greater than at time zero. These results are in accordance with previous studies reporting the induction of heat shock proteins during heat stress (Black et al. 1995, Hayes & King 1995, Fang et al. 1997, Sharp et al. 1997, Gates & Edmunds 1999, Downs et al. 2000, Downs et al. 2002, Downs et al. 2005).

Oxidative stress and nitric oxide signaling. Thermal stress, in synergy with normal to high light levels, leads to the production of ROS in the plastids of zooxanthellae (reviewed in Hoegh-Guldberg 1999, Lesser 2006). The low light levels present during our experiments suggest that the observed bleaching response may not

be reflective of natural bleaching events. In the absence of research-grade PAR measurements, Fv/Fm data, and/or direct measurements of ROS, we cannot determine whether the corals in these experiments experienced oxidative stress conditions thought to induce bleaching when high light is present. It is known, however, that the mitochondrial respiratory chain is a site of ROS generation (Cadenas & Davies 2000, Davidson & Schiestl 2001). Thermal stress-induced mitochondrial ROS generation has been shown in non-photosynthetic organisms, such as yeast (Davidson et al. 1996), clams (Abele et al. 2002), and human keratinocytes (Shin et al. 2008). Even though light levels present during these experiments may not have been high enough to induce significant ROS generation in zooxanthellae plastids, oxidative stress in the coral host is supported given the influence of thermal stress on the mitochondria of both the coral and zooxanthellae.

Regardless of their source, ROS are highly reactive and lead to lipid, protein, and DNA damage. Numerous studies have shown an increased antioxidant response in corals during stress. For example, superoxide dismutase was increased during thermal stress (e.g. Downs et al. 2000, Downs et al. 2002, Lesser & Farrell 2004). Downs *et al.* (2000) established that lipid peroxidation (oxidative damage of lipids) increased during thermal stress, and that glutathione levels decreased during thermal stress. A slight increase in catalase (CAT) during heat and light stress has also been shown in the zoanthid, *Palythoa caribaeorum* (Lesser et al. 1990). We found up-regulated expression of oxidative stress genes in the present experiments – glutathione s-transferase sigma (GST-S) in Experiments 1 and 2, and thioredoxin reductase 1 (TR-

1) and CAT in Experiment 2. The up-regulation of glutathione s-transferase sigma (GST-S) is suggestive of increased detoxification of ROS. GST-S catalyzes the conjugation of lipid peroxides to glutathione in *Drosophila* (Singh et al. 2001). In addition, the up-regulation of TR-1 is a sign of oxidative stress; TR-1 is responsible for keeping thioredoxin in a reduced state capable of detoxifying oxidized molecules (Holmgren 1985). The down-regulation of glutathione s-transferase mu (GST-M) in Experiment 1 is counter-intuitive since this class of GST is well known to be inducible by oxidative stress and active in the detoxification of ROS (Hayes & McLellan 1999). It is possible that GST-M was down-regulated due to the exhaustion of the cellular glutathione pool, or that GST-M in *M. faveolata* functions in roles not related to oxidative stress (Hayes & McLellan 1999). Besides the 'classical' oxidative stress genes mentioned already, protein tyrosine phosphatase 4A1 (also known as Phosphatase of Regenerating Liver-1 (PRL-1)), a member of cluster 7, is consistently up-regulated at all time points relative to time zero. A recent study showed that mRNA and protein expression of PRL-1 was increased during oxidative stress in cultured mammalian retinal cells (Yu et al. 2007).

Nitric oxide (NO) production by the cnidarian host in response to thermal and oxidative stress may be involved in the breakdown in symbiosis; exposure to high temperature led to an increase in NO production by symbiotic anemones followed by bleaching (Perez & Weis 2006). Additionally, zooxanthellae nitric oxide synthase activity was shown to be associated with coral bleaching (Trapido-Rosenthal et al. 2005). While NO can be involved in normal cell signaling processes, in the presence

of ROS, reactive nitrogen species (RNS) can be formed (e.g. peroxynitrite), which have the same damaging qualities as ROS. Furthermore, NO specifically inhibits mitochondrial NADH-ubiquinone reductase activity (Riobo et al. 2001), which directly inhibits ATP production. The collected detriments of ROS, RNS, and NO must invariably lead to diminished metabolism of the coral host. Our results suggest thermal stress and bleaching negatively affect coral host metabolism. Down-regulation of NADH-ubiquinone oxidoreductase (NADH-ubiq) subunits in both experiments (Table 1 and cluster 8) suggests deficiencies in mitochondrial electron transport. Additionally, down-regulation of acyl-carrier protein (cluster 8) points to a decrease in fatty acid synthesis, and down-regulation of both methionine adenosyltransferase 1α and quinoid dihydropteridine reductase (Table 1) suggest decreased amino acid metabolism. While decreased metabolism may be connected to the action of ROS, RNS, and NO, we cannot downplay the role of nutrient exchange between host and symbiont. Zooxanthellae translocate 95% of their photosynthates to the coral (Muscatine 1990), and they supply their host with a wide range of necessary compounds (Trench 1979). The lack of nutrient exchange between the coral and zooxanthellae during bleaching could also result in decreased metabolism of the coral.

Disruption of intracellular Ca^{2+} homeostasis. Intracellular Ca^{2+} homeostasis is critical to a functioning cell as Ca^{2+} is a ubiquitous cell messenger. Oxidative stress can disrupt Ca^{2+} homeostasis (Loven 1988, Orrenius et al. 1992). This disruption is marked by a sustained elevation in intracellular [Ca^{2+}] due to both the release of Ca^{2+} from intracellular stores and the entry of extracellular Ca^{2+}. Evidence from our

experiments points to a disruption of Ca^{2+} homeostasis during bleaching, which is exemplified by the down-regulation of calmodulin (CaM) and an EF-hand protein. CaM is a ubiquitous protein that transduces Ca^{2+} signals via four EF-hands (Ca^{2+}-binding domains); conformational change upon Ca^{2+} binding allows CaM to bind effector molecules. Given the importance of Ca^{2+} signaling in numerous cellular processes, it is surprising that CaM is consistently down-regulated in bleached *M. faveolata*. However, oxidative stress in human skin cells disabled CaM from binding Ca^{2+} and led to decreased CaM expression (Schallreuter et al. 2007). Given that CaM interacts with members of all families of Ca^{2+} channels at the plasma membrane, ER and mitochondria (reviewed in Kasri et al. 2004), disruption of CaM function during oxidative stress would have profound effects on Ca^{2+} homeostasis.

The down-regulation of FKBP12 further supports the notion of disrupted Ca^{2+} homeostasis in bleached *M. faveolata*. FKBP12 modulates the Ca^{2+} flux properties of ryanodine receptors (RyR); RyRs are Ca^{2+} release channels found on all intracellular Ca^{2+} storing organelles (reviewed in Fill & Copello 2002). Binding of both FKBP12 and CaM to a RyR inhibits channel activity, while their removal activates the channel. Moreover, ROS and RNS modify RyRs and thus alter their activity (Hidalgo 2005). These findings suggest that the Ca^{2+} releasing activities of RyRs are altered during oxidative stress via: 1) the down-regulation of FKBP12 and CaM, 2) the inability of CaM to bind Ca^{2+}, and 3) oxidative modifications to RyRs (Figure 3B). NO can also cause an increase in $[Ca^{2+}]$ by activating the release of Ca^{2+} from mitochondria

(Richter 1998), thus providing another mechanism by which Ca^{2+} homeostasis can become disrupted during bleaching.

The role of Ca^{2+} in coral bleaching has been explored previously. Sustained increases in intracellular [Ca^{2+}] during thermal stress were measured over six hours (Fang et al. 1997) and 24 hours (Huang et al. 1998) in isolated coral cells. Both studies found that intracellular [Ca^{2+}] stores were released during heat treatment, and that bleaching required a continuous exogenous supply of Ca^{2+}. Sawyer and Muscatine (2001) used Ca^{2+} channel blockers, Ca^{2+} ionophores, and CaM antagonists to study cold-shock induced bleaching via cell detachment in *Aiptasia*. Interestingly, caffeine treatment (which releases Ca^{2+} from intracellular stores) caused bleaching over 1.5 to 2.5hr, but an increase in intracellular [Ca^{2+}] was not measured during the first 12min of caffeine treatment in isolated cells. Ca^{2+} imaging studies over the time scale of days/weeks of thermal stress are needed in order to unequivocally support the hypothesis of Ca^{2+} homeostasis disruption during coral bleaching.

Modifications to the actin cytoskeleton and cell adhesion. The proposed model of bleaching (Figure 3) follows a scheme where thermal stress, oxidative stress, NO signaling, disruption of Ca^{2+} homeostasis, and decreased metabolism lead to cytoskeletal rearrangement, changes in cell adhesion properties, decreased calcification, and cell death. Cytoskeletal elements are themselves sensitive to damage by thermal stress (e.g. Muller et al. 2007), and a hallmark of Ca^{2+} homeostasis breakdown due to oxidative cell injury is a disruption of the actin cytoskeleton (Loven 1988, Orrenius et al. 1992). Five genes associated with the actin cytoskeleton are

differentially expressed in *M. faveolata* during thermal stress and bleaching. Gelsolin (GSN), lethal giant larvae 2 (LGL2), and tropomyosin (TPM) are down-regulated in response to thermal stress; whereas, myosin 7A (MYO7A) and myosin 9A (MYO9A) are slightly up-regulated. GSN, an actin filament capping and severing protein, and TPM, also an actin-binding protein, are both regulated by intracellular [Ca^{2+}] (Janmey & Stossel 1987, Lees-Miller & Helfman 1991). LGL2 is a heavily studied gene with homologs present in *Drosophila*, yeast, zebrafish, and mammals where it is involved in cytoskeletal organization (Strand et al. 1994). Myosins are a large family of actin-binding motor proteins that mediate various cellular processes. The expression of the aforementioned five genes most likely represents reorganization (or disruption due to thermal damage) of the actin cytoskeleton as a result of thermal stress, oxidative stress, and the disruption of Ca^{2+} homeostasis. It is likely that the cytoskeleton is also reorganized upon thermal stress due to the modulation of cell volume coincident with osmotic stress responses (reviewed in Mayfield & Gates 2007).

Various studies have also implicated LGL2 in cell adhesion processes. For example, the zebrafish homolog is involved in hemidesmosome formation (Sonawane et al. 2005) – hemidesmosomes are essential to the adhesion between cells and their underlying extracellular matrix (reviewed in Litjens et al. 2006). LGL2 mutants in *Drosophila* confirmed its role in cell adhesion. Both Gateff (1978) and Agrawal *et al.* (1995) showed that cell-cell contacts were defective in the absence of functional LGL2. In their description of LGL2, Strand *et al.* (1994) reasoned that all of the

defective cell adhesion symptoms associated with LGL2 mutation could be attributed to the disruption of the cytoskeleton network.

The dual activities of LGL2 in cytoskeletal organization and cell adhesion are reflective of cell adhesion molecules that contain cytoplasmic actin-binding domains or interact with cytoplasmic actin-binding proteins (Halbleib & Nelson 2006, Delon & Brown 2007). We postulate that the differential expression of LGL2 in bleached *M. faveolata* illustrates how disrupted Ca^{2+} homeostasis due to oxidative stress can have effects on both the cytoskeleton and cell adhesion. In addition, a neurofascin (NFASC) homolog is down-regulated in bleached *M. faveolata*. This gene is likely a member of the L1 family of immunoglobulin (Ig) cell adhesion molecules, which are usually implicated in neural cell adhesion (Brummendorf et al. 1998). The topic of cell adhesion in the context of coral bleaching is relevant given that one proposed mechanism of bleaching involves detachment of gastrodermal cells containing zooxanthellae (Gates et al. 1992).

Cell death. Unabated oxidative stress can lead to cell death (e.g. Tiwari et al. 2002), and thus the mounting evidence of oxidative mechanisms involved in bleaching is consistent with recent findings of apoptosis and necrosis in heat-stressed zooxanthellae and cnidarian hosts (Dunn et al. 2002, Dunn et al. 2004, Strychar et al. 2004, Richier et al. 2006, Dunn et al. 2007). An uncontrolled increase in intracellular $[Ca^{2+}]$ can lead to apoptosis (Duchen 2000, Hajnoczky et al. 2003, Orrenius et al. 2003). For example, when elevation of mitochondrial Ca^{2+} occurs in cells during oxidative stress (since Ca^{2+} channels are modified by ROS/RNS), mitochondrial

rupture occurs leading to the release of mitochondrial contents into the cytoplasm and the initiation of cell death. The decision between apoptotic or necrotic modes of cell death is thought to depend on the nature of the stress and the amount of ATP present in the cell (Orrenius et al. 2003). Necrosis proceeds when both intracellular energy levels and mitochondrial function are severely degraded, while apoptosis proceeds during the opposite conditions (Nicotera et al. 1998). Both cell death responses have been documented during thermal bleaching in *Aiptasia* (Dunn et al. 2002, Dunn et al. 2004), and necrotic tissue has been observed repeatedly in histological sections of bleached corals (Lasker et al. 1984, Glynn et al. 1985, Szmant & Gassman 1990, Brown et al. 1995). While our data cannot differentiate between the two modes of cell death, it is important to emphasize that oxidative stress and a disruption in Ca^{2+} homeostasis can lead to both outcomes.

It would have been quite informative to see expression patterns for critical genes in the apoptotic pathway, such as the cell cycle protein p53, an upstream regulator of apoptosis (Lesser & Farrell 2004), and Bcl-2 and caspase homologues (Dunn et al. 2006). Unfortunately, these genes are not present on the microarrays that were used in this study. Their absence is likely a result of the conditions under which the cDNA libraries were made.

Although the microarrays used in this study do not contain classical pro-apoptotic genes (e.g. APAF-1, Bax, and Bad in addition to those mentioned previously), differentially expressed genes identified in the present experiments are suggestive of apoptosis. The down-regulation of voltage-dependent anion-selective

channel 2 (VDAC2) in Experiment 2 is pro-apoptotic (see cluster 6). This anion channel inhibits Bak activation and mitochondrial apoptosis (Cheng et al. 2003, Chandra et al. 2005); thus, down-regulation of VDAC2 suggests the activation of mitochondrial apoptosis. Additionally, the cylindromatosis (CYLD) gene is a member of cluster 7, and thus consistently up-regulated at all time points relative to time zero. CYLD is a de-ubiquitinating enzyme not involved in the ubiquitin-proteasome system. The de-ubiquitinating activities of CYLD are numerous (Simonson et al. 2007); however, CYLD up-regulation leads to apoptosis. Brummelkamp *et al.* (2003) reported that knockdown of CYLD led to activation of NFkB, which is anti-apoptotic. The negative regulation of NFkB by CYLD has been further dissected: de-ubiquitination of TRAF2 (Kovalenko et al. 2003) and NEMO (Kovalenko et al. 2003, Nijman et al. 2005) by CYLD led to the de-activation of NFkB. Most recently, Xue *et al.* (2007) showed that de-ubiquitination of dTRAF2 (the *Drosophila* homolog of TRAF2) by CYLD leads to JNK-dependent apoptosis. These results suggest that up-regulation of CYLD over the time course of thermal stress is a pro-apoptotic signal.

Decreased calcification. The sharp down-regulation of proteins localized to the extracellular matrix (ECM) suggests that the ECM of thermal-stressed corals is structurally different than that of healthy corals. These proteins are thought to be involved in the synthesis of the organic matrix, which is necessary for calcification (Allemand et al. 1998). Decreased calcification resulting from thermal stress was first observed over 25 years ago in both natural (Hudson 1981) and laboratory settings (Jokiel & Coles 1977, Coles & Jokiel 1978). Bleached corals presumably undergo

lower rates of skeletogenesis than healthy corals due to the involvement of zooxanthellae in calcification, a phenomenon known as light-enhanced calcification (reviewed in Allemand et al. 2004). The absence of zooxanthellae does indeed affect the composition of the organic matrix (Cuif et al. 1999). A recently described protein found in the organic matrix of *Galaxea fascicularis*, named galaxin (Fukuda et al. 2003), is highly down-regulated in bleached *M. faveolata* (Table 1). The down-regulation of galaxin, along with that of peroxidasin, procollagen, and an SCP-like extracellular protein, suggests that the ECM of bleached *M. faveolata* is changing in composition to reflect their bleached state. Furthermore, the up-regulation of a matrix metalloproteinase (MMP) suggests increased degradation of the ECM (Shapiro 1998). Although the functions of the scleractinian cysteine-rich peptides (SCRiPs) are unknown, their secreted nature, down-regulation during bleaching, and clustering with known ECM components (data not shown), point to a potential role of these peptides in the process of calcification (Sunagawa et al. 2009a). Calcification is an energy-intensive process as the coral must actively pump Ca^{2+} to the calicoblastic epithelium (Tambutte et al. 1996). While decreased metabolism can explain a decrease in calcification during bleaching, a disruption in Ca^{2+} homeostasis must also be involved since the activity of all cellular Ca^{2+} pumps can be compromised by ROS, RNS, and CaM dysfunction.

Novel responses during thermal stress and bleaching

One of the most striking results from both experiments is the down-regulation during bleaching of transcripts involved in mRNA translation (mainly ribosomal

proteins). In Experiment 1, 12 ribosomal proteins, elongation factor 1α (EF1α), eukaryotic translation initiation factor, and an mRNA splicing factor are down-regulated. In Experiment 2, cluster 2 contains three ribosomal proteins that increase at 1-day and slight bleaching and decrease at partial bleaching relative to time zero. Cluster 4 contains seven ribosomal proteins and EF1α that decrease at all time points relative to time zero. Contrary to these results is ribosomal protein L24 (see cluster 3), which is highly up-regulated at all time points relative to time zero. This contradictory result is probably indicative of continued protein synthesis during thermal stress and bleaching. However, as a whole, these results suggest that after 9-10 days of thermal stress and significant bleaching, a marked down-regulation of many components of protein synthesis occurred. Similar findings are reported with model organisms: heat shock led to a temporary down-regulation of ribosomal protein transcription in yeast (Herruer et al. 1988), and an inhibition of ribosomal protein translation in *Drosophila* (Bell et al. 1988).

Another unexpected result is the apparent increase in transposable element (TE) activity during bleaching. The up-regulation of a transposon, a pol-like protein, and four reverse transcriptase genes in bleached *M. faveolata* during Experiment 1 supports this notion. In Experiment 2, two viral A-type inclusion genes are up-regulated at all thermal stress time points relative to time zero (CAON634 in cluster 5 and CAOO2078 in cluster 7), and two reverse transcriptase genes are up-regulated at all time points relative to time zero (AOSF1088 in cluster 5 and AOSF936 in cluster 7). These findings relate to seminal work showing that maize TEs became active

during chromosomal breakage (McClintock 1950). Further research on plants has shown that TEs are activated upon numerous stressors (McClintock 1984), and virtually all known plant retrotransposons are activated by stress (Wessler 1996). Moreover, thermal stress activated TEs in *Drosophila* (Ratner et al. 1992), silkworm (Kimura et al. 2001), black tiger shrimp (de la Vega et al. 2007), and mouse tissue (Li et al. 1999).

The down-regulation of a PIWI-like protein in bleached *M. faveolata* (Experiment 1) further supports the notion of increased TE activity during thermal stress. Recent research in *Drosophila* has shown that PIWI and related proteins are involved in the silencing of retrotransposons. Vagin *et al.* (2006) showed that transposon silencing in the *Drosophila* germ line functioned through repeat-associated small-interfering RNAs that require members of the PIWI subfamily to operate. Mutation of PIWI resulted in the activation of an endogenous retrotransposon in the testes of *Drosophila* (Kalmykova et al. 2005). These findings suggest that transposon activation during thermal stress in *M. faveolata* may be due to the down-regulation of PIWI-like proteins.

The above hypothesis of heat-induced TE activity assumes that the microarray probe sequences represent mobile genetic elements present in the coral genome; however, it is not clear where the viral genes come from. An alternative hypothesis for the seemingly increased activity of TEs is that a proliferation of viruses within the coral host and/or symbiotic algae occurs during thermal stress. Viral proliferation in response to thermal stress (Wilson et al. 2001) and UV exposure (Lohr et al. 2007) has

been documented in *Symbiodinium*, and viral-like particles were found to be more abundant in heat-stressed corals compared to controls (Wilson et al. 2005). Additionally, the presence of viruses within corals has been found using microscopic (Patten et al. 2008) and bioinformatics techniques (Marhaver et al. 2008). If the microarray results represent heat-induced viral proliferation, then viral sequences must have been cloned during cDNA library construction. Given that an oligo-dT primer was used to target coral mRNAs, it is unlikely (though not impossible) that viral genomes were cloned.

Conclusions

Overall, the findings presented here represent the first medium-scale transcriptomic study focused on elucidating the molecular and cellular foundation of thermal stress-induced coral bleaching. The results suggest that, as a consequence of thermal stress, corals undergo: a heat shock response, oxidative stress, modifications to the cytoskeleton, decreased calcification, decreased metabolism, increased transposon activity, and transcription and translation modifications. The hypothesis that oxidative stress leads to a disruption of intracellular Ca^{2+} homeostasis is powerful, as it would explain why coral bleaching results in cytoskeletal modifications, changes in cell adhesion properties, and the initiation of cell death via apoptosis and necrosis (Figure 3). We hope that the differentially expressed genes reported here will be evaluated as to their potential to serve as field-based biomarkers for coral health, and as a starting point for protein-level expression, localization, and functional studies (e.g. the SCRiPs, PXDN, Galaxin, FKBP12, PIWI, EF-hand, and C/EBPβ). Future

microarray studies on bleaching induced by light, darkness, and/or synergistic factors (e.g. heat and light) will provide further insights into the molecular mechanisms underlying bleaching. Time course studies, while more complex, are important in order to study the temporal patterns of gene expression that produce the bleaching response. Early time points (minutes to hours) are also necessary as large cellular changes are likely to occur on this timescale.

ACKNOWLEDGEMENTS

This chapter was published in *Molecular Ecology* (2008) volume 17 pages 3952-3971. I would like to thank my co-authors for their roles in publishing this work: Shini Sunagawa, Chris Voolstra, Jonathon Stillman, Jodi Schwarz, Alina Szmant, Mary Alice Coffroth, and Monica Medina. I would also like to thank the following people associated with STRI in Panamá: Rachel Collin, Gabriel Jácome, Plínio Gondola and other staff at the Bocas del Toro station, and Eyda Gomez and Javier Jara of Nancy Knowlton's lab at the Naos Laboratory. We would also like to thank Adam Carroll at UCSF for training and aid in printing microarrays. The comments of three anonymous reviewers are also greatly appreciated. This paper was prepared by Michael DeSalvo in partial fulfillment of requirements for a Ph.D. in Quantitative and Systems Biology from the University of California, Merced. This study was supported through a STRI Pre-doctoral Fellowship to Michael DeSalvo and NSF awards to Mónica Medina (BE-GEN 0313708 and IOS 0644438).

SUPPLEMENTARY INFORMATION

Supplementary information can be downloaded at the following website:

http://www3.interscience.wiley.com/journal/120848380/suppinfo

Table S1. qPCR primers used to amplify seven differentially expressed genes and one housekeeping gene (CAON1295).

Table S2. All 309 differentially expressed genes from Experiment 1, a replicate (n=5) dye-swap experiment comparing gene expression between partially bleached and control *M. faveolata* fragments.

Table S3. All 280 differentially expressed genes from Experiment 2, a replicate (n=4) time course experiment (Experiment 2) containing four time points. Expression values in columns E-H represent $\log_2$ ratios. Cluster assignments are based on K-means clustering with eight defined groups.

Table S4. The 57 genes that were consistently differentially expressed in both Experiments 1 and 2. Column E is the fold change difference between the Time Zero and Partially Bleached time points in Experiment 2. This figure should be compared to Column F – the fold change reported in Experiment 1.

Table S5. The variance in gene expression between the five fragments of each condition (control vs. heat-stressed) and the two technical replicates for each microarray hybridization in Experiment 1. Expression data are reported as $\log_2$ / lowess transformed intensities for the seven genes validated using qPCR plus six additional differentially expressed genes.

FIGURES

Figure 1. Zooxanthellae cell count data from both Experiments 1 and 2. The mean cell densities of five (Experiment 1) or four (Experiment 2) replicate fragments are shown with standard deviations. Letters above bars denote statistical significance – two means are significantly different ($p<0.05$) if their letters are different. The difference between control and partially bleached in Experiment 1 is statistically significant (Independent Samples t-test, $p<0.001$). According to a One Way Repeated Measures ANOVA with Tukey post-hoc testing, all pair-wise comparisons in Experiment 2 are significantly different with the exception of time zero vs. 1-day.

Figure 1.

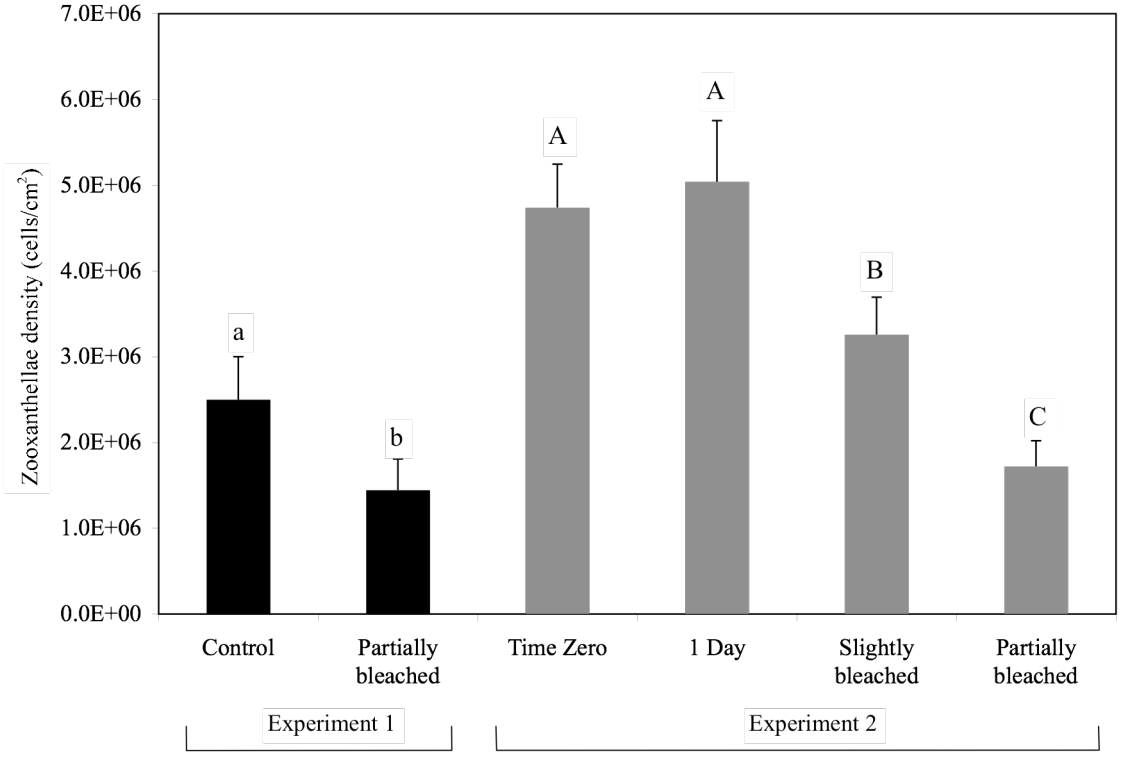
7.0E+06
6.0E+06
5.0E+06
4.0E+06
3.0E+06
2.0E+06
1.0E+06
0.0E+00
Zooxanthellae density (cells/cm^2)
a
b
A
A
B
C
Control
Partially bleached
Time Zero
1 Day
Slightly bleached
Partially bleached
Experiment 1
Experiment 2

Figure 2. Annotated differentially expressed genes from a replicate (n=4) time course experiment (Experiment 2) containing four time points. K-means clustering was performed to group genes by common temporal expression patterns. For clusters 1-4 and 7-8, only annotated genes are presented. For clusters 5 and 6, only those annotated genes that show changes in expression between time points are presented. Asterisks denote genes that were also differentially expressed in Experiment 1 (Table 1): * = opposite patterns of gene expression, and ** = similar patterns of gene expression between Experiments 1 and 2. All clusters are on the scale of -1 to +1 $\log_2$ ratio (upper scale bar), except for clusters 1 and 3 (denoted by a ^), which are on the scale of -3 to +3 $\log_2$ ratio (lower scale bar).

Figure 2.

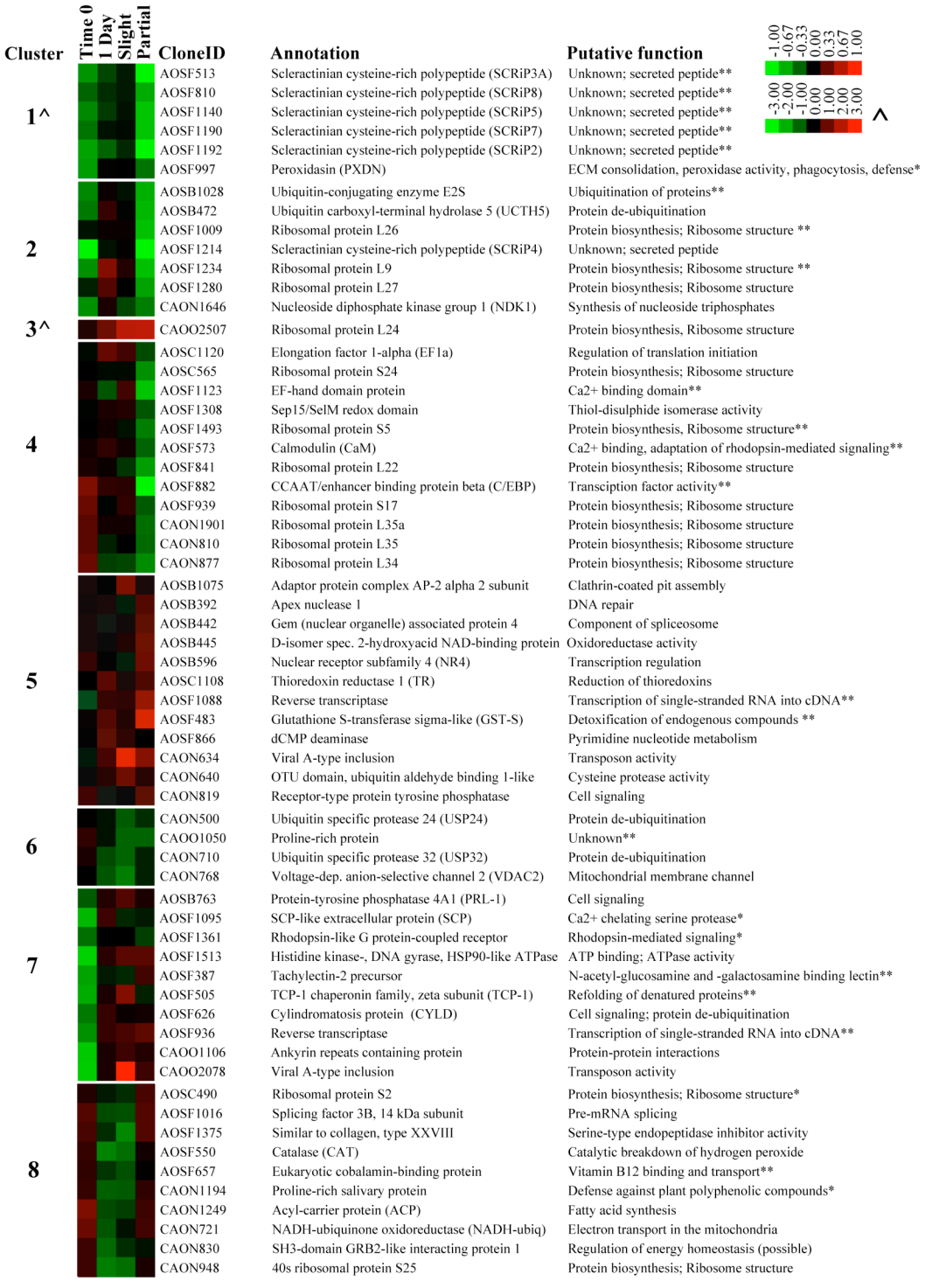

Cluster	CloneID	Annotation	Putative function
1^	AOSF513	Scleractinian cysteine-rich polypeptide (SCRiP3A)	Unknown; secreted peptide**
	AOSF810	Scleractinian cysteine-rich polypeptide (SCRiP8)	Unknown; secreted peptide**
	AOSF1140	Scleractinian cysteine-rich polypeptide (SCRiP5)	Unknown; secreted peptide**
	AOSF1190	Scleractinian cysteine-rich polypeptide (SCRiP7)	Unknown; secreted peptide**
	AOSF1192	Scleractinian cysteine-rich polypeptide (SCRiP2)	Unknown; secreted peptide**
	AOSF997	Peroxidasin (PXDN)	ECM consolidation, peroxidase activity, phagocytosis, defense*
2	AOSB1028	Ubiquitin-conjugating enzyme E2S	Ubiquitination of proteins**
	AOSB472	Ubiquitin carboxyl-terminal hydrolase 5 (UCTH5)	Protein de-ubiquitination
	AOSF1009	Ribosomal protein L26	Protein biosynthesis; Ribosome structure **
	AOSF1214	Scleractinian cysteine-rich polypeptide (SCRiP4)	Unknown; secreted peptide
	AOSF1234	Ribosomal protein L9	Protein biosynthesis; Ribosome structure **
	AOSF1280	Ribosomal protein L27	Protein biosynthesis; Ribosome structure
	CAON1646	Nucleoside diphosphate kinase group 1 (NDK1)	Synthesis of nucleoside triphosphates
3^	CAOO2507	Ribosomal protein L24	Protein biosynthesis, Ribosome structure
4	AOSC1120	Elongation factor 1-alpha (EF1a)	Regulation of translation initiation
	AOSC565	Ribosomal protein S24	Protein biosynthesis; Ribosome structure
	AOSF1123	EF-hand domain protein	Ca2+ binding domain**
	AOSF1308	Sep15/SelM redox domain	Thiol-disulphide isomerase activity
	AOSF1493	Ribosomal protein S5	Protein biosynthesis, Ribosome structure**
	AOSF573	Calmodulin (CaM)	Ca2+ binding, adaptation of rhodopsin-mediated signaling**
	AOSF841	Ribosomal protein L22	Protein biosynthesis; Ribosome structure
	AOSF882	CCAAT/enhancer binding protein beta (C/EBP)	Transciption factor activity**
	AOSF939	Ribosomal protein S17	Protein biosynthesis; Ribosome structure
	CAON1901	Ribosomal protein L35a	Protein biosynthesis; Ribosome structure
	CAON810	Ribosomal protein L35	Protein biosynthesis; Ribosome structure
	CAON877	Ribosomal protein L34	Protein biosynthesis; Ribosome structure
5	AOSB1075	Adaptor protein complex AP-2 alpha 2 subunit	Clathrin-coated pit assembly
	AOSB392	Apex nuclease 1	DNA repair
	AOSB442	Gem (nuclear organelle) associated protein 4	Component of spliceosome
	AOSB445	D-isomer spec. 2-hydroxyacid NAD-binding protein	Oxidoreductase activity
	AOSB596	Nuclear receptor subfamily 4 (NR4)	Transcription regulation
	AOSC1108	Thioredoxin reductase 1 (TR)	Reduction of thioredoxins
	AOSF1088	Reverse transcriptase	Transcription of single-stranded RNA into cDNA**
	AOSF483	Glutathione S-transferase sigma-like (GST-S)	Detoxification of endogenous compounds **
	AOSF866	dCMP deaminase	Pyrimidine nucleotide metabolism
	CAON634	Viral A-type inclusion	Transposon activity
	CAON640	OTU domain, ubiquitin aldehyde binding 1-like	Cysteine protease activity
	CAON819	Receptor-type protein tyrosine phosphatase	Cell signaling
6	CAON500	Ubiquitin specific protease 24 (USP24)	Protein de-ubiquitination
	CAOO1050	Proline-rich protein	Unknown**
	CAON710	Ubiquitin specific protease 32 (USP32)	Protein de-ubiquitination
	CAON768	Voltage-dep. anion-selective channel 2 (VDAC2)	Mitochondrial membrane channel
7	AOSB763	Protein-tyrosine phosphatase 4A1 (PRL-1)	Cell signaling
	AOSF1095	SCP-like extracellular protein (SCP)	Ca2+ chelating serine protease*
	AOSF1361	Rhodopsin-like G protein-coupled receptor	Rhodopsin-mediated signaling*
	AOSF1513	Histidine kinase-, DNA gyrase, HSP90-like ATPase	ATP binding; ATPase activity
	AOSF387	Tachylectin-2 precursor	N-acetyl-glucosamine and -galactosamine binding lectin**
	AOSF505	TCP-1 chaperonin family, zeta subunit (TCP-1)	Refolding of denatured proteins**
	AOSF626	Cylindromatosis protein (CYLD)	Cell signaling; protein de-ubiquitination
	AOSF936	Reverse transcriptase	Transcription of single-stranded RNA into cDNA**
	CAOO1106	Ankyrin repeats containing protein	Protein-protein interactions
	CAOO2078	Viral A-type inclusion	Transposon activity
8	AOSC490	Ribosomal protein S2	Protein biosynthesis; Ribosome structure*
	AOSF1016	Splicing factor 3B, 14 kDa subunit	Pre-mRNA splicing
	AOSF1375	Similar to collagen, type XXVIII	Serine-type endopeptidase inhibitor activity
	AOSF550	Catalase (CAT)	Catalytic breakdown of hydrogen peroxide
	AOSF657	Eukaryotic cobalamin-binding protein	Vitamin B12 binding and transport**
	CAON1194	Proline-rich salivary protein	Defense against plant polyphenolic compounds*
	CAON1249	Acyl-carrier protein (ACP)	Fatty acid synthesis
	CAON721	NADH-ubiquinone oxidoreductase (NADH-ubiq)	Electron transport in the mitochondria
	CAON830	SH3-domain GRB2-like interacting protein 1	Regulation of energy homeostasis (possible)
	CAON948	40s ribosomal protein S25	Protein biosynthesis; Ribosome structure

Figure 3.

A) A proposed model of cellular processes leading to coral bleaching. Thermal stress leads to reactive oxygen species (ROS) formation in the electron transport chains of the zooxanthellae (Z) plastids (C), and the mitochondria (Mt) of both coral and zooxanthellae. ROS cause oxidative stress in the coral cell, the formation of reactive nitrogen species (RNS) in combination with nitric oxide (NO), and a disruption of Ca^{2+} homeostasis (marked by a rise in intracellular [Ca^{2+}]). Disruption of Ca^{2+} homeostasis causes cytoskeletal rearrangement, cell adhesion changes, decreased calcification, and the initiation of cell death. Thermal and oxidative stress in both coral and zooxanthellae lead to decreased metabolism, which also contributes to decreased calcification and cell death. Color-coding is meant to connect cellular processes with differentially expressed genes reported in this study. ER = endoplasmic reticulum, and N = nucleus. For gene abbreviations see Table 1 and Figure 2.

B) A mechanism by which oxidative stress can lead to a disruption in Ca^{2+} homeostasis. In healthy cells, calmodulin (CaM) and FKBP12 inhibit the activity of ryanodine receptors (RyRs) such that Ca^{2+} is only released from the ER during necessary Ca^{2+} signaling events. Our data show that both CaM and FKBP12 are down-regulated during bleaching. These findings, in addition to published reports showing that oxidative stress leads to oxidative modifications to CaM and RyRs, suggest that RyR regulation is inhibited in bleached corals.

Figure 3.

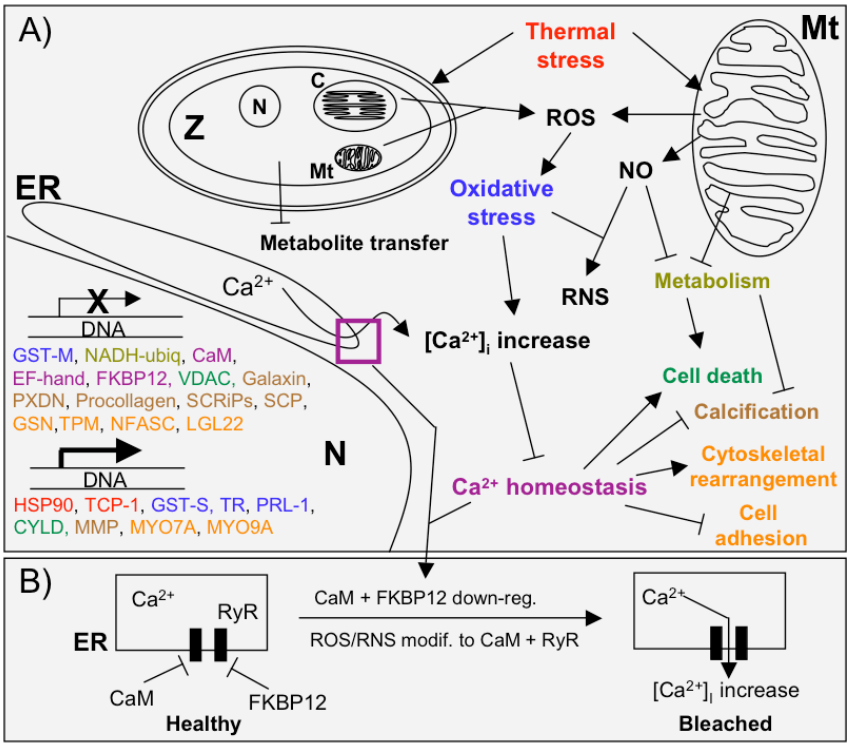
A)
Thermal stress
Mt
C
N
Z
Mt
ROS
NO
ER
Oxidative stress
Metabolite transfer
Ca2+
RNS
Metabolism
X
DNA
[Ca2+]i increase
GST-M, NADH-ubiq, CaM,
EF-hand, FKBP12, VDAC, Galaxin,
PXDN, Procollagen, SCRiPs, SCP,
GSN,TPM, NFASC, LGL22
Cell death
Calcification
DNA
N
Cytoskeletal rearrangement
Ca2+ homeostasis
Cell adhesion
HSP90, TCP-1, GST-S, TR, PRL-1,
CYLD, MMP, MYO7A, MYO9A
B)
Ca2+
RyR
ER
CaM + FKBP12 down-reg.
ROS/RNS modif. to CaM + RyR
Ca2+
CaM
FKBP12
[Ca2+]i increase
Healthy
Bleached

TABLES

Table 1. Annotated differentially expressed genes from a replicate (n=5) dye-swap experiment (Experiment 1) comparing gene expression between partially bleached and control *M. faveolata* fragments. Fold changes of gene expression are shown with Fs values, FDR-adjusted permutation p-values, and qPCR estimates (for six validated genes). Genes are grouped according to GO biological processes, GO cellular components, or manually defined categories. Functional roles are designated by GO molecular function or manually defined functions based on literature and database searches.

Table 1.

GenBank Acc.	Clone ID	Annotation	Putative Functional Role	Fold Δ	Fs val	P val	qPCR
Extracellular matrix proteins							
DR987943	AOSF1176	Galaxin	Soluble protein of the organic matrix	-3.45	71.52	0.000	
DR987689	AOSF997	Peroxidasin (PXDN)	ECM consolidation, peroxidase activity	-2.84	129.32	0.000	-10.36
DR988087	AOSF1268	Procollagen, type I, alpha 2	ECM structural constituent	-2.45	32.58	0.000	
DR987812	AOSF1095	SCP-like extracellular protein (SCP)	Ca2+ chelating serine protease	-1.88	42.83	0.000	
DR987160	AOSF561	Matrix metalloproteinase (MMP)	Metalloendopeptidase activity	1.53	28.43	0.000	2.74
Cysteine-rich peptide activity							
DR987097	AOSF513	Scleractinian cysteine-rich polypeptide 3A (SCRiP3A)	Unknown; secreted peptide	-3.99	68.52	0.000	
DR987884	AOSF1140	Scleractinian cysteine-rich polypeptide 5 (SCRiP5)	Unknown; secreted peptide	-3.62	54.24	0.000	
DR987486	AOSF810	Scleractinian cysteine-rich polypeptide 8 (SCRiP8)	Unknown; secreted peptide	-3.18	44.71	0.000	-22.14
DR987097	AOSF1192	Scleractinian cysteine-rich polypeptide 2 (SCRiP2)	Unknown; secreted peptide	-3.11	38.16	0.000	-6.53
DR987965	AOSF1190	Scleractinian cysteine-rich polypeptide 7 (SCRiP7)	Unknown; secreted peptide	-1.67	19.10	0.000	
DR987831	AOSF1109	Scleractinian cysteine-rich polypeptide 1 (SCRiP1)	Unknown; secreted peptide	-1.21	8.68	0.018	
Oxidative stress proteins							
DR988371	AOSF1447	Glutathione s-transferase mu (GST-M)	Detoxification of endogenous compounds	-1.29	10.46	0.009	
DR987313	AOSF666	Zinc RING finger protein 7 (SAG)	Lipid peroxide defense; protein ubiquitination	1.15	11.14	0.007	
DR987062	AOSF483	Glutathione S-transferase sigma-like (GST-S)	Detoxification of endogenous compounds	1.26	7.14	0.033	
Heat shock proteins							
DR988373	AOSF1451	90-kda heat shock protein (HSP90)	Refolding of denatured proteins	1.28	14.93	0.001	
DR987088	AOSF505	TCP-1 chaperonin family, zeta subunit (TCP-1)	Refolding of denatured proteins	1.36	30.02	0.000	
Ca2+ homeostasis proteins							
DR987851	AOSF1123	EF-hand domain protein	Ca2+ binding domain	-1.66	35.56	0.000	-2.58
DR987178	AOSF573	Calmodulin (CaM)	Ca2+ binding, adaptation of rhodopsin-mediated signaling	-1.38	16.56	0.001	
DR987514	AOSF836	FK506-binding protein 12 (FKBP12)	Refolding of denatured proteins; Ca2+ channel regulation	-1.35	33.49	0.000	
Cytoskeletal proteins / Cell adhesion molecules							
DR988150	AOSF1307	Gelsolin (GSN)	Calcium-regulated, actin-severing protein	-1.83	29.72	0.000	
DR986355	AOSB404	Tropomyosin (TPM)	Actin-binding cytoskeletal component	-1.52	9.45	0.014	
DR988440	CAOO655	Neurofascin homolog (NFASC)	Neural cell-cell adhesion	-1.32	10.27	0.010	
FE039783	CAON1906	Lethal giant larvae homolog 2 (LGL2)	Cytoskeleton organization, hemidesmosome assembly	-1.25	24.18	0.000	
DR988233	AOSF1357	Myosin 9A (MYO9A)	Actin-dependent ATPase activity	1.12	7.72	0.026	
DR987660	AOSF976	Fat tumor suppressor homolog 1 (FAT1)	Cadherin-mediated adhesion and signaling	1.14	9.30	0.014	
DR987650	AOSF969	Myosin 7A (MYO7A)	Actin-dependent ATPase activity	1.28	30.41	0.000	
Transposon activity							
DR988354	AOSF1434	PAZ domain/Piwi-like subfamily (PIWI)	Retrotransposon regulation	-1.51	12.70	0.004	
DR988240	CAON1787	Reverse transcriptase	Transcription of single-stranded RNA into cDNA	1.11	6.99	0.035	
DR988440	AOSF1490	Novel transposon	Transposable element activity	1.20	11.67	0.005	
FE039892	CAON537	Pol-like protein	Nuclease/transposase/RNase activity	1.23	8.45	0.020	
DR988412	AOSF1473	Reverse transcriptase	Transcription of single-stranded RNA into cDNA	1.30	13.34	0.003	
DR987618	AOSF 936	Reverse transcriptase	Transcription of single-stranded RNA into cDNA	1.33	9.27	0.014	
DR987618	AOSF1088	Reverse transcriptase	Transcription of single-stranded RNA into cDNA	1.52	38.90	0.000	

Table 1, continued.

GenBank Acc.	Clone ID	Annotation	Putative Functional Role	Fold Δ	Fs val	P val	qPCR
Cell signaling proteins							
DR988240	AOSF1361	Rhodopsin-like G protein-coupled receptor	Rhodopsin-mediated signaling	-1.77	29.41	0.000	
DR987569	AOSF882	CCAAT/enhancer binding protein β (C/EBPβ)	Transcription factor activity	-1.52	25.38	0.000	-2.55
DR986829	AOSC957	Ets domain transcription factor (Pointed subfamily)	Transcription factor activity	-1.14	7.15	0.033	
Nucleosome / Transcription related proteins							
DR987246	AOSF622	H2A histone family, member V, isoform 1	Nucleosome assembly	-1.47	19.45	0.000	
DR988012	AOSF1219	Histone protein H3	Nucleosome assembly	-1.40	18.76	0.000	
DR988033	AOSF1233	Histone H2A, isoform 1	Nucleosome assembly	-1.28	6.24	0.047	
FE040071	CAON876	High mobility group AT-hook 2 (HMGA2)	Maintenance of chromatin architecture; transcriptional reg.	-1.21	8.50	0.019	
DR986454	AOSB760	SNF2 and DEXH-box helicase domain protein	Unwinding of DNA double helix	1.05	6.96	0.035	
FE039615	CAON1597	Bromodomain containing 8 (Brd8)	Component of histone acetylase complex	1.15	22.11	0.000	
Metabolic proteins							
FE040151	CAON999	Methionine adenosyltransferase 1α (MAT1α)	S-adenosylmethionine biosynthesis	-1.86	89.05	0.000	
DR988384	AOSF1456	Quinoid dihydropteridine reductase (QDPR)	Amino acid metabolism; tetrahydrobiopterin biosynthesis	-1.37	10.25	0.010	
FE040110	CAON943	NADH-ubiquinone oxidoreductase (NADH-ubiq)	Mitochondrial electron transport	-1.20	12.20	0.004	
DR987599	AOSF914	CDGSH iron sulfur domain 1	Iron transport into mitochondria	-1.18	11.67	0.005	
DR987302	AOSF657	Eukaryotic cobalamin-binding protein	Vitamin B12 binding and transport	-1.16	7.85	0.025	
FE039547	CAON1459	Ferritin (FTN)	Iron binding and homeostasis	-1.11	9.53	0.013	
Protein synthesis							
DR986615	AOSF1234	Ribosomal protein L9	Protein synthesis; structural constituent of ribosome	-1.47	7.42	0.029	
DR988446	AOSF1167	Ribosomal protein S3	Protein synthesis; structural constituent of ribosome	-1.34	11.91	0.005	
DR988446	AOSF1493	Ribosomal protein S5	Protein synthesis; structural constituent of ribosome	-1.31	24.70	0.000	
DR987242	AOSF620	Eukaryotic translation initiation factor	Regulation of translation initiation	-1.30	20.59	0.000	
DR988266	AOSF1376	Ribosomal protein S7	Protein synthesis; structural constituent of ribosome	-1.24	12.01	0.005	
DR987703	CAOO2477	Ribosomal protein L23	Protein synthesis; structural constituent of ribosome	-1.24	12.19	0.004	
DR988328	AOSF1416	Ribosomal protein X-linked	Protein synthesis; structural constituent of ribosome	-1.23	7.77	0.025	
DR986825	AOSC944	Ribosomal protein S25	Protein synthesis; structural constituent of ribosome	-1.23	7.62	0.027	
FE040377	CAOO2543	Splicing factor, arginine/serine-rich 4	Regulation of pre-mRNA splicing	-1.20	6.83	0.037	
DR987703	AOSF1009	Ribosomal protein L26	Protein synthesis; structural constituent of ribosome	-1.19	10.14	0.010	
DR986810	AOSC908	Ribosomal protein L12	Protein synthesis; structural constituent of ribosome	-1.18	21.94	0.000	
DR986717	AOSC713	Ribosomal protein L3	Protein synthesis; structural constituent of ribosome	-1.17	6.95	0.035	
DR988078	AOSF1264	Ribosomal protein L14	Protein synthesis; structural constituent of ribosome	-1.17	6.89	0.036	
DR986615	AOSC490	Ribosomal protein S2	Protein synthesis; structural constituent of ribosome	-1.14	8.64	0.018	
FE040562	CAOO902	Elongation factor 1α (EF1α)	Regulation of translation initiation	-1.12	16.13	0.001	
Miscellaneous proteins							
DR987865	AOSF1131	Green fluorescent protein homolog (GFP)	Energy transfer acceptor	-1.67	27.47	0.000	
DR988485	AOSF1521	USP-like protein	Universal stress protein (Bacteria)	-1.58	27.58	0.000	
DR987591	AOSF907	BPTI/Kunitz family of serine protease inhibitors	Serine-type endopeptidase inhibitor activity	-1.51	16.12	0.001	
DR986515	AOSB1028	Ubiquitin-conjugating enzyme E2S	Ubiquitination of proteins	-1.46	7.75	0.025	
FE040166	CAOO1050	Proline-rich protein	Unknown	-1.18	8.13	0.022	
DR988087	CAOO526	Probable transport protein sec61 alpha subunit	Protein targeting, transport, secretion	-1.14	6.26	0.046	
DR987207	AOSF595	Astacin domain containing protein	Zinc-regulated peptidase	1.09	31.45	0.000	
DR987088	AOSF387	Tachylectin-2 precursor	Lectin that binds N-acetyl-glucosamine and -galactosamine	1.10	7.14	0.033	
DR988170	AOSF1319	Zinc finger, NFX1-type containing 1	Zinc ion-binding transcription factor	1.12	7.86	0.024	
DR988384	CAON1194	Proline-rich salivary protein	Defense against plant polyphenolic compounds	1.22	7.57	0.028	
DR987159	AOSF560	Ubiquitin specific protease 24 (USP24)	De-ubiquitination of proteins	1.27	11.53	0.006	

CHAPTER 2

TRANSCRIPTOMIC RESPONSES TO HEAT STRESS AND BLEACHING IN THE ELKHORN CORAL *ACROPORA PALMATA*

ABSTRACT

The emergence of genomic tools for reef-building corals and symbiotic anemones comes at a time when alarming losses in coral cover are being observed worldwide. These tools hold great promise in elucidating novel and unforeseen cellular processes underlying the successful mutualism between corals and their dinoflagellate endosymbionts (*Symbiodinium* spp.). Since thermal stress triggers a breakdown in the symbiosis (coral bleaching), measuring the transcriptomic response to thermal stress-induced bleaching offers an extraordinary view of the cellular processes specific to coral-algal symbioses. In the present study, we utilized a cDNA microarray containing 2,059 genes of the threatened Caribbean Elkhorn coral *Acropora palmata* to identify genes differentially expressed upon thermal stress. Fragments from replicate colonies were exposed to elevated temperature for two days, and samples were frozen for microarray analysis after 24 and 48 hours. 204 genes were differentially expressed in samples collected one day after thermal stress, and 104 genes were differentially expressed in samples collected two days after thermal stress. Analysis of the differentially expressed genes indicate a cellular stress response in *A. palmata* involving: (1) growth arrest; (2) chaperone activity; (3) nucleic acid stabilization and repair; and (4) the removal of damaged macromolecules. Other differentially expressed processes include sensory perception, metabolite transfer

between host and endosymbiont, nitric oxide signaling, and modifications to the actin cytoskeleton and extracellular matrix. The results are compared to those from a previous coral microarray study of thermal stress in *Montastraea faveolata* pointing to an overall evolutionary conserved bleaching response in scleractinian corals.

INTRODUCTION

Coral reefs represent the most diverse marine ecosystem, yet numerous anthropogenic stressors currently threaten their vitality (Hoegh-Guldberg et al. 2007). Understanding how scleractinian corals and their associated microbes (especially the photosynthetic dinoflagellates of the genus *Symbiodinium*) will respond to future stress requires knowledge of the molecular and cellular basis of the symbiosis itself and the events that lead to the collapse in symbiosis (i.e. bleaching). Genomic-scale approaches can help attain a new level of understanding, which in turn can propel the study of coral symbiosis into the realm of systems biology, whereby predictive mathematical models can more efficiently extract information from genomic studies.

Initial ventures into the field of coral functional genomics have focused on environmental stress in natural populations of *Montastraea faveolata* (Edge et al. 2005, Morgan et al. 2005, Edge et al. 2008), thermal stress and bleaching in *M. faveolata* (DeSalvo et al. 2008), development in *Acropora millepora* (Grasso et al. 2008), and the transcriptomic response to symbiosis establishment in *M. faveolata* and *Acropora palmata* (Voolstra et al. 2009). Also relevant to this burgeoning discipline are microarray studies on the temperate symbiotic anemone *Anthopleura elegantissima*. Rodriguez-Lanetty et al. (2006) measured transcriptomic differences

between symbiotic and aposymbiotic anemones, and (Richier et al. 2008) quantified gene expression following UV and thermal stress. These initial studies have provided a wealth of information on the molecular basis of cnidarian-algal symbioses and the transcriptomic response to thermal stress and bleaching. Not only have studies on stress corroborated early findings (e.g. the involvement of oxidative stress and apoptosis), but they have also revealed new aspects of cnidarian physiology (e.g. the involvement of cytoskeletal remodeling, ribosomal protein transcript down-regulation, and Ca^{2+} homeostasis disruption) relevant to thermal stress and bleaching (DeSalvo et al. 2008, Richier et al. 2008).

Perhaps the most exciting results from early transcriptomic studies on cnidarian stress are transcripts encoding cell signaling molecules, transcription factors, transport proteins, and extracellular matrix proteins differentially expressed during stress. These newly identified focal molecules are prime candidates for future inquiries given that the precise cellular signaling mechanisms of bleaching are still unknown. For example, the following candidates overlap between the differentially expressed genes reported in DeSalvo et al. (DeSalvo et al. 2008) and (Richier et al. 2008): CCAAT/enhancer binding protein transcription factors, tropomyosin (an actin binding cytoskeletal protein), sec61 (an ER protein translocation channel), and tissue factor pathway inhibitor (a member of the BPTI/Kunitz family of serine protease inhibitors).

Studying bleaching mechanisms in zooxanthellate cnidarians such as *A. elegantissima*, *Aiptasia pallida*, and scleractinian corals offers the advantage of taking an evolutionary comparative approach. The aforementioned anemones are highly

amenable to laboratory culture and manipulation and thus hold much promise in the study of cnidarian bleaching mechanisms (Weis et al. 2008). In the interest of directly studying bleaching in reef-building corals, we have taken a comparative approach by investigating the transcriptomic response to bleaching in the Robust clade coral *M. faveolata* (DeSalvo et al. 2008) and the Complex clade coral *A. palmata* (present study). This approach enables us to ask questions such as: do coral species separated by 240-288 Ma (Medina et al. 2006) respond similarly (on transcriptomic and organismal levels) to thermal stress and bleaching? Despite known differences in the bleaching susceptibilities of branching versus encrusting corals (e.g. Loya et al. 2001), we hypothesized that the overall transcriptomic responses to bleaching are consistent in these divergent species. A similar approach used by Voolstra et al. (Voolstra et al. 2009) found that larvae of *A. palmata* and *M. faveolata* responded similarly to infection by competent and incompetent strains of *Symbiodinium* spp.

In the present study, we report a microarray-based experiment of thermal stress and bleaching in *Acropora palmata*. The experiment was performed concurrently with our previous study on thermal stress and bleaching in *Montastraea faveolata* (DeSalvo et al. 2008). While *A. palmata* bleached faster given the same temperature increase, the transcriptomic response was very similar to the one observed in *M. faveolata.* Specific similarities and differences are discussed in-depth, and the functional annotations of differentially expressed genes are discussed in the context of previous findings, thus extending the current view of both the cellular stress response and the cellular mechanisms underlying coral bleaching.

MATERIALS AND METHODS

Field experiment

The field experiment was performed at the Smithsonian Tropical Research Institute's Bocas del Toro field station in Panamá during September and October 2006. Four colonies of *A. palmata* were sampled from two separate reefs 21 km apart (two colonies from Isla Solarte – 9°19'56.78" N and 82°12'54.65" W, and two colonies from Cayos Zapatillas – 9°15'08.79" N and 82°02'24.63" W). Each colony was broken into six fragments using a hammer and chisel. For each colony, three fragments were placed in a control aquarium, and three fragments were placed in an experimental aquarium fitted with two 200-Watt aquarium heaters (each colony was represented by a pair of 75 liter aquaria). The four control and four experimental aquaria were each placed in large fiberglass ponds equipped with continuous water flow to buffer ambient temperature fluctuations.

All aquaria were exposed to shaded ambient light, and each aquarium was a closed system (but contained a pump to generate continuous water flow). Fragments were kept at a depth of ~25cm. HOBO Pendant Temperature/Light Data Loggers (Onset Corp UA-002-64) recorded temperature and light data every three minutes. These data loggers are not designed to measure photosynthetically active radiation; therefore, relative light levels in the aquaria are reported as the percentage of the average 10am to 2pm light intensity measured on a reef ~4m deep in Bocas del Toro (9°22'68.4" N and 82°18'24.6" W) during September and October 2007. Light intensity differed slightly between the four aquaria fitted with HOBOs (control aquaria

1 – 43%; control aquaria 2 – 46%; heated aquaria 1 – 35%; and heated aquaria 2 – 34% of reef light).

After an acclimation period of four days at the natural temperature of the seawater system (mean temperature = 30.29±0.07^{o}C), a fragment from each control and experimental aquaria was sampled (t0C and t0H). After time zero sampling, the heaters in each of the experimental aquaria were turned on. The temperatures of the experimental aquaria increased to ca. 32^{o}C over three hours. The mean temperature of the control aquaria during the entire experiment was 29.74±0.03^{o}C, and the mean temperature of the heated aquaria was 32.72±0.32^{o}C. Control and experimental fragments were sampled again one day (1dC and 1dH) and two days (2dC and 2dH) after turning on the heaters. Heated fragments from one of the colonies (colony 3) showed extreme bleaching after one day of thermal stress. The remaining fragment of colony 3 was removed at this time to avoid fouling of the water due to death. Thus, there are four replicates for t0C, t0H, 1dC, and 1dH, and three replicates for 2dC and 2dH. All samples were taken at night and frozen in liquid nitrogen. Immediately prior to freezing, a polyp-size tissue scraping (~12.6 mm^2) was preserved in 1 mL of 3.7% formaldehyde for *Symbiodinium* cell density counts.

Symbiodinium cell counts and 18S rRNA gene RFLP analysis

The formaldehyde-fixed tissue scrapings were homogenized by maceration with a dissecting needle and vortexed. Cell counts were performed with a hemocytometer. Eight replicate cell counts were averaged for each coral genotype at each time point. After testing for normality and equal variances within time points,

significance between time points was assessed using a one-way ANOVA and pairwise post-hoc testing via the Fisher LSD method. All statistical tests were performed using SigmaStat 3.11.

Genomic DNA was isolated from frozen coral powder (see below) using the PowerPlant DNA Isolation kit (MoBio). *The Symbiodinium* 18S ribosomal RNA gene was amplified from all samples using the primers ss5 and ss3Z (Rowan & Powers 1991). The resulting 1.5kb fragment was digested with TaqI restriction enzyme, and the resulting fragments were compared to *Symbiodinium* clade standards (Rowan & Knowlton 1995).

RNA extraction and microarray hybridization

Total RNA from all frozen coral fragments was isolated using QIAzol lysis reagent (Qiagen). Coral tissue was chiseled off each coral fragment and homogenized using a pre-chilled mortar and pestle (this method did not efficiently lyse endosymbiont cells). The frozen powder was transferred directly to QIAzol. Three chloroform extractions were performed, followed by isopropanol precipitation and three washes in 70% ethanol. RNA pellets were re-dissolved in nuclease-free water and cleaned with RNeasy Mini columns (Qiagen). RNA quantity and integrity were assessed with a NanoDrop ND-1000 spectrophotometer and an Agilent 2100 Bioanalyzer, respectively.

The microarray used in this study consisted of 2,059 PCR-amplified cDNAs (spotted in duplicate) chosen from coral host-specific cDNA libraries described in Schwarz et al. (2008). Microarray post-processing and hybridization protocols

followed previously published methods (DeSalvo et al. 2008), with a few slight changes. Briefly, one μg of total RNA was amplified using the MessageAmp II aRNA kit (Ambion), and 3 μg of aRNA per sample were primed with 10 μg random nonamer for 10 min at 70°C. Reverse transcription (RT) lasted for 2 hr at 50°C using a master mix containing a 4:1 ratio of aminoallyl-dUTP to TTP and SuperScript III reverse transcriptase (Invitrogen). Following RT, single-stranded RNA was hydrolyzed by incubating the RT reactions in 10 μL 0.5M EDTA and 10 μL 1M NaOH for 15 min at 65°C. After hydrolysis, RT reactions were cleaned using MinElute Reaction Cleanup columns (Qiagen). Cy3 and Cy5 dyes (GE Healthcare) were dissolved in 18 μL DMSO, and the coupling reactions lasted for 1 hr at room temperature in the dark. Dye-coupled cDNAs were cleaned (MinElute), and Cy3- and Cy5-labeled cDNAs were mixed together in a hybridization buffer containing 0.25% SDS, 25 mM HEPES, and 3x SSC. The hybridization mixtures were boiled for 2 min at 99°C then allowed to cool at room temperature for 5min. The cooled hybridization mixtures were pipetted under an mSeries Lifterslip (Erie Scientific), and hybridization took place in custom-fabricated hybridization chambers overnight at 63°C. Microarrays were washed twice in 0.6x SSC and 0.01% SDS followed by a rinse in 0.06x SSC and dried via centrifugation.

Microarray data analysis

Slides were immediately scanned using an Axon 4000B scanner (Molecular Devices) where care was taken to balance photomultiplier tube (PMT) settings. Gridding was performed using GenePix Pro 6.0. TIGR Express Converter was used to

convert GenePix results files into .mev files for input into TIGR MIDAS 2.19 (Saeed et al. 2003). Data for a particular spot were discarded according to the stringent one bad channel policy. Additional data were discarded if spots had been flagged during gridding in GenePix, and if the intensity in either channel was less than 30,000 units. After filtering, background-subtracted median intensity values were LOWESS normalized, and in-slide duplicates were averaged. Both PMT balancing and LOWESS normalization equalize for differing amounts of host RNA input (a potential issue when processing tissue where endosymbiont densities can vary). Microarray hybridization data (both raw and normalized) are deposited in GEO with the series record number GSE16151.

We employed a reference design where all control and heat-stressed samples (labeled with Cy5) were compared to a pooled reference aRNA sample (labeled with Cy3) composed of aRNA from the four t0C fragments. Since all RNA samples were compared to the reference sample, direct comparisons of gene expression across all time points and conditions can be performed. Furthermore, dye swapping is not needed in a reference design since all samples contain the same dye bias.

Genes were included in statistical analyses only if there were data for three out of four replicates for t0C, t0H, 1dC, and 1dH, and two out of three replicates for 2dC and 2dH. This left 1,697 genes for statistical analyses of gene expression. Missing values were imputed using PAMR (Tibshirani et al. 2002). The ratio between the fluorescence intensity of the two channels was then used as input for BAGEL (Bayesian Analysis of Gene Expression Levels) (Townsend & Hartl 2002). The

BAGEL software uses Bayesian probability to infer a relative expression level of each gene and statistical significance of differentially expressed genes. BAGEL computes an estimated mean and 95% credible interval of the relative level of expression of each gene in each treatment and time point (i.e. t0C, t0H, 1dC, 1dH, 2dC, and 2dH). We used the conservative gene-by-gene criterion of non-overlapping 95% credible intervals to regard a gene as significantly differentially expressed. Genes significant at 1day satisfied the following conditions: t0C=t0H, 1dH≠t0C, 1dH≠t0H, 1dH≠1dC. Genes significant at 2days satisfied the following conditions: t0C=t0H, 2dH≠t0C, 2dH≠t0H, and 2dH≠2dC. Genes significantly different at both days were the overlap between the previous two tests. Genes significantly different between 1dH and 2dH had to be among those genes significant on both days and also satisfy the additional test 1dH≠2dH. Clustering of genes differentially expressed at both 1d and 2d were performed in TIGR TMEV 4.0 (Saeed et al. 2003) using hierarchical clustering according to Euclidean distance and average linkage. To assess over-representation of Gene Ontology (GO) terms in the lists of significant genes, we used default values in GOEAST (Zheng & Wang 2008) except no correction was made for multiple testing, and the significance cutoff was set to $\alpha = 0.01$. These parameters were empirically chosen as they produced results that were best reflected by the data. All clone annotations are available via our EST database: http://sequoia.ucmerced.edu/SymBioSys/index.php.

Quantitative real-time PCR (qRT-PCR)

In order to validate and complement microarray gene expression patterns, qRT-PCR was performed for three housekeeping genes (HKGs) and three differentially expressed genes. Additionally, we quantified the expression of eight genes in order to evaluate pathways thought to be involved in the cellular mechanisms of cnidarian bleaching. cDNAs were synthesized from 1 μg of aRNA using SuperScript III reverse transcriptase (Invitrogen). cDNA synthesis reactions were diluted ten-fold to a final volume of 200 μL. qRT-PCR primers (Table S1) were designed using Primer Express 3.0 (Applied Biosystems) based on available *A. palmata* EST sequences, and test-PCRs confirmed specific amplification of the desired amplicons (70-100 bp). Two μL of cDNA were used in triplicate 12.5 μL qPCR reactions with 0.2 μM primers and Power SYBR Green PCR Master Mix (Applied Biosystems) for 40 cycles. Six candidate HKGs were identified using previously described quantitative methods (Rodriguez-Lanetty et al. 2008). The three most stable HKGs were identified using geNORM software (Vandesompele et al. 2002). The pairwise variation of the normalization factor based on the three HKGs was 0.082 (less than the 0.15 cut-off suggested in Vandesompele et al. (2002)). The three HKGs were: (1) AOKF904 – BUD13 homolog ($E=1e^{-46}$) – an mRNA splicing protein; (2) AOKF1782 – Ribokinase ($E=8e^{-88}$) – a protein involved in D-ribose metabolism; and (3) AOKF1657 – a Ca^{2+}-dependent protein kinase ($E=6e^{-6}$). Using calculations outlined in Vandesompele et al. (2002), the qRT-PCR expression values for the assayed genes were normalized to the geometric mean of the three HKGs. Statistical significance in qRT-PCR data was assessed on the normalized expression levels for

each timepoint and treatment using SigmaStat 3.11. If normality and equal variance tests were satisfied, then a one-way ANOVA and Holm-Sidak post-hoc testing was performed. If a normality test failed, then a Kruskal-Wallis one-way ANOVA on ranks was performed with post-hoc testing via Dunn's method.

RESULTS

Visual observations of bleaching and Symbiodinium cell densities

Heat-treated *Acropora palmata* displayed a high, yet variable sensitivity to a 3˚C temperature increase. While one replicate (colony 1) showed no appreciable bleaching after one day of stress, two replicates (colony 2 and colony 4) showed definite slight bleaching, and the final replicate (colony 3) showed extreme bleaching. After two days of thermal stress, colony 1 and colony 2 showed significant partial bleaching, and colony 4 displayed near full bleaching.

Densities of *Symbiodinium* within the experimental coral fragments largely corroborate visual observations. After one day of thermal stress, colony 1 experienced no reduction in *Symbiodinium* density; colony 2 and colony 4, roughly 50% reductions; and colony 3, a 75% reduction. This high variability can be seen in Figure 1 (high standard deviation for the 1day heated replicates). In contrast, the *Symbiodinium* densities of the three heat-stressed replicates displayed low variability after 2 days. Colony 1 experienced a 60% reduction; colony 2, a 50% reduction; and colony 4, a 70% reduction. The results of a one-way ANOVA revealed a significant difference among the treatment groups ($p=0.01$), and post-hoc pairwise testing

revealed significant differences in the following comparisons: t0C vs. 1dH ($p=0.008$); and all controls vs. 2dH ($p<0.05$) (Figure 1).

Symbiodinium 18S rRNA gene RFLP genotyping analyses revealed that all fragments housed *Symbiodinium* clade A (data not shown). This finding is consistent with previous reports documenting the monoassociation of *A. palmata* with clade A (Baker et al. 1997).

Microarray gene expression analysis

Genes that were differentially expressed across the entire experiment represent the overlap between 1day and 2day significant genes (see below). Seventy-four genes were identified (Figure 2), which showed stable expression among the non-heat-treated groups and marked changes upon thermal stress. Of these 74 genes, 43 were down-regulated (56% annotated), and 31 were up-regulated (58% annotated). Fold changes and functional groupings for selected genes presented in Figure 2 are listed in Table 1 (annotations and fold changes for all differentially expressed genes can be found in Table S2).

GOEAST identified 23 statistically over-represented GO terms among the list of 74 significant genes (Table S3). Over-representation of the cellular component *chromatin* (GO:0000785), the biological process *DNA replication* (GO:0006260), and the molecular function *chromatin binding* (GO:0003682) strongly suggest reduced DNA replication and cell division in heat-stressed samples given that all of the differentially expressed genes in these categories were down-regulated (see "Cell cycle regulation" in Table 1 and "CC" superscript in Figure 2). Additionally, the up-

regulation of 11-*cis* retinol dehydrogenase (AOKF1403) and syntenin-1 (CAOH975), and the down-regulation of eyes absent homolog 3 (AOKG2092) led to the over-representation of the biological processes *sensory perception* (GO:0007600) and *neurological system process* (GO:0050877) (see "Sensory perception" in Table 1).

We identified 204 differentially expressed in the 1day heat-stressed samples. Of these 204 genes, 115 were up-regulated, and 89 were down-regulated following thermal stress. 54% of the up-regulated genes were annotated, and 56% of the down-regulated genes were annotated. These 204 genes contain the 74 genes differentially expressed across the entire experiment (above), which leaves 130 genes unique to the 1day samples. Some clear trends emerge from studying the 130 genes expressed after one day of thermal stress. Modification of the actin cytoskeleton, down-regulation of cell cycle transcripts, up-regulation of protein folding transcripts, up-regulation of transport transcripts, and differential expression of many signaling molecules and transcription factors emerge as cellular processes being effected following one day of thermal stress (Table 1). GOEAST over-representation analysis of these 130 genes corroborates some of these findings. For example, the molecular functions *heat shock protein binding* (GO:0031072) and *transcription factor activity* (GO:0003700) were over-represented. In addition, the up-regulation of polyadenylate-binding protein 4 (AOKF1142), selenoprotein S (AOKF908), and transcriptional repressor NF-X1 (AOKG1293) transcripts led to the over-representation of the biological processes *response to external stimulus* (GO:0009605) and *inflammatory response* (GO:0006954) (Table S3).

In the 2day heat-stressed samples, 105 genes were differentially expressed. Of these 105 genes, 44 were up-regulated, and 61 were down-regulated following thermal stress. 56% of the up-regulated genes were annotated, and 61% of the down-regulated genes were annotated. Again, these 105 genes contain the 74 genes significant across the entire experiment, which leaves 31 genes uniquely expressed at 2days. Some notable differentially expressed genes are listed in Table 1. The up-regulation of isocitrate lyase (AOKF1837), 1,4-α-glucan-branching enzyme (AOKF1308), synaptic glycoprotein SC2 (AOKF818), and carnitine O-acetyltransferase (CAOG693) transcripts led to the statistically significant over-representation of the GO biological processes *carbohydrate metabolic process* (GO:0005975), *carboxylic acid metabolic process* (GO:0019752), and *lipid metabolic process* (GO:0006629). Another notable over-represented GO category was the cellular component *ribonucleoprotein complex* (GO:0030529) represented by the down-regulation of three ribosomal protein transcripts and the up-regulation of La-related protein 7 transcripts (Table S3).

We were also interested in genes differentially expressed between 1dH and 2dH. Among the 74 genes significant across the entire experiment (Figure 2), only two genes were significantly different between 1dH and 2dH. NF-κB p105 subunit (Death domain – AOKF1682) decreases in expression from 1dH to 2dH, as does CAOI1144 (non-annotated). Thus, over 90% of the genes differentially expressed at both 1day and 2day did not change expression as bleaching progressed.

Quantitative real-time PCR

For the three genes that we validated via qRT-PCR, their direction of change was consistent with the microarray results. However, their normalized expression estimates were less than (26S proteasome non-ATPase regulatory subunit 5), greater than (11-cis retinol dehydrogenase), or highly similar to (NF-κB) the microarray-estimated fold changes (Table 2). Instead of confirming the significance of more differentially expressed genes, we chose to assay eight genes not present on the microarray in order to evaluate pathways thought to be involved in the cellular mechanisms of cnidarian bleaching. Three of these eight genes were not significantly differentially expressed in the thermally stressed samples (Cu/ZnSOD, E3 ubiquitin-protein ligase Mdm2, and caspase-3). Of the remaining five genes, two were up-regulated upon thermal stress: TNF receptor-associated factor 3 (TRAF3) and NF-κB p105 (Rel homology domain); and three were down-regulated upon thermal stress: nitric oxide synthase-interacting protein (NOSIP), TP53-regulated inhibitor of apoptosis 1 (p53CV), and autophagy-related protein 12.

DISCUSSION

The cellular stress response in Acropora palmata

Many differentially expressed genes identified in the present study are involved in the cellular stress response, which can be defined as the response of the coral to stress-induced damage to cellular macromolecules. In the case of symbiotic corals, multiple stressors can lead to bleaching. For example, thermal stress causes bleaching, but the bleaching process is invariably the result of both thermal stress and oxidative stress (Lesser 1997) given that thermal stress causes reactive oxygen species

(ROS) formation in the host mitochondria (Dykens et al. 1992, Nii & Muscatine 1997), and heat and light stress causes ROS generation in *Symbiodinium* chloroplasts (Lesser 1996, Jones et al. 1998). As the number of endosymbionts dwindles and metabolites cease to be transferred from endosymbiont to host and *vice versa*, osmotic stress is produced (Mayfield & Gates 2007).

Our results provide solid evidence of thermal and oxidative stress, and include possible signatures of osmotic stress. We identified transcripts encoding four heat shock proteins (HSPs) up-regulated in the 1day samples (Table 1). Interestingly, no HSPs were differentially expressed in the 2day samples, which is consistent with the idea that HSP expression ramps up in waves consistent with protein turnover (Gates & Edmunds 1999). With respect to oxidative stress, the up-regulation of transcripts encoding glutaredoxin-3 (AOKG480) and selenoprotein S (AOKF908) represents increased protective mechanisms against ROS. Additionally, oxidative stress-responsive transcription factors were up-regulated during thermal stress: nuclear factor erythroid 2-related factor 3 (Nrf3) homologs (AOKF942 and AOKF1550) (Vargas et al. 2006) and cAMP-dependent transcription factor ATF4 (CAOH936) (Harding et al. 2003). Interestingly, copper/zinc superoxide dismutase (Cu/ZnSOD – CCHX1276), measured via qRT-PCR, was not significantly up-regulated in thermally stressed samples, although the 1day stressed samples had an increase in expression (Table 2). This protein was previously shown to increase in expression during thermal and light stress (Downs et al. 2000, Lesser & Farrell 2004). Low light levels present during our experiments may explain the insignificant Cu/ZnSOD up-regulation. With respect to

osmotic stress, the up-regulation of transcripts involved in ion/macromolecular transport (Table 1) may indicate osmoregulation. In our earlier study on *M. faveolata* (DeSalvo et al. 2008), we observed transcriptomic signatures of heat and oxidative stress but not osmotic stress.

Growth arrest. Discussed in Kultz (2003), the cellular stress response is highly conserved in all organisms, and includes four main mechanisms: (1) growth arrest; (2) up-regulation of chaperones (shown above); (3) nucleic acid stabilization and repair; and (4) removal of damaged macromolecules. We found a marked down-regulation of numerous genes involved in DNA replication and cell cycle progression in the present study (Table 1 and Figure 2). Suppressing cell proliferation during stress conserves energy and ensures that cells with damaged DNA do not divide. This transcriptomic response was found in the fish *Gillichthys mirabilis* exposed to hypoxia (Gracey et al. 2001) and thermal stress (Buckley et al. 2006) and in murine kidney cells in response to hyperosmotic stress (Kultz et al. 1998). The need to conserve energy during cellular stress is also the likely reason behind the observed down-regulation of ribosomal protein transcripts, which is consistent with previous studies in yeast (Herruer et al. 1988), *Drosophila* (Bell et al. 1988), and *M. faveolata* (DeSalvo et al. 2008).

Nucleic acid stabilization and repair. Our results do not show the up-regulation of classic DNA repair proteins; however, Kultz (2003) mentions p53 and NF-κB as eukaryotic pathways involved in DNA repair and chromatin stabilization. The p53 transcription factor was previously found to be up-regulated during heat and light stress in *M. faveolata* (Lesser & Farrell 2004). p53 is not present on our

microarray, nor is it present in our *A. palmata* EST libraries. However, we quantified the expression of two genes within the p53 pathway using qRT-PCR: E3 ubiquitin-protein ligase Mdm2 (CCHX13018.g1) and TP53-regulated inhibitor of apoptosis 1, also known as p53CSV (CCHX1211) (Table 2). Mdm2-p53 binding prevents p53 from acting as a transcription factor and targets p53 for proteolytic degradation (Prives & Hall 1999). Mdm2 was not differentially expressed in *A. palmata.* While Mdm2 down-regulation would have suggested p53 activation, our results suggest that corals may regulate p53 activity via phosphorylation and acetylation, which is consistent with other study systems (Prives & Hall 1999). p53CSV mediates survival in a p53-dependent manner (Park & Nakamura 2005). We found this gene to be 2-fold down-regulated in thermal stressed samples. Interestingly, Park and Nakamura (2005) found that p53CSV was not induced during severe DNA damage. Thus, our results indicate either severe DNA damage, or lack of p53 activation.

The NF-κB family of transcription factors regulates genes that control cell death, cell adhesion, innate immunity, proliferation, inflammation, the cellular stress response, and tissue remodeling (Perkins 2007). One member of this family is the NF-κB p105 precursor, which encodes a protein that contains a Rel homology domain (RHD), an ankyrin repeat domain (ARD), and death domain (DD). The p105 precursor is post-translationally modified to generate the p50 subunit (RHD-containing transcription factor) and I-κB (an inhibitor of the p50 subunit containing the ARD and DD) (Pereira & Oakley 2008). Differences in NF-κB p105 gene architecture are apparent in cnidarians. In *Nematostella vectensis*, all characterized NF-κB genes lack

the I-κB-like sequences; however, loci distinct from NF-κB encode for I-κB-like genes (Sullivan et al. 2007). Our results show the up-regulation of transcripts encoding two proteins that contain homology to NF-κB p105: (1) CAOH485 (2-fold up-regulated at 1day), which contains the ARD; and (2) AOKF1682 (over 5-fold up-regulated on both days), which contains the DD (Table 1). Additionally, we performed qRT-PCR on CCHX9815, another EST with homology to NF-κB p105 (containing the RHD) and found it to be over 5-fold up-regulated in the heat stressed samples (Table 2). Based on our most current EST assembly, CAOH485 (an I-κB-like sequence) and CCHX99815 (an NF-κB-like sequences) contain a poly-A tail, but AOKF1682 does not. While further sequencing is needed to resolve NF-κB p105 gene architecture in *A. palmata*, our results preliminarily indicate that the gene architecture in *A. palmata* is similar to *N. vectensis* in that NF-κB genes may be encoded by loci distinct from I-κB genes. We also quantified the expression of TNF receptor-associated factor 3 (TRAF3 – CCHX4259.b1), a protein involved in the activation of NF-κB, via qRT-PCR. TRAF3 was up-regulated over 20-fold in heat stressed samples (Table 2). Interestingly, the expression levels of the I-κB-like sequences became non-significant (CAOH485) or decreased (AOKF1682) after two days of stress, but the levels of the transcription factor and the activator increased. These results show for the first time the role of NF-κB in signaling mechanisms during coral bleaching and suggest that the balance between NF-κB inhibition and activation may have been tipped towards activation in our experiment.

Removal of damaged macromolecules. Thermal and oxidative damage to cellular proteins leads to increased protein degradation via ubiquitin/proteasome-mediated proteolysis. In the context of coral health, increased protein levels of ubiquitin were found in stressed corals (Downs et al. 2000, Downs et al. 2002, Downs et al. 2005). We clearly see up-regulation of transcripts involved in protein degradation. Ubiquitin (AOKF1154), E3 ubiquitin protein ligase NRDP1 (AOKF1969), and ubiquitin-conjugating enzyme E2A (AOKG649) were 1.5 to 2.9 fold up-regulated at 1day. Furthermore, E3 ubiquitin protein ligase DZIP3 (CAOG662) was up-regulated at both days (Table 1). The up-regulation of ubiquitin and ubiquitin-conjugating enzyme E2A clearly suggests increased targeting of proteins for degradation in the proteasome.

When stress intensity increases to a point at which the organism can no longer maintain homeostasis, cell death pathways are often initiated as part of the stress response (Kultz 2003). Apoptosis, or programmed cell death, has received considerable attention in the coral bleaching field, and indeed, numerous studies have found apoptotic bodies or apoptosis molecular markers in bleached tissue preparations (reviewed in Weis 2008). Two additional bleaching mechanisms have recently been studied in symbiotic cnidarians: autophagy, the process by which a cell degrades its own components, e.g. organelles (Dunn et al. 2007); and symbiophagy, an autophagic process whereby the host consumes its endosymbiont (Downs et al. 2009).

Our previous study (DeSalvo et al. 2008) contained two pro-apoptotic signals; however, the present study contains both pro- and anti-apoptotic signals.

Transcriptional repressor NF-X1 (AOKG1293) and polyadenylate-binding protein 4 (PABP4 – AOKF1142), whose transcripts were both up-regulated at 1day (Table 1), together stimulate telomerase reverse transcriptase, which enhances anti-apoptotic signaling during oxidative stress (Katzenellenbogen et al. 2007). The up-regulation of apoptosis regulator R1 (AOKF1649) is also anti-apoptotic. This gene is a member of the Bcl-2 family, which contains potent inhibitors of cell death (Hockenbery et al. 1990, Shimizu et al. 1996, Clem et al. 1998). We measured the mRNA transcript levels of caspase-3 (CCHX15353.b1) via qRT-PCR and found that the gene was not differentially expressed during thermal stress (Table 2). This likely reflects previous findings that caspase-3, an executioner caspase, requires activation via post-translational modification (Boatright & Salvesen 2003). The only pro-apoptotic signal among the differentially expressed genes was the aforementioned down-regulation of TP53-regulated inhibitor of apoptosis 1 (CCHX1211). This protein mediates survival by inhibiting the activation of caspases (Park & Nakamura 2005), thus down-regulation would seem to be pro-apoptotic. Simultaneous pro- and anti-apoptotic signals likely point to tissue-specific responses to thermal stress.

Autophagy and symbiophagy also represent mechanisms by which the coral can rid itself of damaged macromolecules, organelles, and endosymbionts. We quantified the transcript abundance of Autophagy-related protein 12 (CCHX2749.b1) via qRT-PCR and found it to be nearly 2-fold down-regulated in stressed *A. palmata* (Table 2). Since this protein is required for autophagy (Mizushima et al. 1998), this

result provides evidence against autophagic processes occurring in the present experiment.

Other patterns of differential gene expression

Restructuring of the extracellular matrix. Thermal stress and bleaching in *A. palmata* was marked by a strong differential expression of ECM protein transcripts (Table 1). Collagen α-1(II) chain (AOKF900) was the most differentially expressed gene in the experiment – over 20-fold down-regulated in both 1day and 2day samples. Interestingly, the ortholog of AOKF900 in *M. faveolata* (AOSF1268) was also down-regulated during bleaching (DeSalvo et al. 2008). The down-regulation of collagen either indicates: (1) reduced calcification during stress since this type of collagen is an ECM structural constituent (GO:0005201) involved in chondrocyte differentiation and skeleton formation in vertebrates (Cheah et al. 1991, Li et al. 1995); or (2) modified cell adhesion properties since ECM deposition in coral cells (composed mainly of collagen) was previously shown to mediate cell-cell and cell-substrate adhesion (Helman et al. 2008). Disrupted cell adhesion in *A. palmata* may point to bleaching via cell detachment (Gates et al. 1992). The remaining differentially expressed ECM genes were up-regulated in the stressed samples. Papilin (AOKF939) and carboxypeptidase inhibitor SmC1 (AOKF1161) are both Kunitz-type serine protease inhibitors. The activities of these enzymes warrant further study since the ortholog of AOKF1161 in *M. faveolata* (AOSF907) was responsive to thermal stress (DeSalvo et al. 2008), and a protein with a Kunitz domain was also identified in *Anthopleura elegantissima* exposed to UV stress (Richier et al. 2008). Tolloid-like protein 2

(AOKF1669) – an ECM matrix metalloprotease involved in skeletogenesis (Scott et al. 1999) – also represents a candidate for further study.

Sensory perception. Another group of differentially expressed genes in *A. palmata* are related to *neurological system processes* (GO:0050877) and *visual perception* (GO:0007601). 11-*cis* retinol dehydrogenase (AOKF1403 – 8-fold and 6.4-fold up-regulated at 1day and 2days, respectively) catalyzes the final step in the biosynthesis of 11-cis retinaldehyde, the universal chromophore of visual pigments. Cnidarian visual ecology consists of a large body of literature dedicated to the camera-type eye of the cubozoan *Tripedalia cystophora* (e.g. Kozmik et al. 2008) and eyeless photoreception in *Hydra* (e.g. Santillo et al. 2006). It is worthy to note that our *A. palmata* EST libraries include other vision-related genes such as micropthalmia-associated transcription factor – Mitf (CCHX11178), opsin-1 (CCHX12957.b1), and phosducin-like protein (CCHX14045.b1). Additionally, cryptochrome-1 (AOKF2211 – involved in circadian rhythms) was up-regulated 1.5-fold at 1day. How these sensory perception proteins may be involved in thermal stress responses, bleaching, or be affected by the breakdown in symbiosis is unknown. Given the control aquaria received roughly 10% more light than the heated aquaria, there also exists the possibility that the differential expression of sensory genes was confounded by the different light fields present during the experiment. Another possibility unrelated to vision is that the up-regulation of 11-*cis* retinol dehydrogenase is related to nuclear retinoic acid receptor activation and transcription regulation (Ross 1993).

Metabolite transfer between host and endosymbiont. The transfer of metabolites between the coral host and *Symbiodinium* is at the core of this ecologically successful mutualism. The coral host provides the *Symbiodinium* with glycine, ammonium, nitrate, sulfate, and guanine; the *Symbiodinium* provide the coral host with glycolic acid, glycerol, glucose, alanine, lipids, and CO_2; and both partners shuttle cystine, methionine, and cystathione back and forth (e.g. Muscatine 1967, Patton et al. 1977, Trench 1979, Papina et al. 2003). The down-regulation of the following protein transcripts suggests changes in the dynamics of transfer from host to endosymbiont: (1) multifunctional protein ADE2 (AOKF1956) -- involved in purine synthesis (Chen et al. 1990, Gavalas et al. 1993); (2) methylenetetrahydrofolate reductase (AOKF1692) -- involved in methionine synthesis (Yamada et al. 2005); and (3) a neutral and basic amino acid transporter (AOKF878) -- involved in the transport of cystine.

Conversely, the down-regulation of the following protein transcripts suggests changes in the dynamics of transfer from endosymbiont to host; (1) 1,4-α-glucan-branching enzyme (AOKF1308) -- needed to increase the solubility of glycogen, the stored form of glucose; (2) glyceraldehyde-3-phosphate dehydrogenase (AOKG2283) -- responsible for transforming glycerol into glyceraldehyde-3-phosphate; and (3) vitellogenin-2 (CAOH1099) -- the major precursor of egg-yolk proteins. The ortholog of vitellogenin-2 in *M.faveolata* (AOSF1022) was also down-regulated during bleaching (DeSalvo et al. 2008). While the activities of the first two genes listed above indicate the lack of exchange of glucose and glycerol from endosymbiont to host,

suppressed host metabolism during thermal stress can also explain these observations. Additionally, the activity of vitellogenin-2 may also be due to less vitellogenesis in stressed corals, which is consistent with findings of lower reproduction in bleached corals (Ward et al. 2002). Lastly, the up-regulation of cAMP-dependent transcription factor ATF4 (CAOH936), which is responsive to amino acid starvation (Harding et al. 2003), supports the idea that the coral host loses the amino acid input from their endosymbionts during bleaching.

In addition to identifying genes involved in the transfer of metabolites, our results also indicate the presence of an alternative metabolic pathway in corals – the glyoxylate cycle. Isocitrate lyase converts isocitrate to succinate and glyoxylate during the first step in the glyoxylate cycle. The glyoxylate cycle allows for the use of fats to synthesize carbohydrates (Kornberg & Madsen 1958). The pathway is present in bacteria, yeast, plants, nematodes, and has more recently been discovered in insects and vertebrates (Popov et al. 2005). The near 3-fold up-regulation of isocitrate lyase (AOKF1837) at 2days suggests the host is not receiving sufficient carbohydrates from their endosymbionts. In addition to isocitrate lyase, malate synthase is another glyoxylate cycle-specific enzyme present in our EST libraries (CCHX12543.b1). Malate synthase catalyzes the transformation of glyoxylate and acetyl-coA into malate. Both malate synthase and isocitrate lyase are also present in the aposymbiotic larval transcriptome of *Acropora millepora* (Meyer et al. 2009), and phylogenetic analysis shows that both enzymes were acquired by cnidarians through horizontal gene transfer (Kondrashov et al. 2006).

Nitric oxide signaling. Perez and Weis (2006) provide evidence that nitric oxide (NO) signaling is involved in the bleaching process. They showed that exogenous NO causes bleaching in *Aiptasia pallida,* and that oxidative stress triggers host production of NO. The hypothesized signaling events lead from ROS production to activation of NF-κB which causes up-regulation of inducible nitric oxide synthase (iNOS). NO then acts as a secondary messenger leading to cell death and thereby bleaching. While neither our EST libraries nor our microarray contains iNOS, our results do support this hypothesized pathway given the strong up-regulation of NF-κB at both 1day and 2days of stress. We targeted eNOS interacting protein (NOSIP – CCHX14559.b1) for qRT-PCR analysis to further study NO signaling events during bleaching. NOSIP is a negative modulator of eNOS activity in vertebrates (Dedio et al. 2001); therefore, down-regulation of NOSIP indicates increased NO production. Indeed, our qRT-PCR results show a significant down-regulation of NOSIP transcripts in thermally stressed samples (Table 2). Lastly, the 2.2-fold up-regulation of HSP90 (AOKF986) at 1day is noteworthy in the context of NO signaling since HSP90 is an allosteric enhancer of iNOS (Yoshida & Xia 2003).

Comparison with bleaching in Montastraea faveolata

Our previous microarray study documented the transcriptomic response to thermal stress and bleaching in *Montastraea faveolata* (DeSalvo et al. 2008). Despite less than 30% of the differentially expressed genes having functional annotation, we were able to corroborate past findings and provide new information regarding the cellular mechanisms of cnidarian bleaching. In the present study, differentially

expressed genes were nearly 60% annotated. The gene overlap between the two microarray platforms is small (~10%) (Voolstra et al. 2009). Regardless of low overlap and differences in the level of annotation between both microarrays, there are many parallels between the two studies. We identified the following transcriptomic responses in both studies: (1) an increase in heat shock protein (HSP) expression; (2) an increase in antioxidant enzymes; (3) a decrease in expression of Ca^{2+} homeostasis proteins; (4) a restructuring of the ECM; (5) a rearrangement of the actin cytoskeleton; and (6) a decrease in ribosomal protein expression. In contrast, the following responses identified in the present study were not seen in *M. faveolata*: (1) osmotic stress; (2) p53 and NF-κB signaling; (3) sensory perception; (4) the glyoxylate cycle; and (5) nitric oxide signaling. Overall, the bleaching model presented in (DeSalvo et al. 2008) is supported by the present study, and in addition, we have identified numerous other proteins (e.g. cell signaling molecules and ECM proteins) that await future functional work to assess their specific role in the coral-algal symbiosis.

A remarkable difference between the two studies is related to temporal patterns of bleaching. Given the same increase in temperature, *M. faveolata* experienced a 60% reduction in *Symbiodinium* cell density after 9 days. In the present study, *A. palmata* reached a 60% reduction in *Symbiodinium* cell density after only 2 days. Thus, the intensity of stress felt by *A. palmata* was greater than that of *M. faveolata*. This could be the reason why fold change estimates in *A. palmata* were (on average) higher than those measured in *M. faveolata*. This difference in bleaching susceptibility is consistent with previous studies showing that branching corals, especially acroporids,

are more susceptible to bleaching compared to encrusting/hemispherical corals (Harriott 1985, Glynn 1988, Hoeksema 1991, Gleason 1993, Glynn 1993, Hoegh-Guldberg & Salvat 1995, Marshall & Baird 2000, Loya et al. 2001). Loya et al. (2001) provide a sound discussion of likely differences between branching and encrusting colonies that underlie their differential bleaching susceptibilities. They found that massive and encrusting species have thicker tissue, which renders them less susceptible to bleaching because thicker tissue is more photoprotective and self-shading, especially when polyps are retracted (Brown 1997, Hoegh-Guldberg 1999). Another hypothesis posited by Loya et al. (2001) involves differential mass transfer. These ideas are discussed further in Nakamura and van Woesik (2001) and hold that high water flow allows for more efficient transfer of mass (i.e. metabolites, and ROS), which is especially needed during stress. Indeed, higher coral survival was evident in high compared to low flow regimes (Nakamura et al. 2003). These notions ultimately apply to colony morphology – flat, encrusting coral colonies experience higher flow than branching colonies.

While bleaching susceptibility due to colony morphology is likely involved in the observed differential response between *M. faveolata* and *A. palmata*, we also cannot ignore the influence of *Symbiodinium* genotype (Rowan et al. 1997, Baker et al. 2004, LaJeunesse et al. 2007, Sampayo et al. 2008). Given that we observed no differences in bleaching susceptibility between clade A-associated and multi-clade-associated *M. faveolata* in (DeSalvo et al. 2008), and that subclade genotyping to differentiate between clade A within *M. faveolata* and clade A within *A. palmata* is

not available, we cannot state whether a *Symbiodinium* clade effect influenced the differential response between *M. faveolata* and *A. palmata*. Differences in *Symbiodinium* clades might also contribute to the greater fold changes measured in *A. palmata*. Given that the *Symbiodinium*-effect on the host transcriptome can be greater than thermal stress (DeSalvo, Sunagawa et al., in review), controlling for the *Symbiodinium* clade content within experimental fragments is likely to increase the resolution at which gene expression can be measured.

Conclusions and future outlook

Despite little overlap between the *A. palmata* and *M. faveolata* microarrays, we found similar processes differentially expressed in response to thermal stress and bleaching in both species. Much of this conserved transcriptomic stress response is part of the cellular stress response already present in the last universal common ancestor (i.e. predating the evolution of the three domains of life) (Kultz 2003, 2005).

Focusing on the cellular stress response and how it has allowed corals to persist through geologic time is incomplete without taking into consideration the contribution of their endosymbionts in the evolutionary success of the Scleractinia. For example, the adaptive radiation of scleractinians in the Late Triassic (200-228 Ma) may be correlated with the initiation of symbiosis with dinoflagellate endosymbionts (Stanley 1981). Thus, it is also important to identify scleractinian- and symbiosis-specific cellular responses to thermal stress. For example, while down-regulation of cytoskeletal components (also seen in *M. faveolata*) is certainly related to the conserved cellular stress response (Loven 1988, Shyy et al. 1989, Chowdhury et al.

1992, Orrenius et al. 1992, Muller et al. 2007), we cannot ignore the possibility that the cytoskeleton must reorganize as cells change their adhesion properties and/or become devoid of their intracellular endosymbionts. A rearrangement of the ECM (also seen in *M. faveolata*), along with the metabolite transfer systems, which involve molecules specific to different symbioses (Trench 1979), are more likely to be bleaching-responsive processes specific to zooxanthellate corals.

Identifying responses specific to symbiosis breakdown represents a daunting task. Future transcriptomic studies using stressors other than thermal stress (i.e. cold shock, darkness, high light, etc…) in corals and other symbiotic cnidarians will allow us to identify cellular processes common between different stressors. Utilizing the amenable symbiotic cnidarian *Aiptasia pallida* (Weis et al. 2008, Sunagawa et al. 2009c), one could measure the transcriptomic response to a given stressor in both symbiotic and aposymbiotic anemones and thus use a subtractive approach to determining symbiosis-specific stress responses. These experimental approaches will ultimately lead to a more complete understanding of the molecular mechanisms of coral symbiosis and bleaching.

Finally, our study demonstrates how genomic tools are helping to reconstruct the ancestral coral and how it was equipped to cope with stress over geologic time. For example, early scleractinian corals survived many paleoclimatic changes, such as sea-level rise and climatic warming in the Late Triassic, the Paleocene-Eocene thermal maximum, and repeated sea level and climatic changes during the Neogene (Stanley & van de Schootbrugge 2009). The resilience of coral community structure during global

climate fluctuations of the Pleistocene (Pandolfi & Jackson 2006) also suggests that corals are equipped to survive drastic environmental transitions. While the resiliency of corals over geologic time suggests that they may indeed be able to cope with thermal stress related to contemporary climate change, it is becoming abundantly clear that numerous other human impacts are acting synergistically with climate change to shift coral community structure (Hughes et al. 2003, Pandolfi et al. 2003, Pandolfi & Jackson 2006).

ACKNOWLEDGEMENTS

This chapter was published in *Marine Ecology Progress Series* (2010) volume 402, pages 97-113. I would like to thank my co-authors for their aid in all aspects of completing and publishing this work: Shini Sunagawa, Chris Voolstra, and Monica Medina. We would like to thank the following people associated with STRI in Panamá: R. Collin, G. Jácome, P. Gondola and other staff at the Bocas del Toro station, and E. Gomez and J. Jara of N. Knowlton's lab at the Naos Laboratory. We would also like to thank M. A. Coffroth for initial input with tank experiments, and three anonymous reviewers whose comments greatly improved the manuscript. M. DeSalvo prepared this manuscript in partial fulfillment of requirements for a Ph.D. in Quantitative and Systems Biology from the University of California, Merced. This study was supported through a STRI Pre-doctoral Fellowship and an NSF award to M. D. (OISE 0837455), and NSF awards to M. M. (BE-GEN 0313708 and IOS 0644438). This is contribution #2 of the STRI Caribbean Reef Futures initiative.

SUPPLEMENTARY INFORMATION

Supplementary information can be downloaded at the following website:

http://www.int-res.com/articles/suppl/m402p097_app.xls

Table S1. Primers used for qRT-PCR analyses.

Table S2. Complete list of differentially expressed genes.

Table S3. Complete list of over-represented GO categories identified using GOEAST.

FIGURES

Figure 1. Symbiodinium cell count data illustrating bleaching over 2 days in *Acropora palmata*. The mean cell densities of four replicate fragments are shown with standard deviations. Asterisks above bars denote statistically significant differences. According to a one-way ANOVA with post-hoc pairwise testing via the Fisher LSD Method, the 1 day heated samples (*) were significantly different than the time zero control samples only ($P<0.01$). The 2 day heated samples (**) were significantly different than all non-heated samples ($P<0.05$).

Figure 1.

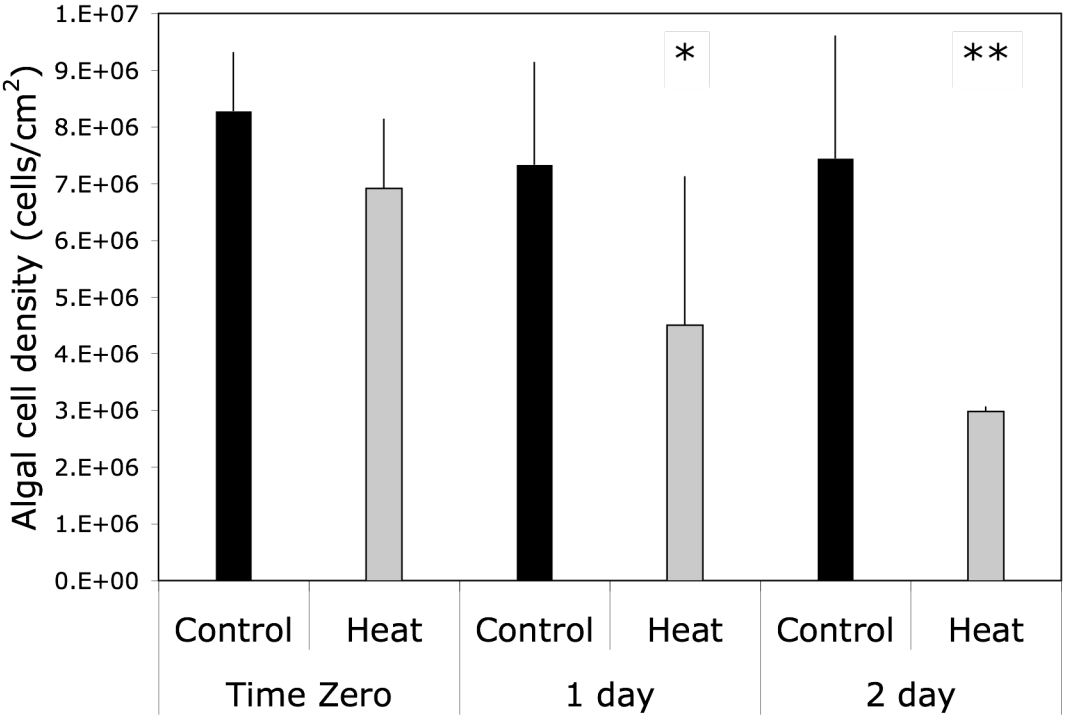
1.E+07
9.E+06
8.E+06
7.E+06
6.E+06
5.E+06
4.E+06
3.E+06
2.E+06
1.E+06
0.E+00
Algal cell density (cells/cm2)
*
**
Control
Heat
Control
Heat
Control
Heat
Time Zero
1 day
2 day

Figure 2. Heat map of genes differentially expressed at both 1day and 2days post-heat stress. For each gene, BAGEL assigns the value of 1 to the class with the lowest expression, and calculates the expression of the other classes relative to 1. Thus, down-regulated genes are > 1 in the controls and approach 1 in the heat stressed samples. Conversely, in up-regulated genes, the controls approach 1 and the heat stressed samples are > 1. Superscripts in the functional annotation column denote categories used in Table 1: CC = cell cycle regulation; SIG = cell signaling/transcription factor activity; ECM = extracellular matrix proteins; SP = sensory perception; PD = protein degradation; AC = actin cytoskeleton; and MT = metabolite transfer.

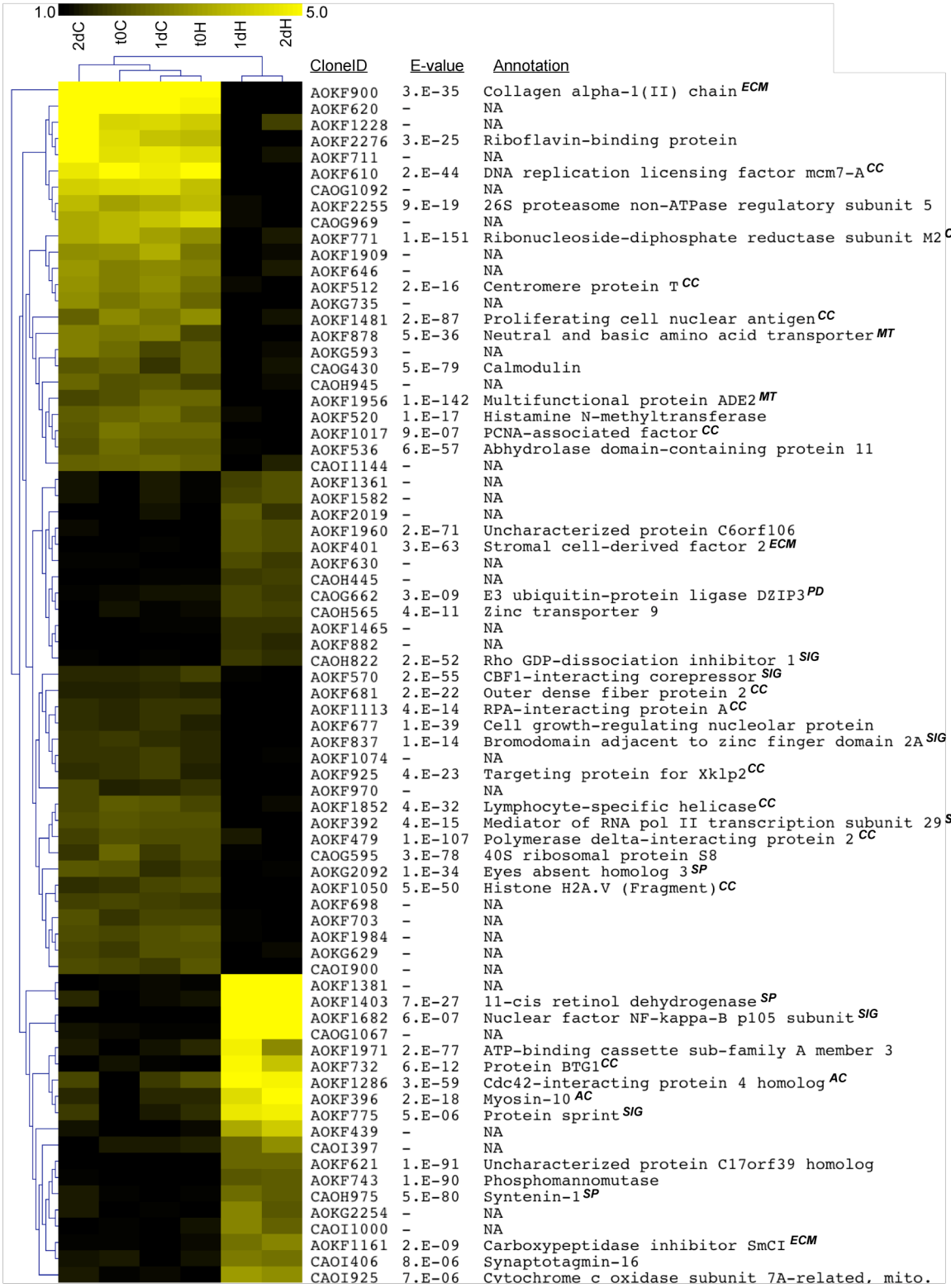

CloneID	E-value	Annotation
AOKF900	3.E-35	Collagen alpha-1(II) chain ECM
AOKF620	-	NA
AOKF1228	-	NA
AOKF2276	3.E-25	Riboflavin-binding protein
AOKF711	-	NA
AOKF610	2.E-44	DNA replication licensing factor mcm7-A CC
CAOG1092	-	NA
AOKF2255	9.E-19	26S proteasome non-ATPase regulatory subunit 5
CAOG969	-	NA
AOKF771	1.E-151	Ribonucleoside-diphosphate reductase subunit M2 CC
AOKF1909	-	NA
AOKF646	-	NA
AOKF512	2.E-16	Centromere protein T CC
AOKG735	-	NA
AOKF1481	2.E-87	Proliferating cell nuclear antigen CC
AOKF878	5.E-36	Neutral and basic amino acid transporter MT
AOKG593	-	NA
CAOG430	5.E-79	Calmodulin
CAOH945	-	NA
AOKF1956	1.E-142	Multifunctional protein ADE2 MT
AOKF520	1.E-17	Histamine N-methyltransferase
AOKF1017	9.E-07	PCNA-associated factor CC
AOKF536	6.E-57	Abhydrolase domain-containing protein 11
CAOI1144	-	NA
AOKF1361	-	NA
AOKF1582	-	NA
AOKF2019	-	NA
AOKF1960	2.E-71	Uncharacterized protein C6orf106
AOKF401	3.E-63	Stromal cell-derived factor 2 ECM
AOKF630	-	NA
CAOH445	-	NA
CAOG662	3.E-09	E3 ubiquitin-protein ligase DZIP3 PD
CAOH565	4.E-11	Zinc transporter 9
AOKF1465	-	NA
AOKF882	-	NA
CAOH822	2.E-52	Rho GDP-dissociation inhibitor 1 SIG
AOKF570	2.E-55	CBF1-interacting corepressor SIG
AOKF681	2.E-22	Outer dense fiber protein 2 CC
AOKF1113	4.E-14	RPA-interacting protein A CC
AOKF677	1.E-39	Cell growth-regulating nucleolar protein
AOKF837	1.E-14	Bromodomain adjacent to zinc finger domain 2A SIG
AOKF1074	-	NA
AOKF925	4.E-23	Targeting protein for Xklp2 CC
AOKF970	-	NA
AOKF1852	4.E-32	Lymphocyte-specific helicase CC
AOKF392	4.E-15	Mediator of RNA pol II transcription subunit 29 SIG
AOKF479	1.E-107	Polymerase delta-interacting protein 2 CC
CAOG595	3.E-78	40S ribosomal protein S8
AOKG2092	1.E-34	Eyes absent homolog 3 SP
AOKF1050	5.E-50	Histone H2A.V (Fragment) CC
AOKF698	-	NA
AOKF703	-	NA
AOKF1984	-	NA
AOKG629	-	NA
CAOI900	-	NA
AOKF1381	-	NA
AOKF1403	7.E-27	11-cis retinol dehydrogenase SP
AOKF1682	6.E-07	Nuclear factor NF-kappa-B p105 subunit SIG
CAOG1067	-	NA
AOKF1971	2.E-77	ATP-binding cassette sub-family A member 3
AOKF732	6.E-12	Protein BTG1 CC
AOKF1286	3.E-59	Cdc42-interacting protein 4 homolog AC
AOKF396	2.E-18	Myosin-10 AC
AOKF775	5.E-06	Protein sprint SIG
AOKF439	-	NA
CAOI397	-	NA
AOKF621	1.E-91	Uncharacterized protein C17orf39 homolog
AOKF743	1.E-90	Phosphomannomutase
CAOH975	5.E-80	Syntenin-1 SP
AOKG2254	-	NA
CAOI1000	-	NA
AOKF1161	2.E-09	Carboxypeptidase inhibitor SmCI ECM
CAOI406	8.E-06	Synaptotagmin-16
CAOI925	7.E-06	Cytochrome c oxidase subunit 7A-related, mito.

TABLES

Table 1. Significantly differentially expressed genes identified in a cDNA microarray experiment comparing gene expression between control and heat-stressed fragments from four colonies of *Acropora palmata*. Common names and E-values are for the top BLAST hit to the SwissProt database. Fold changes in 1day and 2day heat-stressed fragments (1dH and 2dH) are relative to the average of the four control groups (t0C, t0H, 1dC, and 2dC).

Table 1.

CloneID	Common Name	E-val	Fold Changes 1dH	2dH
Cell cycle regulation				
AOKG1979	Cell division cycle protein 20 homolog	1E-129	-1.53	-
AOKF610	DNA replication licensing factor mcm7-A	2E-44	-4.66	-5.03
CAOH556	G1/S-specific cyclin-D2	7E-80	-2.53	-
AOKF732	Protein BTG1	6E-12	4.49	3.56
AOKF1223	Protein regulator of cytokinesis 1	1E-35	-1.84	-
AOKF1767	Ribonucleoside-diphosphate reductase large subunit	1E-107	-2.20	-
AOKF771	Ribonucleoside-diphosphate reductase subunit M2	1E-151	-3.40	-2.44
Cell signaling / Transcription factor activity				
CAOH623	cAMP-responsive element-binding protein-like 2	2E-18	2.32	-
AOKF917	Cyclic AMP-dependent transcription factor ATF-2	8E-31	2.70	-
CAOH936	Cyclic AMP-dependent transcription factor ATF-4	1E-13	2.42	-
CAOH485	NF-κB p105 subunit (Ankyrin repeat domain)	2E-37	2.01	-
AOKF1682	NF-κB p105 subunit (Death domain)	6E-07	7.12	5.57
AOKF1550	Nuclear factor erythroid 2-related factor 3	5E-08	2.99	-
AOKF942	Nuclear factor erythroid 2-related factor 3	5E-08	2.77	-
AOKF775	Protein sprint	5E-06	3.28	3.42
AOKF1938	Receptor-type tyrosine-protein phosphatase alpha	6E-45	1.83	-
AOKF494	Serine/threonine-protein kinase 6	1E-109	-	-1.96
AOKF654	Transcription initiation factor TFIID subunit 13	5E-21	-	-1.71
AOKG1293	Transcriptional repressor NF-X1	8E-36	1.59	-
CAOI879	Transmembrane emp24 domain-containing protein 1	2E-25	-	1.58
Extracellular matrix proteins				
AOKF1161	Carboxypeptidase inhibitor SmCI	2E-09	2.26	2.56
AOKF900	Collagen alpha-1(II) chain	3E-35	-20.69	-22.16
AOKF939	Papilin	2E-12	-	1.89
AOKF401	Stromal cell-derived factor 2	3E-63	2.08	1.90
AOKF1669	Tolloid-like protein 2	2E-30	1.49	-
Sensory perception				
AOKF1403	11-*cis* retinol dehydrogenase	7E-27	7.99	6.39
AOKF2211	Cryptochrome-1	9E-74	1.54	-
AOKG2092	Eyes absent homolog 3	1E-34	-1.91	-1.73
CAOH975	Syntenin-1	5E-80	2.14	1.96
Protein degradation				
CAOG662	E3 ubiquitin-protein ligase DZIP3	3E-09	1.54	1.41
AOKF1969	E3 ubiquitin-protein ligase NRDP1	6E-52	2.40	-
AOKF1154	Ubiquitin	4E-35	1.49	-
AOKG649	Ubiquitin-conjugating enzyme E2 A	1E-78	2.85	-
Actin cytoskeleton				
CAOH739	Actin, cytoplasmic	0E+00	-2.28	-
CAOG410	Gelsolin	1E-47	-1.82	-
AOKF396	Myosin-10	2E-18	3.18	3.63
CAOH671	Myosin-2 essential light chain	4E-25	-1.80	-

CloneID	Common Name	E-val	Fold Changes 1dH	2dH
AOKF554	Tropomyosin	8E-14	-	-2.13
AOKF1962	Tropomyosin-2	2E-21	-1.53	-
Heat shock proteins				
CAOH1088	DnaJ homolog subfamily A member 2	1E-10	1.83	-
AOKF1222	DnaJ homolog subfamily B member 11	1E-112	2.11	-
AOKG405	Heat shock cognate 71 kDa protein	2E-38	1.56	-
AOKF986	Heat shock protein HSP 90-alpha	0E+00	2.20	-
Metabolite transfer				
AOKF1308	1,4-α-glucan-branching enzyme	6E-30	-	-2.08
CAOG693	Carnitine O-acetyltransferase	5E-61	-	1.86
AOKG2283	Glyceraldehyde-3-phosphate dehydrogenase	5E-163	-2.17	-
AOKF1837	Isocitrate lyase	1E-151	-	2.85
AOKF1692	Methylenetetrahydrofolate reductase	1E-22	-1.86	-
AOKF1956	Multifunctional protein ADE2	1E-142	-2.21	-2.14
AOKF878	Neutral and basic amino acid transporter	5E-36	-2.53	-2.51
AOKF818	Synaptic glycoprotein SC2	2E-88	-	-2.23
CAOH1099	Vitellogenin-2	4E-22	-5.74	-
Ribosomal proteins				
CAOH815	40S ribosomal protein S15a	6E-60	-	-1.76
CAOG595	40S ribosomal protein S8	3E-78	-1.70	-1.95
CAOH441	60S acidic ribosomal protein P1	2E-17	-	-1.82
CAOG952	60S ribosomal protein L11	5E-82	-	-1.47
Ca2+ homeostasis proteins				
AOKF800	Calcyphosin-like protein	5E-52	-	-2.04
CAOG430	Calmodulin	5E-79	-2.12	-1.60
CAOI402	Sarcoplasmic reticulum histidine-rich Ca-binding protein	7E-15	-1.85	-
AOKF1965	Troponin C, skeletal muscle	1E-11	-1.84	
Oxidative stress				
AOKG480	Glutaredoxin-3	1E-110	1.94	-
AOKF1142	Polyadenylate-binding protein 4	2E-55	1.51	-
AOKF908	Selenoprotein S	2E-20	1.80	-
Vesicle/ion/macromolecule transport				
AOKF1016	ADP-ribosylation factor GTPase-activating protein 3	2E-27	1.74	-
AOKF1971	ATP-binding cassette sub-family A member 3	2E-77	3.74	2.26
AOKF1543	BTB/POZ domain-containing protein KCTD7	3E-18	-	-1.58
CAOH817	Pituitary tumor-transforming gene 1 interacting protein	2E-20	2.41	-
CAOH1006	Protein RER1	4E-54	2.15	-
AOKF821	Vacuolar proton pump subunit E	7E-66	1.64	-
Miscellaneous				
AOKF1649	Apoptosis regulator R1 (Fragment)	1E-20	1.65	-
AOKG615	Atrial natriuretic receptor A	7E-47	1.68	-
AOKF638	Cytochrome b-245 light chain	2E-36	1.70	-
AOKG407	Endothelin-converting enzyme 1	1E-16	2.19	-
AOKF2276	Riboflavin-binding protein	3E-25	-4.68	-4.30

Table 2. Results of qRT-PCR analyses on control and heat-stressed fragments from four colonies of *Acropora palmata*. We validated the microarray-based results for the first three genes listed, and chose an additional eight genes not present on the microarray to further implicate certain cellular processes involved in the thermal stress response and bleaching. Common names and E-values are for the top BLAST hit to the SwissProt database. Similar to the microarray data output from BAGEL, we set the lowest expression class to 1 and calculated the expression of the other classes relative to 1. qRT-PCR-estimated expression for the controls is represented by the mean of the four control groups (t0C, t0H, 1dC, and 2dC). Asterisks (*) represent statistically significant differences in the heat stressed samples (1dH and 2H) according to a one-way ANOVA and post-hoc testing ($p<0.05$).

Table 2.

Clone ID	Common name	E-val	qRT-PCR Controls Mean (± SD)	Heat-stressed 1dH	Heat-stressed 2dH	Microarray Fold Change 1dH	Microarray Fold Change 2dH
AOKF1403	11-cis retinol dehydrogenase	7E-27	2.10 ± 1.67	56.38*	186.76*	7.99	6.39
AOKF1682	NF-κB p105 (Death domain)	6E-07	1.21 ± 0.26	7.91*	5.45*	7.12	5.57
AOKF2255	26S proteasome non-ATPase reg. subunit 5	9E-19	1.77 ± 0.08	1.06*	1*	-3.08	-3.62
CCHX1276	CuZn superoxide dismutase (Cu/ZnSOD)	2E-56	1.17 ± 0.12	1.50	1	-	-
CCHX14559.b1	NOS-interacting protein (NOSIP)	3E-60	1.56 ± 0.15	1.12*	1*	-	-
CCHX13018.g1	E3 ubiquitin-protein ligase Mdm2	3E-13	1.30 ± 0.25	1.01	1.09	-	-
CCHX1211	TP53-regulated inhibitor of apoptosis 1	5E-16	2.35 ± 0.33	1.21*	1*	-	-
CCHX2749.b1	Autophagy-related protein 12	6E-24	2.19 ± 0.43	1.16*	1*	-	-
CCHX15353.b1	Caspase-3	4E-36	1.06 ± 0.06	1.06	1.03	-	-
CCHX4259.b1	TNF receptor-assoc. factor 3 (TRAF3)	6E-53	1.27 ± 0.22	27.04*	29.24*	-	-
CCHX9815	NF-κB p105 (Rel homology domain)	1E-38	1.96 ± 0.77	12.97*	13.29*	-	-

CHAPTER 3

CORAL HOST TRANSCRIPTOMIC STATES ARE CORRELATED WITH *SYMBIODINIUM* GENOTYPES

ABSTRACT

A mutualistic relationship between reef-building corals and endosymbiotic dinoflagellates (*Symbiodinium* spp.) forms the basis for the existence of coral reefs. Genotyping tools for *Symbiodinium* spp. have added a new level of complexity to studies concerning cnidarian growth, nutrient acquisition, and stress. For example, the response of the coral holobiont to thermal stress is connected to the host-*Symbiodinium* genotypic combination, as different partnerships can have different bleaching susceptibilities. In this study, we monitored *Symbiodinium* physiological parameters and profiled the coral host transcriptional responses in acclimated, thermally stressed, and recovered fragments of the coral *Montastraea faveolata* using a custom cDNA gene expression microarray. Interestingly, gene expression was more similar among samples with the same *Symbiodinium* content rather than the same experimental condition. In order to discount for host-genotypic effects, we sampled fragments from a single colony of *M. faveolata* containing different symbiont types, and found that the host transcriptomic states grouped according to *Symbiodinium* genotype rather than thermal stress. As the first study that links coral host transcriptomic patterns to the clade content of their *Symbiodinium* community, our results provide a critical step to elucidating the molecular basis of the apparent variability seen among different coral-*Symbiodinium* partnerships.

INTRODUCTION

Reef-building corals are critically important to the functioning of tropical coral reefs, the most biologically diverse and complex marine ecosystems. A mutualistic partnership between coral hosts and photosynthetic dinoflagellates in the diverse genus *Symbiodinium* is a well-documented driving force of the trophic and structural integrity of coral reef ecosystems. By trapping solar energy and nutrients, *Symbiodinium* provide up to 95% of the energy requirements of the coral hosts, which precipitate calcium carbonate skeletons at high rates (Muscatine 1990).

In recent decades, coral mortality and extinction risk have increased dramatically, predominantly owing to mass "bleaching" events that have become more intense and more frequent (Hughes et al. 2003, Carpenter et al. 2008). The term "bleaching" describes the paling of the coral tissue due to a disruption of the symbiosis between coral hosts and their obligate dinoflagellate endosymbionts resulting in a loss of endosymbiont cells and/or their photosynthetic pigments. Although bleaching can be triggered by a number of factors, high temperature and light stress are commonly considered as the ecologically most significant (Hoegh-Guldberg 1999). Under short or mild thermal stress conditions, corals may recover; although, adverse effects such as reduced growth and fecundity, as well as higher disease susceptibility, have been observed in subsequent periods (Bruno et al. 2007, Harvell et al. 2007, Sunagawa et al. 2009b).

Our knowledge of the complexity underlying coral-dinoflagellate symbioses has increased with the advent of molecular genotyping tools for *Symbiodinium* spp.

(Baker 2003, Coffroth & Santos 2005, Pochon et al. 2006, Stat et al. 2006). Clade genotyping via restriction fragment length polymorphism (RFLP) of the 18S rRNA gene (Rowan & Powers 1991), and subclade genotyping via differential gradient gel electrophoresis (DGGE) of the internal transcribed spacer 2 (ITS2) region are now in common practice (LaJeunesse & Trench 2000). Many coral species house only one clade (Goulet 2006), some species house many different clades (Rowan & Knowlton 1995, Toller et al. 2001b, Mieog et al. 2007, Frade et al. 2008), and some species can shuffle their *Symbiodinium* clade content following bleaching events (Toller et al. 2001a, Berkelmans & van Oppen 2006, Rodriguez-Roman et al. 2006, Thornhill et al. 2006, Jones et al. 2008). The composition of coral-*Symbiodinium* partnerships has been shown to affect a number of important properties, including (1) adaptation to different environmental optima (Rowan & Knowlton 1995, Iglesias-Prieto et al. 2004), (2) differences in growth rates (Little et al. 2004, Mieog et al. 2009), (3) photosynthate transfer and carbon fixation efficiencies (Loram et al. 2007, Stat et al. 2008, Cantin et al. 2009), and (4) susceptibility to thermal stress (Rowan et al. 1997, Baker et al. 2004, Middlebrook et al. 2008, Sampayo et al. 2008, Mieog et al. 2009).

Given the evidence that different symbiont genotypes can affect these processes, correlations between the *Symbiodinium* clade content and coral gene expression have the potential to inform us on the molecular basis of differences in coral-*Symbiodinium* partnerships. Gene expression microarrays have been widely used to investigate changes in the expression of all or a subset of transcribed genes (i.e. the transcriptome) under varying conditions. Gene expression differences in cnidarian

holobionts have thus far been studied in symbiotic versus aposymbiotic anemones (Rodriguez-Lanetty et al. 2006), under thermal and UV stress (DeSalvo et al. 2008, Richier et al. 2008), during acclimatization of different source populations to different environmental conditions (Bay et al. 2009), during the onset of symbiosis (Voolstra et al. 2009), and across distinct developmental stages (Grasso et al. 2008, Reyes-Bermudez et al. 2009).

In this study, we measured *Symbiodinium* physiological parameters and profiled host gene expression in acclimated, thermally stressed, and recovered fragments from different colonies of *Montastraea faveolata* – a coral known to associate with multiple clades of *Symbiodinium* (Rowan & Knowlton 1995, Toller et al. 2001a, Iglesias-Prieto et al. 2004, Thornhill et al. 2006). In a parallel experiment, fragments harboring different *Symbiodinium* clades were sampled from a single host colony in order to control for the host genotypic background. Based on photochemical efficiency and host gene expression measurements in fragments containing different *Symbiodinium* clades, we demonstrate that the coral host transcriptional state, as well as the magnitude of the thermal stress response, is correlated with the symbiont genotype.

MATERIALS AND METHODS

Sample Collection and Tank Experiment

On 31 July 2007, six replicate fragments were collected using a hammer and chisel from the top sun-exposed surface of five different, healthy-looking *Montastraea faveolata* colonies near Puerto Morelos, Quintana Roo, México ($20^{o}52'28.77"$N and

86°51'04.53"W). These 30 fragments were used in a time-series experiment of control, thermal stress, and recovery (referred to as the "time-series experiment"). In addition, six replicate fragments were sampled from the top (2.7m), middle (3.7m), and bottom (5.2m) of a single colony of *M. faveolata*. These 18 fragments were used in a single time point experiment of control vs. thermally stressed (referred to as the "single host genotype experiment"). All fragments were transported to the UNAM - Instituto de Ciencias del Mar y Limnología field station within 1 h and divided evenly between two 50 L aquaria (i.e., 3 fragments from each colony and 3 fragments from top, middle, and bottom parts of one single colony were placed into each tank) that received a constant flow of seawater (0.6 L min^{-1}) from the same source.

Acclimation of collected coral fragments

Control and experimental aquaria were placed in a large common fiberglass tank with constantly flowing water to equilibrate the temperature of incoming seawater and to buffer temperature fluctuations. Both aquaria were exposed to the same shaded ambient light condition in order to control for the light-related factors that determine the ecological zonation of *Symbiodinium* spp. within *M. faveolata*. Each aquarium was fit with a water pump connected to a spray-bar to provide constant water movement and aeration. All coral fragments were mounted on plasticene and kept at a depth of 7 cm. From 10 to 19 August 2007, both aquaria received an average water temperature of 27.9 ± 0.6°C (as recorded by HOBO Light/Temperature Data Loggers, Onset Corp.). Beginning on 11 August, dark-adapted maximum quantum yields for charge separation (*Fv/Fm*) were measured at dusk for all coral fragments

using a DIVING-Pulse Amplitude Modulated (PAM) fluorometer (Walz, Germany). Photosynthetically active radiation (PAR) was measured at noon and averaged 318 ± 129 μmol m^{-2} s^{-1}. From 20 to 21 August 2007, all coral fragments were brought inside during the passage of Hurricane Dean. On 22 August, the experiment was reconstituted.

During acclimation of the coral fragments, top fragments in the single host genotype experiment did not show any significant variation in *Fv/Fm* (0.575 ± 0.030) relative to the values observed in the field (0.550 ± 0.028). Likewise, none of the 30 fragments in the time-series experiment displayed a significant decrease in *Fv/Fm* throughout the acclimation period. In contrast, middle fragments in the single host genotype experiment experienced a significant reduction in *Fv/Fm* upon transfer to the experimental tanks from 0.582 ± 0.023 in the field to 0.481 ± 0.054 after 48 hours in the tanks. Similarly, bottom fragments experienced a dramatic reduction of *Fv/Fm* after transfer to the experimental tanks from 0.610 ± 0.030 in the field to 0.348 ± 0.042 after 48 hrs of exposure to the experimental tank conditions. However, at the end of the control period (see below), all coral fragments were completely acclimated to the experimental tank conditions (Figure S1).

The control period of the experiments started on 23 August (day 1) and lasted until 1 September (day 10). During this time, both aquaria received a mean water temperature of 28.5 ± 0.8^{o}C, and mean PAR of 371 ± 169 μmol m^{-2} s^{-1}. On the night of day 1, control time point samples from five different colonies were collected from each tank. Afterward, one 200-Watt aquarium heater was turned on in the treatment

aquarium (rate: 0.35^{o}C h^{-1}). A second heater was turned on 3 days later. During the thermal stress period, the control aquarium received mean water temperature of 28.8 ± 1.2^{o}C, the heated aquarium 31.5 ± 1.1^{o}C, and both tanks received mean PAR of 420 ± 152 µmol m^{-2} s^{-1}. On the night of day 16, all fragments in the single host genotype experiment were flash-frozen in liquid nitrogen. On day 20, and day 58, one sample each from the five colonies used in the time-series experiment was collected from both tanks for the thermal stress and recovery time point, respectively. All samples were exported to the USA through a CITES permit (MX-HR-007-MEX). See SI Text for methods related to statistical analysis of *Fv/Fm* data.

Symbiodinium and Coral Host Genotyping

Genomic DNA was isolated from approximately 100-200 mg of frozen coral powder using the PowerPlant DNA Isolation kit (MoBio). The *Symbiodinium* 18S ribosomal RNA gene was amplified using the primers ss5 and ss3Z (Rowan & Powers 1991) and digested with TaqI restriction enzyme. The resulting fragments were compared to *Symbiodinium* clade standards (Rowan & Knowlton 1995). The internal transcribed spacer region 2 (ITS2) was PCR amplified using cycling conditions and primers ITSintfor2 and ITS2CLAMP (without the clamp sequence) reported in (LaJeunesse & Trench 2000). ITS2 amplicons were cloned, sequenced, and assigned to *Symbiodinium* clades based on both BLASTn results and phylogenetic reconstruction using reference sequences (see SI Text for details). All ITS2 sequences were deposited in GenBank with the accession numbers FJ223886-FJ224080 and

FJ811907-FJ811960. Coral hosts were genotyped (see SI Text for details) using five microsatellite loci (Severance et al. 2004).

Microarray Gene Expression Analysis of Coral Host Gene Expression

Total RNA from all samples was isolated and checked for quality as previously described (DeSalvo et al. 2008). Contamination of total RNA with *Symbiodinium* RNA is expected to be low as determined by microscopic analysis of re-suspended coral powder, which revealed *Symbiodinium* cells to be intact. For the time-series experiment, a pool of amplified RNA from all control tank fragments was used as a reference RNA sample, against which each of the 15 amplified RNA samples from the treatment tank (5 control, 5 stressed, 5 recovered) was competitively hybridized. For the single genotype experiment, the reference sample constituted a pool of total RNA from all 18 samples. Fifteen micrograms of total RNA from control (3 replicates per region) and heat-stressed (3 replicates per region) samples were competitively hybridized against an equal amount of reference RNA resulting in a total of 18 hybridizations. Dye swaps were not performed, as any dye bias present is equal in all comparisons to the reference.

Samples were hybridized to *M. faveolata* microarrays containing 2,620 features (1,310 genes spotted in duplicate) that were annotated based on BLASTx hits (E-value cutoff: 1e-5) to the UniProt Knowledgebase database SwissProt (The_UniProt_Consortium 2008) and its GO-term associations (UniProt GOA, March 2008). All sequences/clone IDs are searchable at: http://sequoia.ucmerced.edu/SymBioSys/index.php. Based on hybridization of

Symbiodinium RNA directly to the *M. faveolata* microarray, we determined the potential for cross-hybridization with *Symbiodinium* transcripts to be below 8% (data not shown). All microarrays were scanned using an Axon 4000B scanner (Molecular Devices) where care was taken to manually balance photomultiplier tube (PMT) settings. TIFF images were generated with GenePix Pro 6.0, and gridding was performed using TIGR Spotfinder 3.1.1 (Saeed et al. 2003) with the *Otsu* segmentation method. The top 25% of background pixels were discarded prior to the estimation of the median local background intensity, which was subsequently subtracted from the median foreground intensity. Using TIGR MIDAS 2.19 (Saeed et al. 2003), background-corrected data were LOWESS normalized, and in-slide duplicates were averaged. Both PMT balancing and LOWESS normalization equalize for differing amounts of host RNA input (a potential issue when processing tissue where symbiont densities can vary). Genes were included in statistical analyses only if at least 60% of representative spots were called positive in each condition tested. This corresponds to three out of five (time course experiment), or two out of three (single host genotype experiment) hybridizations for a given category (i.e., control, thermal stress, recovery, or top-control, top-treatment, etc., respectively). After this filtration step, 1,012 (time-series experiment) and 1,236 (single host genotype experiment) genes were used for subsequent analyses. Microarray hybridization data (both raw and normalized) along with methodological details are deposited in GEO with the series record number GSE15262.

The ratio between the fluorescence intensity of the two channels was used as input for BAGEL (Bayesian Analysis of Gene Expression Levels) (Townsend & Hartl 2002). The BAGEL software uses Bayesian probability to infer a relative expression level of each gene. An estimated mean and 95% credible interval of the relative level of expression of each gene is computed in each treatment and time point. We used the conservative gene-by-gene criterion of non-overlapping 95% credible intervals to regard a gene as significantly differentially expressed. The following pair-wise statistical tests were performed: control>stressed, control<stressed, control>recovered, control<recovered, stressed>recovered, and stressed<recovered (time-series experiment) and control>stressed, control<stressed (single genotype experiment). Similarly, gene expression in top (T), middle (M), and bottom (B) fragments under both control and stressed conditions were tested: T>M, T<M, T>B, T<B, M>B, and M<B. The genes found to be differentially expressed under these conditions were further grouped into 12 possible gene expression patterns, i.e.: B>M>T, B<M<T, B=M>T, B=M<T, B>M=T, B<M=T, B=T>M, B=T<M, B>M<T and B>T, B<M>T and B<T, B>M<T and B<T, and B<M>T and B>T.

Hierarchical clustering of gene expression was performed using TIGR TMEV 4.0 (Saeed et al. 2003). Array trees were created according to average linkage and Euclidean distance metric on $\log_2$ ratios of signal intensities, which were normalized across arrays in the case of the time-series experiment. Signal intensities from control and stressed replicate fragments (n=3) from top, middle, and bottom were averaged prior to hierarchical clustering. The stability of clusters was tested using the R-

package pvclust by calculating approximately unbiased p-values via multiscale bootstrap resampling; a measure that has been demonstrated to provide a better indicator for cluster support than regular bootstrapping procedure (Suzuki & Shimodaira 2006). To assess over-representation of Gene Ontology (GO) terms in the lists of significant genes, we used default statistical tests and multiple-testing adjustments in GOEAST (Zheng & Wang 2008) except the significance cutoff was set to $\alpha = 0.001$.

RESULTS

Experimental Thermal Stress and Recovery

We measured dark-adapted maximum quantum yields for charge separation (*Fv/Fm*) in fragments sampled from five biological replicates of the coral *M. faveolata* throughout the time course of a thermal stress experiment (Figure 1A, Table S1). A significant decrease in *Fv/Fm* in previously acclimated coral fragments was observed four days after increasing the water temperature. The total duration of the thermal stress treatment was 10 days and the difference in *Fv/Fm* became insignificant two days after termination of the treatment (Figure 1A). The initial decrease in *Fv/Fm* was linear, whereas its increase during the recovery period was explained best by a logarithmic function (Figure S2, Table S2).

Differences in *Fv/Fm* among the sampled colonies were observed in all experimental periods ($p_{adj}<0.001$; Table S1). Post-hoc analyses revealed that *Fv/Fm* averages in colonies C1 and C2 were significantly different from those in colonies C3, C4, and C5 during the control period. Colony C2 showed very little reduction in

Fv/Fm upon heat treatment, and *Fv/Fm* values were significantly higher than in all other colonies during the stress and recovery periods. The differences between colonies were most likely due to a combinatorial effect of differences in *Symbiodinium* (Table 1) and host genotypes (Figure S3).

Restriction fragment length polymorphism (RFLP) analysis and sequencing of internal transcribed spacer 2 (ITS2) loci were used to genotype the *Symbiodinium* clades hosted by the experimental coral fragments. In the control samples, the dominant *Symbiodinium* clades were clade A in colonies 1 and 2, clade B in colonies 4 and 5, and clade C in colony 3. In thermally stressed samples, clade A was the dominant type in colony 3, whereas clade A and clade B remained the dominant clade types in colonies 1 and 2, and colonies 4 and 5, respectively (Table 1). While the 5 replicate colonies initially harbored a range of symbiont clades (A, B, and C), following recovery from bleaching all colonies harbored clade A, i.e., the dominant *Symbiodinium* clade type residing in colonies 3, 4 and 5 changed from clade C/B to clade A. ITS2 sequencing results were generally congruent with RFLP analyses in control fragments, and additionally allowed for both the determination of relative contributions of different *Symbiodinium* subtypes in fragments hosting more than one clade type and an increase in resolution of *Symbiodinium* clades to the subclade level. Based on both BLASTn results and phylogenetic reconstruction (Figure S4), we found the dominant haplotype of clade A, clade B, and clade C ITS2 sequences to be type A3 (most similar to EU074857), type B1 (EU074875), and type C7 (AF499797), respectively.

Analysis of a Single Host Genotype Harboring Different Symbiodinium Clades

In a parallel experiment, we sampled replicate fragments from top, middle and bottom parts of a single coral colony to obtain samples containing different *Symbiodinium* clade types in one host genetic background. *Fv/Fm* values began to decline following exposure to elevated temperature (Figure 1B). The bottom fragments showed a significant decrease relative to their controls two days after heating. Top fragments also showed a significant decrease after two days albeit less than the bottom fragments. The middle fragments showed a significant decrease after four days. By the end of the experiment, all heat-stressed fragments had significantly lower *Fv/Fm* values compared to their controls, and the top and bottom heat-stressed fragments had significantly lower maximum quantum yields than the middle heat-stressed fragments (Figure 1B). RFLP analyses revealed that middle and bottom fragments harbored mainly clade C; top fragments, mainly clade B (Table 1). Again, ITS2 sequencing results were largely consistent with RFLPs analyses (Table 1). After sequence alignment and phylogenetic analyses (Figure S4), we found that the dominant haplotype of clade C sequences was identical to type C7 (AF499797), and the dominant haplotype of clade B sequences was identical to type B17 (EU449083).

Microarray Gene Expression Analysis

After the generation of *Symbiodinium* physiological and genotypic data, we were interested in differentially expressed genes in control, thermally stressed, and recovered coral fragments from different coral colonies (Figure 2A). In addition, control and thermally stressed coral fragments from different regions of a single host

colony were analyzed for differentially expressed genes (Figure 2B), a design that eliminated potential differences due to host genotypic background effects.

Pair-wise comparisons between control, stressed, and recovered samples resulted in a relatively small number (n=57-84) of differentially expressed genes, which is most likely attributable to the different *Symbiodinium* genotypes that were hosted by the control and stressed fragments (Table 1). Nevertheless, a gene ontology (GO) enrichment analysis revealed that genes related to regulation of transcription and response to stress were significantly enriched ($p<0.001$) among the annotated, differentially expressed genes (Figure 2A, Table S3). A direct comparison between control and thermally stressed samples from a single host colony yielded only 28 differentially expressed genes with low fold-changes ranging from 1.08 to 1.53 (Figure 2B, Table S3).

Next, we performed hierarchical cluster analyses (using Euclidean distance) on all assayed (1,000+) genes to group together samples with similar transcriptomic activity, and mapped *Symbiodinium* physiological and genotypic data onto the resulting array trees (Figure 3). With respect to the time-series experiment, the array tree reveals four major groups, which displayed congruency with *Symbiodinium* clade content and possibly with host genotypic differences. All recovered samples, which exclusively harbored *Symbiodinium* clade A, clustered together (Group 1, Figure 3A). In contrast, neither control nor thermally stressed samples were grouped together, i.e. according to experimental conditions. Instead, they were divided into groups that suggest the influence of both host and *Symbiodinium* genotype effects. Control and

stressed samples from colony 2, which was determined to be genetically distinct from all other colonies (Figure S3), contained mainly symbionts of clade A (Group 2, Figure 3A). Group 3 was formed by control and stressed fragments from colonies 1 and 3, which mainly contained clade A symbionts. The only exception to this observation was that the control fragment of colony 3 was dominated by clade C. These two colonies were genetically different from each other as well as different from colonies 2, 4 and 5 (Figure S3). Finally, different to all other control and stressed fragments, colonies 4 and 5 could not be genetically differentiated (Figure S3) and contained mainly clade B (Group 4, Figure 3A).

Another aspect of our analyses revealed an apparent trend between the magnitude of the transcriptomic response to thermal stress (determined by the distance between the control and stressed samples in Figure 3) and the symbiont genotype. In clade A (colonies 1 and 2) or clade C (colony 3) hosting fragments, the difference was relatively small (branch length distances between control and stressed samples: 37.02, 36.08, and 31.56, respectively) compared to those dominated by clade B (44.55 and 61.86 for colonies 4 and 5, respectively).

Unlike in the time-series experiment, differences in gene expression between samples originating from a single host genotype were not biased by host genotypic background, thus strengthening the observed correlation between host transcriptomic states and *Symbiodinium* clade contents (Figure 3B). We found that middle and bottom control fragments (both dominated by clade C symbionts) exhibited gene expression patterns more similar to each other than to clade B-dominated top fragments (Figure

3B top panel). This association was highly significant according to cluster support. However, the correlation between host transcriptomic states and *Symbiodinium* clade contents noticeably diminished in the top, middle, and bottom stressed fragments (Figure 3B lower panel). Not only were the transcriptomic states of the top and bottom stressed fragments more similar to each other than to the middle stressed fragments, but the branch lengths and cluster support were lower compared to the control tree (Figure 3B top panel). This pattern is consistent with the PAM data showing that *Symbiodinium* within top and bottom fragments experienced more stress than those within middle fragments (Figure 1B).

Expression Patterns of Differentially Expressed Genes

Testing for pair-wise differences between colony locations showed that among the control samples, many genes were differentially expressed between top and middle (n=204) and top and bottom (n=312); however, a very small number of genes were differentially expressed between middle and bottom (n=24). These numbers were substantially lower for the corresponding analysis of thermally stressed samples: top vs. middle (n=51); top vs. bottom (n=96); and middle vs. bottom (n=49) (see Table S3 for all gene expression results).

We further analyzed differentially expressed genes between top, middle, and bottom samples by grouping them into 12 major expression patterns. Among control samples, 173 genes were sorted into 8 different patterns. The vast majority (90%) of these genes were either upregulated (B=M<T, n=105) or downregulated (B=M>T, n=50) in top versus middle/bottom samples (Figure 4, Table S3). The distribution into

distinct patterns for stressed samples was more even, further supporting a diminishing correlation between transcriptomic states and *Symbiodinium* genotypes during thermal stress as previously mentioned (Figure 3B). Nevertheless, similar to the control samples, the majority (60%) of differentially expressed genes were either upregulated (B=M<T, n=20) or downregulated (B=M>T, n=6) in top versus middle/bottom samples (Figure 4, Table S3).

GO enrichment analysis of the most populated patterns, i.e. those with *Symbiodinium* genotype differences among the control samples (B=M<T and B=M>T), showed genes involved in protein metabolism (e.g., translation, protein folding/degradation) to be significantly ($p<0.001$) enriched (Figure 5).

DISCUSSION

Host and Symbiodinium Factors Affect Dark-Adapted Maximum Quantum Yields (Fv/Fm)

Maximum quantum efficiencies in *Symbiodinium* sp. type C7-associated with *Montastraea faveolata* were previously shown to decrease more in response to experimental thermal stress compared to type B1-associated with *M. faveolata* (Warner et al. 2006). In our study, however, type B1-hosting colonies actually decreased more in *Fv/Fm* than type A3- and type C7-containing colonies (Figure 3A). Similarly, type B17-containing top fragments experienced a greater decrease in *Fv/Fm* than type C7-containing middle fragments. However, the response of B17-containing top fragments was similar to C7-containing bottom fragments. Marked differences were also found in the degree of photoinactivation of PSII between different colonies

that hosted the same *Symbiodinium* type. For example, colony 2 experienced hardly any reduction in *Fv/Fm* while colony 1 experienced a sharp decrease in *Fv/Fm*, yet both housed clade A.

The discrepancies between our study and Warner *et al*. (2006), in addition to the differences between middle and bottom fragments and the fact that colonies 1 and 2 differed in thermal susceptibility, argues against the idea that thermal stress-susceptibility of corals is solely linked to symbiont genotype (Iglesias-Prieto et al. 2004, Rowan 2004, Tchernov et al. 2004, LaJeunesse et al. 2007, Sampayo et al. 2008). Instead, our results and other studies (Brown et al. 2002, Bhagooli & Hidaka 2003, Goulet et al. 2005) support the notion that host contributions and/or effects of previous conditions (Brown et al. 2002, Middlebrook et al. 2008) must be taken into account when discussing differences in stress-induced *Fv/Fm* losses with respect to differences in *Symbiodinium* type.

Host gene expression profiling during thermal stress and recovery

In a previous coral microarray study on heat stress, we assayed gene expression changes in fragments from a single colony and fragments from different colonies (DeSalvo et al. 2008). We found that while using biological replicates (i.e., different colonies) increased our ability to draw conclusions beyond the limits of a single genotype, it confounded our ability to detect significant changes in genes that show only a small difference in expression given a similar number of microarrays. Nevertheless, many genes identified in the single-genotype experiment were corroborated in the multi-colony experiment (DeSalvo et al. 2008). In the present

study, we followed a similar two-pronged experimental design by using multiple replicates from a single host colony, in combination with sampling different colonies.

Unexpectedly, we found: (1) few genes differentially expressed in response to thermal stress and recovery, and (2) low overlap with previous results (DeSalvo et al. 2008). In our previous experiment greater than 20% of genes were found differentially expressed upon induction of bleaching (DeSalvo et al. 2008). These discrepancies might be explained by differences in experimental procedures such as: acclimation time (4 days vs. 21 days), initial rate of temperature change (0.73°C h^{-1} vs. 0.35 °C h^{-1}), sampling time points, water quality, light regime, etc. However, we provide strong evidence that the symbiont genotype had a substantial influence on host gene expression (see below), and thus diminished our ability to detect more genes differentially expressed during thermal stress and recovery. Nevertheless, we found an enrichment of genes related to transcription regulation and stress response (Figure 2). Interestingly, a number of those genes are differentially expressed between control and recovered samples. These genes (e.g., heat shock factor protein) represent candidates for future studies given their possible involvement in the acquisition of experience-mediated thermal stress resistance (Brown et al. 2002).

The results from comparing control and stressed fragments from the same host genotype, an approach that allowed us to disentangle the contribution of host genetic background and the *Symbiodinium* type hosted, yielded a low number (about 2% of all assayed genes) of differentially expressed genes with fold-changes less than 1.53. This is in stark contrast to the single-genotype experiment described in DeSalvo *et al.* 2008,

where 24% of all assayed genes were found differentially expressed. Intriguingly, all fragments in the 2008 study hosted the same *Symbiodinium* genotype (clade A), which, besides methodological differences, supports the notion that the host gene expression is correlated with the symbiont-genotype hosted.

Based on the results found in this study, i.e. an influence of *Symbiodinium* genotypes on coral transcriptomes, and the variability in transcriptomic responses seen in different experiments, the identification of a core set of stress-responsive genes represents a daunting challenge. Such an endeavor will require accounting for differences in both abiotic and biotic factors such as experimental procedures (acclimation conditions, rate and magnitude of temperature increase, stress exposure time, etc.) and host and symbiont genotypic backgrounds, respectively.

Integration of Host Gene Expression and Symbiodinium Genotyping Analyses

Numerous studies support the notion that different symbionts have far-reaching effects on host physiology. Growth rates in *Aiptasia pulchella* (Kinzie & Chee 1979) and in juvenile *Acropora millepora* and *Acropora tenuis* (Little et al. 2004, Mieog et al. 2009) are dependent on the symbiont genotype. Host growth is likely dependent on nutrient availability; thus, differential growth as a result of symbiont genotype may be related to the type (Loram et al. 2007) and amount (Stat et al. 2008, Cantin et al. 2009) of nutrients translocated from the symbiont to the host. Furthermore, a recent study investigated growth, survival, and thermal tolerance in different host-*Symbiodinium* combinations and found that *Symbiodinium* type was a better predictor of holobiont fitness than host genetic effects (Mieog et al. 2009). Finally, during natural bleaching

of *Montastraea* spp., clade A- and C-associated colony regions were less susceptible to thermal stress compared to clade B- and C-associated regions (Rowan et al. 1997).

In both of our experiments, acclimation of field-collected samples to the same light and temperature conditions for 4 weeks did not cause homogenization of *Symbiodinium* genotypes as seen in the control samples. Thus, it is possible that the observed patterns in host gene expression could have resulted from long-term acclimatization effects (months, years) to different environmental conditions in the field (e.g., light levels and temperature). The homogenization of *Symbiodinium* genotypes following thermal stress (all recovered fragments hosted *Symbiodinium* clade A) could also be interpreted as host physiology determining symbiont type dominance or alternatively, symbiont type content driving host gene expression. Taken together, we acknowledge that our experimental design did not allow disentangling a cause and effect relationship, i.e. whether a change in environmental conditions changed host physiology, and in turn a change in *Symbiodinium* type dominance, or that a change in environmental conditions caused a change in *Symbiodinium* type dominance and in turn a change host physiology (reflected in transcriptomic states). Nevertheless, the congruency between the array tree groupings and the *Symbiodinium* community compositions (Figure 3), which is seen in both experiments presented here, constitutes strong evidence that there exists a correlation between different *Symbiodinium* genotypes and the state of the coral host transcriptome. Our statistical analyses corroborate these findings in that the greatest differences in gene expression were found between clade B hosting top fragments and

clade C hosting middle/bottom fragments (Figure 4). However, in thermally stressed top, middle, and bottom samples the correlation notably diminished as seen by the lower number of differentially expressed genes compared to the corresponding analysis in control samples (Figure 4). The observed reduction was due to genes becoming more similar in their expression during stress rather than an increase in variation (Table S3).

The comparison between top, middle, and bottom fragments suggests that pathways involved in protein translation, folding, and degradation, in addition to other genes listed in Figure 5, are differentially affected in coral fragments hosting different *Symbiodinium* genotypes. Since these results are based on a single host genotype and a relatively small microarray, they set the stage for an in-depth analysis of differentially regulated pathways involving a multi-colony experimental design. If we are to succeed in such an effort, then surveying host and symbiont genotypic diversity must precede and thus inform the design of future experiments. At the time of writing, a *M. faveolata* microarray containing greater than 10,000 features is under fabrication, which will be utilized in the future to address this important gap of knowledge.

Conclusions and outlook

While the order of events, i.e. host physiology driving symbiont content and/or symbiont content driving host physiology, requires further investigation, the convergent findings of the two experiments outlined in this study strongly argues for the existence of a correlation between host transcriptional states and the symbiont genotype. It would thus be interesting to hypothesize that different symbiont types

may modulate the host transcriptome in more or less stress-responsive configurations, which would add a host transcriptomic perspective to a *Symbiodinium*-centric view of bleaching susceptibility.

Advancement in the understanding of the apparent differences observed in bleaching susceptibility of different coral-*Symbiodinium* partnerships are of particular relevance given the grim outlook of coral populations in the face of large-scale climate change-induced bleaching events. The ability of some corals to multi-associate most likely arose because symbiont effectiveness changes with environmental conditions (Douglas 1998). This scenario is consistent with the idea that organisms gain robustness to environmental perturbation by extending their system boundary via the integration of foreign biological entities such as symbionts (Kitano & Oda 2006). This is exemplified by different coral-*Symbiodinium* genotypic combinations being locally adapted to irradiance (Rowan & Knowlton 1995, Iglesias-Prieto et al. 2004). So far, only a handful of studies have addressed the effects of mutualistic symbionts on animal host transcriptomes, e.g. human gut microbiome (Hooper et al. 2001), *Vibrio*-squid symbiosis (Chun et al. 2008), and *Symbiodinium*-coral larvae and *Symbiodinium*-anemone symbioses (Rodriguez-Lanetty et al. 2006, Voolstra et al. 2009). These examples illustrate effects on host gene expression upon infection by different symbionts, whereas our study extends this body of knowledge by describing a correlation between symbiont genotype and the host transcriptome in both established symbioses and responses to thermal stress.

ACKNOWLEDGEMENTS

This chapter was published in *Molecular Ecology* (2010) volume 19, pages 1174-1186. I would like to thank my co-authors for their aid in all aspects of completing and publishing this work: Shini Sunagawa, Paul Fisher, Chris Voolstra, Roberto Iglesias-Prieto, and Monica Medina. We would like to thank the members of the Medina Lab at UCM and the members of the Photobiology group in Puerto Morelos for aid in many aspects of this study. We would like to especially thank Xavier Hernández-Pech of UNAM, Erika Diaz-Almeyda of UCM, Keith Bayha of UCM, Lolo Cardenas of the Roy Genomics Shared Facility at UCM, and the Functional Genomics Lab at UC Berkeley. Nicholas Polato and Iliana Baums at Penn State University are thanked for genotyping coral colonies. The comments of anonymous reviewers greatly improved this manuscript. This study was supported by a UC MEXUS Dissertation Research Grant to MKD, two Sigma Xi Grants-in-Aid of Research to MKD and SS, a UC MEXUS-CONACYT Collaborative Grant to RI-P and MM, NSF awards to MM (BE-GEN 0313708 and IOS 0644438), start-up funds from UC Merced to MM, and Coral Reef Targeted Research Program Funds to RI-P.

SUPPLEMENTARY INFORMATION

Supplementary information is downloadable at the following website:

http://www3.interscience.wiley.com/journal/123276178/suppinfo

Figure S1. Recovery of relative Fv/Fm values of Montastraea fragments during acclimation to the experimental tanks.

Figure S2. Reflectance measurements and best statistical Fv/Fm models for each period.

Figure S3. Host genotyping using published microsatellite markers.

Figure S4. Maximum-likelihood-based phylogenetic tree of *Symbiodinium* spp. based on ITS2 sequences.

Table S1. Linear models used to test for differences between colonies and tanks. Raw and adjusted p-values are shown for tanks and colonies or fragments.

Table S2. Parameters of statistical models for Fv/Fm during each experimental period are shown with the best model determined by a comparison of R2 and p-values.

Table S3. Results of gene expression analyses.

FIGURES

Figure 1. Relative *Fv/Fm* changes before, during, and after exposure of coral fragments to thermal stress. Dark-adapted maximum quantum yields relative to control samples were measured in five biological replicates during an experimental heat stress experiment (A) and in top (black), middle (red), and bottom fragments (blue) collected from a single coral colony (B). After acclimation, experimental coral fragments were exposed to elevated temperatures (shown by shaded areas) before being collected for microarray analyses at time points indicated by arrows. *Fv/Fm* data are averages (± standard error) of treatment tank replicates relative to the average of coral fragments maintained at control temperature. Horizontal bars above the plot indicate periods during which the difference between control and heat-stressed fragments were significant ($p<0.05$).

Figure 1.

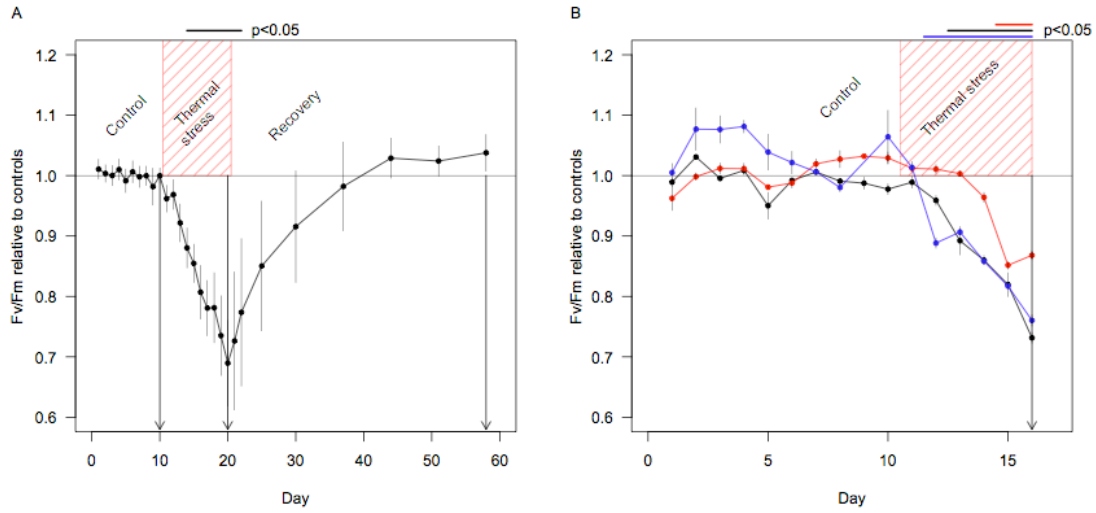
A
p<0.05
Control
Thermal stress
Recovery
Fv/Fm relative to controls
Day
B
p<0.05
Control
Thermal stress
Fv/Fm relative to controls
Day

Figure 2. Heat map of stress-responsive differentially expressed genes. Annotated differentially expressed genes identified in the time-series (A) and single host genotype experiment (B) are shown with clone IDs and annotations. Color scales correspond to BAGEL-computed gene expression estimates where a value of 1 is assigned to the class with the lowest expression. Boldfaced genes are involved in transcription regulation and stress response according to GO enrichment analysis.

Figure 2.

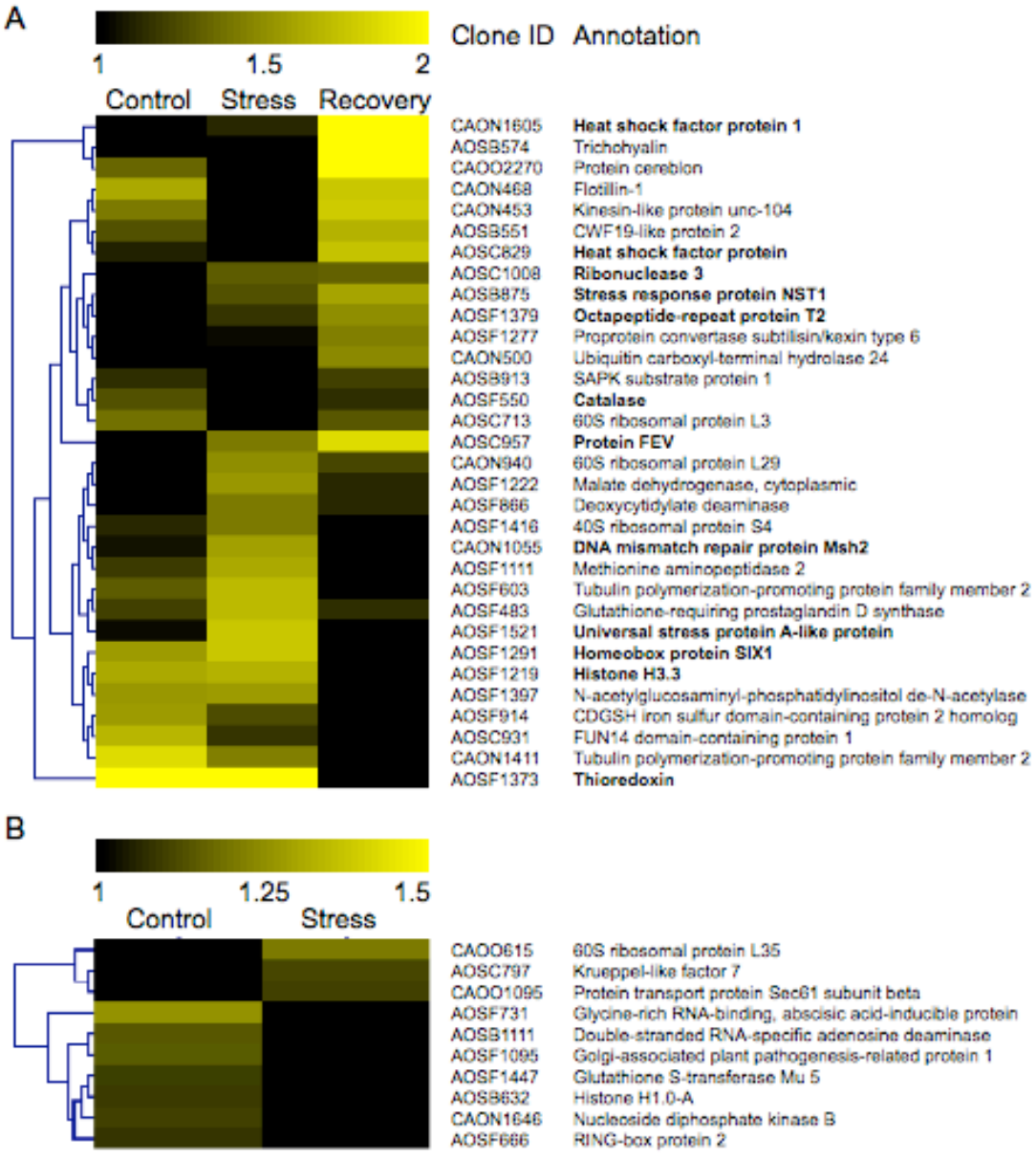
A
1
1.5
2
Control
Stress
Recovery
Clone ID
Annotation
CAON1605 Heat shock factor protein 1
AOSB574 Trichohyalin
CAOO2270 Protein cereblon
CAON468 Flotillin-1
CAON453 Kinesin-like protein unc-104
AOSB551 CWF19-like protein 2
AOSC829 Heat shock factor protein
AOSC1008 Ribonuclease 3
AOSB875 Stress response protein NST1
AOSF1379 Octapeptide-repeat protein T2
AOSF1277 Proprotein convertase subtilisin/kexin type 6
CAON500 Ubiquitin carboxyl-terminal hydrolase 24
AOSB913 SAPK substrate protein 1
AOSF550 Catalase
AOSC713 60S ribosomal protein L3
AOSC957 Protein FEV
CAON940 60S ribosomal protein L29
AOSF1222 Malate dehydrogenase, cytoplasmic
AOSF866 Deoxycytidylate deaminase
AOSF1416 40S ribosomal protein S4
CAON1055 DNA mismatch repair protein Msh2
AOSF1111 Methionine aminopeptidase 2
AOSF603 Tubulin polymerization-promoting protein family member 2
AOSF483 Glutathione-requiring prostaglandin D synthase
AOSF1521 Universal stress protein A-like protein
AOSF1291 Homeobox protein SIX1
AOSF1219 Histone H3.3
AOSF1397 N-acetylglucosaminyl-phosphatidylinositol de-N-acetylase
AOSF914 CDGSH iron sulfur domain-containing protein 2 homolog
AOSC931 FUN14 domain-containing protein 1
CAON1411 Tubulin polymerization-promoting protein family member 2
AOSF1373 Thioredoxin
B
1
1.25
1.5
Control
Stress
CAOO615 60S ribosomal protein L35
AOSC797 Krueppel-like factor 7
CAOO1095 Protein transport protein Sec61 subunit beta
AOSF731 Glycine-rich RNA-binding, abscisic acid-inducible protein
AOSB1111 Double-stranded RNA-specific adenosine deaminase
AOSF1095 Golgi-associated plant pathogenesis-related protein 1
AOSF1447 Glutathione S-transferase Mu 5
AOSB632 Histone H1.0-A
CAON1646 Nucleoside diphosphate kinase B
AOSF666 RING-box protein 2

Figure 3. Hierarchical clustering of gene expression intensities shows that samples group according to differences in *Symbiodinium* clade content.

(A) Samples from a thermal stress and recovery experiment using replicates from five different coral colonies were clustered into the following groups: (1) all recovered fragments, containing exclusively *Symbiodinium* clade A, (2) fragments from colony 2 containing predominantly clade A, (3) fragments from colonies 1 and 3 containing mainly clade A, and (4) fragments from colonies 4 and 5 containing predominantly clade B. (B) Averaged samples (n=3) from top, middle, and bottom parts of a single coral host colony group according to *Symbiodinium* genotypes in control (top panel), but not thermally stressed samples (bottom panel). Legend: sample names (1-5: sampled colony; T: top, M: middle, B: bottom; Con: control, Str: thermally stressed, Rec: recovered) and RFLP analysis results are shown as color-coded rectangles. Pie charts illustrate proportions of *Symbiodinium* clades based on ITS2 sequence analysis in selected fragments (note: red indicates type B1 in panel A and type B17 in panel B). Numbers next to rectangles represent the percent differences in *Fv/Fm* between treated and untreated fragments. Approximately unbiased p-values are shown next to tree nodes.

Figure 3.

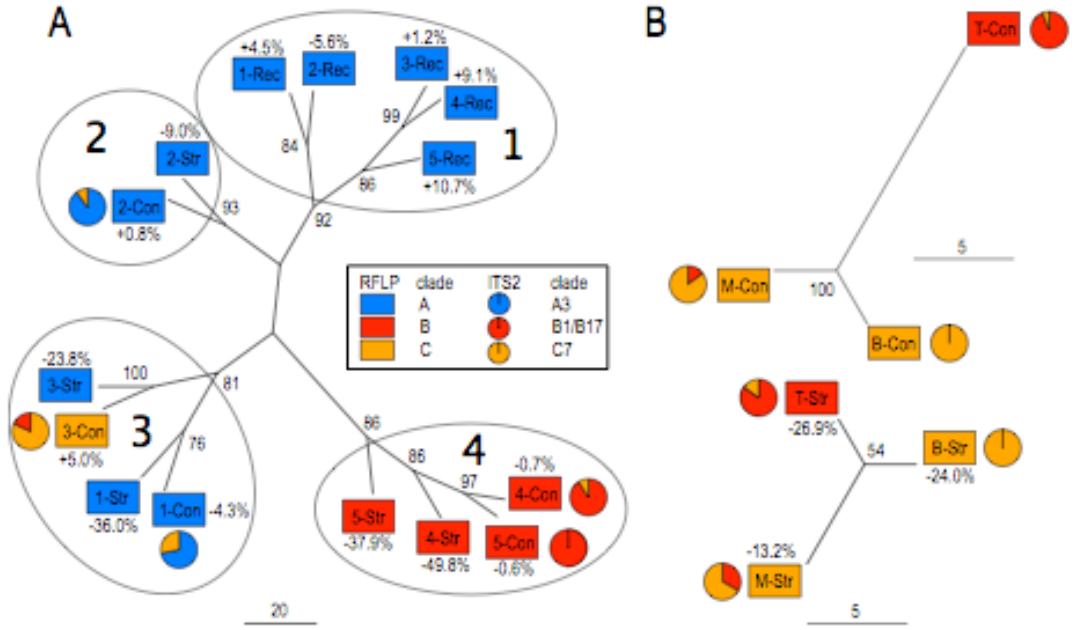
A
B
+4.5%
1-Rec
-5.6%
2-Rec
+1.2%
3-Rec
+9.1%
4-Rec
5-Rec
+10.7%
1
2
-9.0%
2-Str
2-Con
+0.8%
3
-23.8%
3-Str
3-Con
+5.0%
1-Str
-36.0%
1-Con
-4.3%
4
-0.7%
4-Con
5-Str
-37.9%
4-Str
-49.8%
5-Con
-0.6%
99
84
86
92
93
100
81
76
86
97
RFLP clade
A
B
C
ITS2 clade
A3
B1/B17
C7
20
T-Con
5
M-Con
100
B-Con
T-Str
-26.9%
54
B-Str
-24.0%
-13.2%
M-Str
5

Figure 4. Pattern analysis of differentially expressed genes. Genes that were differentially expressed between top, middle, and bottom control (left panel) and stressed (right panel) fragments were sorted into groups of distinct expression patterns. Heat map intensities were calculated by averaging the BAGEL-estimated expression levels for all genes within each pattern. Of the 12 patterns tested, only those containing at least one gene are depicted.

Figure 4.

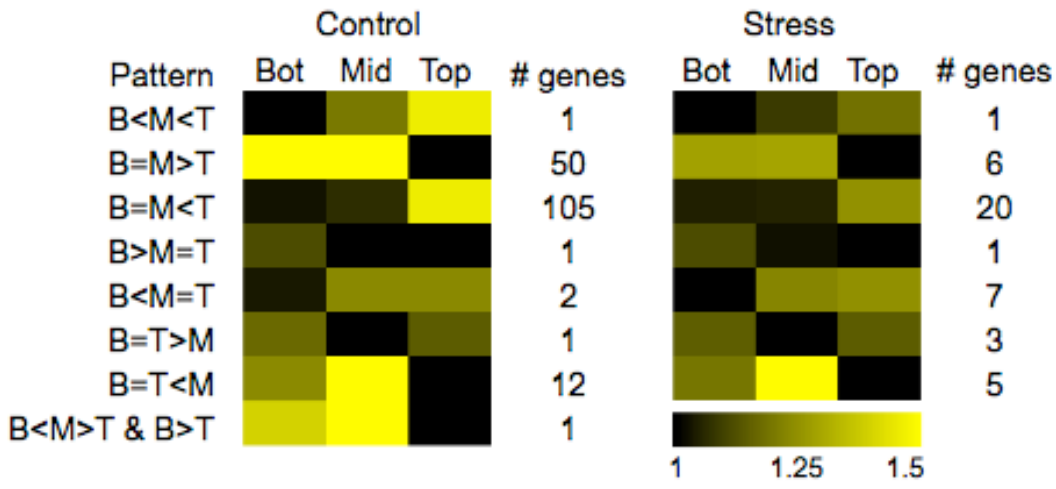
Control
Stress
Pattern
Bot
Mid
Top
genes
Bot
Mid
Top
genes
B<M<T
1
1
B=M>T
50
6
B=M<T
105
20
B>M=T
1
1
B<M=T
2
7
B=T>M
1
3
B=T<M
12
5
B<M>T & B>T
1
1
1.25
1.5

Figure 5. Heat map of genes differentially expressed between top, middle, and bottom control fragments. Annotated differentially expressed genes identified in the single host genotype experiment are shown with clone IDs and annotations. Color scales correspond to BAGEL-computed gene expression estimates where a value of 1 is assigned to the class with the lowest expression. Boldfaced genes are involved in protein metabolism (e.g., translation, protein folding/degradation) according to GO enrichment analysis.

Figure 5.

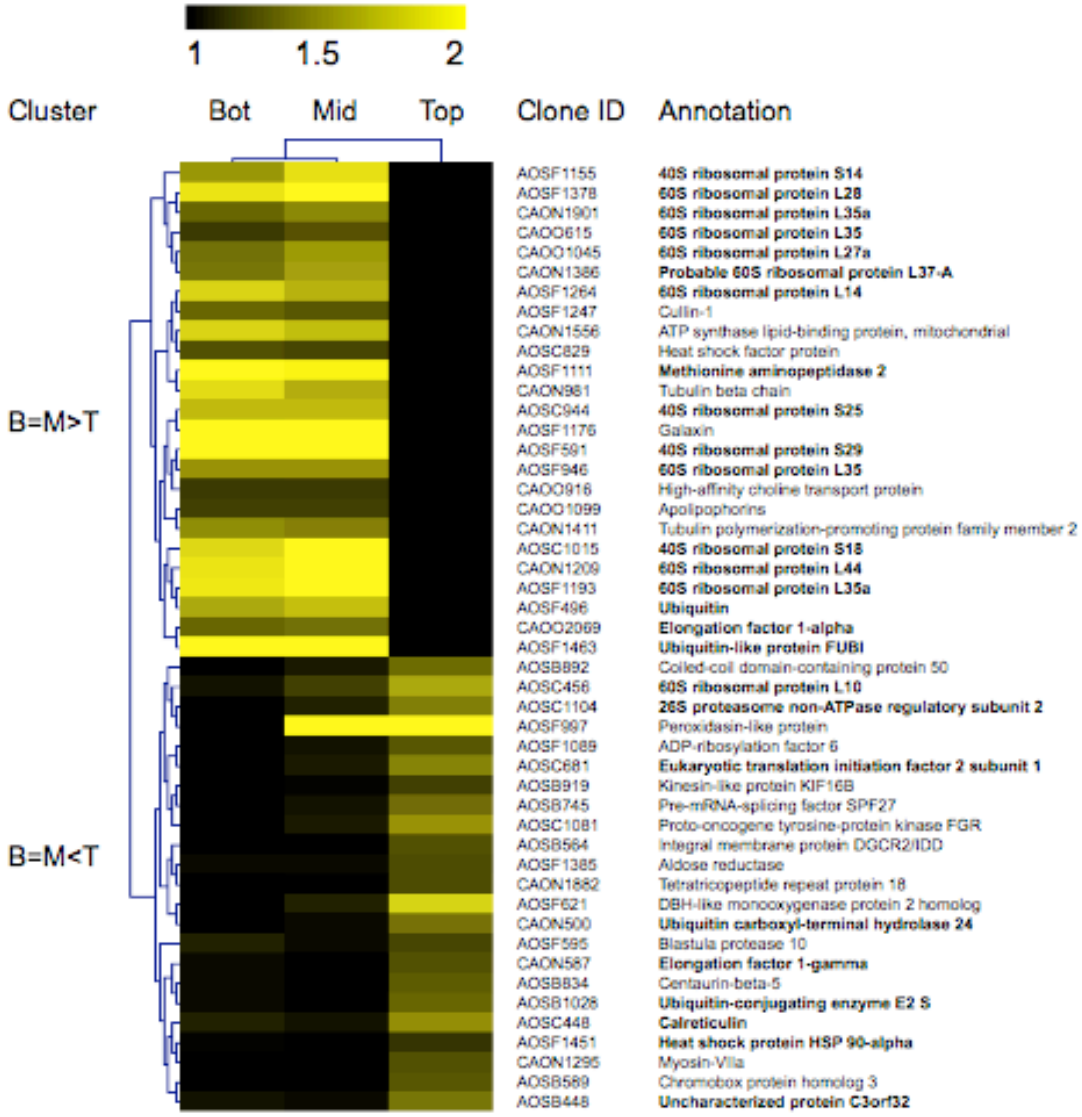
1
1.5
2
Cluster
Bot
Mid
Top
Clone ID
Annotation
B=M>T
B=M<T
AOSF1155 40S ribosomal protein S14
AOSF1378 60S ribosomal protein L28
CAON1901 60S ribosomal protein L35a
CAOO615 60S ribosomal protein L35
CAOO1045 60S ribosomal protein L27a
CAON1386 Probable 60S ribosomal protein L37-A
AOSF1264 60S ribosomal protein L14
AOSF1247 Cullin-1
CAON1556 ATP synthase lipid-binding protein, mitochondrial
AOSC829 Heat shock factor protein
AOSF1111 Methionine aminopeptidase 2
CAON981 Tubulin beta chain
AOSC944 40S ribosomal protein S25
AOSF1176 Galaxin
AOSF591 40S ribosomal protein S29
AOSF946 60S ribosomal protein L35
CAOO916 High-affinity choline transport protein
CAOO1099 Apolipophorins
CAON1411 Tubulin polymerization-promoting protein family member 2
AOSC1015 40S ribosomal protein S18
CAON1209 60S ribosomal protein L44
AOSF1193 60S ribosomal protein L35a
AOSF496 Ubiquitin
CAOO2069 Elongation factor 1-alpha
AOSF1463 Ubiquitin-like protein FUBI
AOSB892 Coiled-coil domain-containing protein 50
AOSC456 60S ribosomal protein L10
AOSC1104 26S proteasome non-ATPase regulatory subunit 2
AOSF997 Peroxidasin-like protein
AOSF1089 ADP-ribosylation factor 6
AOSC681 Eukaryotic translation initiation factor 2 subunit 1
AOSB919 Kinesin-like protein KIF16B
AOSB745 Pre-mRNA-splicing factor SPF27
AOSC1081 Proto-oncogene tyrosine-protein kinase FGR
AOSB564 Integral membrane protein DGCR2/IDD
AOSF1385 Aldose reductase
CAON1882 Tetratricopeptide repeat protein 18
AOSF621 DBH-like monooxygenase protein 2 homolog
CAON500 Ubiquitin carboxyl-terminal hydrolase 24
AOSF595 Blastula protease 10
CAON587 Elongation factor 1-gamma
AOSB834 Centaurin-beta-5
AOSB1026 Ubiquitin-conjugating enzyme E2 S
AOSC448 Calreticulin
AOSF1451 Heat shock protein HSP 90-alpha
CAON1295 Myosin-VIIa
AOSB589 Chromobox protein homolog 3
AOSB448 Uncharacterized protein C3orf32

TABLES

Table 1. Results of *Symbiodinium* genotyping assays. The top half corresponds to the time series experiment, the bottom half to the single host colony experiment. When more than one sample appears on the same row, they contained the same *Symbiodinium* type and proportions. Abbreviations used: C, B, R followed by a number denote control, bleached, and recovered fragments, respectively.

Table 1.

	18S rRNA RFLP		ITS2 sequencing				
Fragment(s)	1°	2°	1°	%	2°	%	n
C1	A	-	A3	73	C7	27	11
C2	A	-	A3	90	C7	10	10
C3	C	B	C7	82	B1	18	11
C4	B	-	B1	91	C7	9	11
C5	B	-	B1	100	-	-	11
B1-3	A	-	n/a				
B4	B	A	n/a				
B5	B	-	n/a				
R1-5	A	-	n/a				
Top 1,3,6	B	-	B17	100	-		11,11,12
Top 2	B	C	B17	83	C7	17	12
Top 4	B	C	B17	80	C7	20	10
Top 5	B	C	B17	73	C7	27	11
Middle 1,4	C	-	C7	100	-		14,15
Middle 2	C	-	C7	69	B17	31	13
Middle 3	C	-	C7	82	B17	18	11
Middle 5	C	B	B17	75	C7	25	12
Middle 6	C	-	C7	67	B17	33	12
Bottom 1-6	C	-	C7	100	-		8-9

CONCLUSIONS

Review of the dissertation

The preceding three chapters described experiments that were conducted in order to understand the molecular events surrounding the collapse in symbiosis between reef-building corals and their dinoflagellate endosymbionts. True to the original motivation, comparing the transcriptomic responses to heat stress and bleaching in two evolutionary distant corals (Chapters 1 and 2) revealed both conserved and putative species-specific cellular processes. Interestingly, the results of Chapter 3 described a surprising result – that the coral host transcriptome can be correlated with *Symbiodinium* type more than stress condition. Taken together, this dissertation has exposed the immense utility of cDNA microarrays for the study of coral biology. Furthermore, the descriptive, discovery-based nature of microarray studies has unearthed a plethora of hypotheses that can now be tested in order to eventually describe the precise molecular and cellular events underlying the onset, maintenance, and breakdown of the coral-algal symbiosis.

Microarray analyses of thermal stress and bleaching in A. palmata and M. faveolata

The results described in Chapters 1 and 2 have greatly enhanced the body of knowledge surrounding the molecular and cellular responses to thermal stress and bleaching in scleractinian corals. Table 1 lists the cellular processes and components affected by thermal stress as measured in the microarray experiments from Chapters 1 and 2.

Conserved cellular processes/components involved in the coral stress response. Not surprisingly, responses involved in the conserved cellular stress response (CSR), such as growth arrest and up-regulation of chaperones (Kultz 2003), were among the differentially expressed processes found in both coral species. Interestingly though, the differentially expressed genes (DEGs) within each process were often different for both species. For example, growth arrest in *M. faveolata* was indicated by the down-regulation of ribosomal proteins (less protein synthesis) and histones (less DNA replication). In *A. palmata*, growth arrest was also indicated by the down-regulation of ribosomal proteins; however, histone down-regulation was not detected, but rather a sharp down-regulation of cell cycle checkpoint transcripts was detected (a response not seen in *M. faveolata*). Given that the best estimate of the overlap between the microarrays for both species is approximately 10% (Voolstra et al. 2009), it is possible that these observatioins may be due to biases in the genes represented on the microarrays.

Likewise, the remaining processes involved in the CSR, i.e. nucleic acid stabilization/repair and the removal of damaged macromolecules (Kultz 2003), were measured unequivocally in *A. palmata* but not detected in *M. faveolata*. These differences provoke two explanations that are not mutually exclusive: (1) the level of stress felt in both was species was different; and (2) as mentioned above, the cDNA libraries used to construct the microarrays contained little overlap. The first explanation is valid given the major difference in the timing of bleaching – *A. palmata* lost 60% of its symbionts after two days, and *M. faveolata* reached a similar level of

bleaching after nine days. Despite these fundamental differences, the results of both studies have confirmed past findings and revealed new exciting avenues of inquiry in coral symbiosis research.

The following responses measured in *A. palmata* and *M. faveolata* confirm past findings: antioxidant up-regulation (e.g. Lesser 1997, Downs et al. 2002), heat shock protein expression (e.g. Black et al. 1995), removal of damaged macromolecules (Downs et al. 2005), cell death (e.g. Dunn et al. 2004, Strychar et al. 2004), and nitric oxide signaling (Perez & Weis 2006). Similarly, the following processes (in addition to the CSR processes mentioned above) are expected to be differentially expressed given general eukaryotic stress physiology and coral-algal symbiotic interactions: calcium homeostasis (Orrenius et al. 1992) and metabolite transfer between host and symbiont (Trench 1979).

By studying two different species, both of which have abundant sequence resources, stronger claims can be assigned to DEGs that arise in experiments for both species. Despite evolutionary separation and observed sensitive/resistant phenotypic differences, a gene that is differentially expressed in both species is likely to be involved in the core cellular response to stress and bleaching. Table 2 contains DEGs that overlap between the *A. palmata* and *M. faveolata* experiments. Some of the DEGs are orthologs, whereas the rest have the same or similar BLAST hits. Perusal of Table 2 shows the immense importance of actin cytoskeletal (AC) components, extracellular matrix (ECM) proteins, and DNA binding/transcription factors. While the activity of actin and other proteins that bind actin (e.g. gelsolin and myosins) may be tied to

simple heat stress effects (Coakley 1987), oxidative stress (Huot et al. 1997), and/or osmotic stress effects (Chowdhury et al. 1992), it is tempting to speculate that differential expression of these genes is tied to loss of endosymbiotic algae. Whether the algae are being lost via cell detachment (Gates et al. 1992), exocytosis (Steen & Muscatine 1987), or autophagy/symbiophagy (Dunn et al. 2007, Downs et al. 2009), the AC is likely involved. Integrin-mediated cell adhesion involves the AC (Delon & Brown 2007), and exocytosis or degradation of membrane-bound vesicles involves modifications to the AC (Ridley 2006). Given the involvement of the AC in the numerous cellular mechanisms that lead to symbiont loss, it is interesting to note that the expected 'complexity' in cellular bleaching mechanisms may actually be quite simple. Adopting an AC-centric view of bleaching mechanisms could serve to unify past and present studies and refine future research inquiries.

Given the role of the AC in these possible mechanisms of symbiont loss, future experiments must investigate how the AC changes during bleaching. An appropriate way to achieve this objective, which is used routinely in cell culture of model organisms, is by acquiring fixed and live cell images using confocal microscopy (Douglass & Vale 2008). Actin-specific stains are readily available, and other AC components could be targeted with antibodies. Furthermore, fluorophore-tagged proteins-of-interest can be generated via transfection of cells. The main impediment to these types of analyses in the context of coral bleaching is the absence of coral cell lines. While numerous investigators have succeeded in culturing coral cells (Kopecky & Ostrander 1999, Domart-Coulon et al. 2001, Helman et al. 2008, Khalesi 2008,

Reyes-Bermudez & Miller 2009), longevity of the culture is rarely achieved. However, most investigators note that symbiotic cells survive tissue dissociation, which holds promise for these future endeavors. See below for discussions on ECM proteins and transcription factors.

Novel cellular processes/components involved in the coral stress response. Perhaps the most exciting results from the first two chapters are the cellular processes/components revealed in *A. palmata* and *M. faveolata* that have never before been implicated in bleaching mechanisms and coral stress physiology. These processes/components include ECM proteins, the glyoxylate cycle, and cell signaling molecules, which I will discuss further below.

Extracellular matrix proteins. The ECM is of particular interest in the context of coral molecular biology because this part of the cellular milieu is critical to both symbiosis and calcification. First, consider the algal symbionts. They exist in membrane-bound vesicles known as 'symbiosomes', and thus they are effectively *outside* of the host cell. ECM proteins existing at the interface of the host and symbiont (i.e. the symbiosome membrane) must be essential to the maintenance of the symbiosis. Second, consider the calcification process. The calicoblastic epithelium is the layer of tissue that secretes the organic matrix, which controls the formation of the calcium carbonate skeleton (Puverel et al. 2005). Considering both symbiosis and calcification, a down-regulation of ECM proteins during bleaching could mean (1) a loss of symbionts and thus a lowered need for proteins active at the symbiosome membrane, and/or (2) a decrease in calcification as a result of stress.

Discerning which of these two processes an ECM DEG is involved in poses a serious challenge. A prime example is the observed down-regulation of a family of coral-specific genes in *M. faveolata.* The so-called SCRiPs, or small cysteine-rich polypeptides (Sunagawa et al. 2009a), may be involved in either of the two aforementioned processes. Evidence for a role in calcification comes from hierarchical clustering of DEGs – four SCRiPs cluster tightly with galaxin, a known constituent of the coral organic matrix (Fukuda et al. 2003) (see Figure 3 in Sunagawa *et al.* 2009). Down-regulation of calcification-related molecules is expected given numerous observations of decreased coral growth following bleaching events (e.g. Jokiel & Coles 1977). In reality though, it is not clear whether the SCRiPs are involved in symbiosis or calcification. *In situ* hybridization with labeled probes specific to SCRiPs transcripts can at least elucidate where the SCRiPs are active. Localization to the symbiosome membrane or the calicoblastic epithelium would be hugely informative.

Three ECM proteins listed in Table 2, collagen alpha-1(II), a Kunitz-type peptidase inhibitor, and papilin are very intriguing given that orthologs in *A. palmata* and *M. faveolata* were differentially expressed in the respective experiments. Collagens are structural molecules ubiquitous among animals. While it is impossible to say exactly what process this specific collagen is involved in, it is worthy to note that Helman *et al.* (2008) found the ECM of two coral species to have high amounts of collagen. However, it is still unclear what this means in the context of coral bleaching. If collagen is a critical component of the organic matrix, then down-regulation during bleaching is simply related to less calcification. Other possibilities exist, though, for

example a down-regulation of collagen may reflect a change in cell adhesion properties during bleaching, or perhaps the symbiosome membrane is reinforced with host-derived collagen.

The Kunitz-type peptidase inhibitor (orthologs AOSF907 and AOKF1161) and papilin (AOKF939) also present a challenge when trying to explain their differential expression during bleaching. The *A. palmata* ortholog of the Kunitz-type inhibitor was up-regulated, but inconsistently, the *M. faveolata* ortholog was down-regulated. Papilin was up-regulated in *A. palmata*. Regardless of direction, the functions of these proteins are not clear. At the most basic level, these proteins are peptidase inhibitors, i.e. they inhibit proteolytic enzymes. Peptidases are essential to cellular physiology being involved in myriad processes such as digestion and apoptosis. Peptidase inhibitors exist in order to keep the activity of peptidases in check (reviewed in Rawlings et al. 2004). Both of these peptidase inhibitors contain Kunitz/BPTI and Thyroglobulin type-1 repeat domains, which suggests that they inhibit serine and/or cysteine proteases (see PF00086 and PF00014 – http://pfam.sanger.ac.uk/). Among the many described functions of peptidase inhibitors, an example relevant to symbiotic systems is that of parasites avoiding host digestion by releasing peptidase inhibitors (Martzen et al. 1990). It is tempting to hypothesize that these proteins are involved in mechanisms underlying the establishment and maintenance of the coral-algal partnership; however, an alternate hypothesis assumes these peptidase inhibitors are involved in the remodeling of the organic matrix for calcification purposes.

The glyoxylate cycle. The presence of an alternative metabolic strategy in corals, by which lipids can be broken down to produce carbohydrates, is particularly intriguing given the dependence of the coral host on the algal symbiont for fixed carbon. Based on bioinformatics analyses, the glyoxylate cycle had previously been implicated in cnidarian metabolism by the presence of the glyoxylate cycle-specific enzymes isocitrate lyase and malate synthase in sequence databases (Kondrashov et al. 2006). The transcriptomic response to bleaching in *A. palmata* (Chapter 2) showed for the first time an active glyoxylate cycle in a cnidarian. Future studies can assess the contribution of the glyoxylate cycle to the fixed carbon pool of a coral during a diurnal cycle (via radioisotope labeling), and whether the glyoxylate cycle is a general metabolic strategy in stressed/bleached corals (via qPCR analysis).

Cell signaling: transcription factors. Precise cell signaling cascades likely underpin the observed up-regulation of the glyoxylate cycle during bleaching (as measured in *A. palmata*). Similarly, there must be cell signaling mechanisms underlying the breakdown in coral-algal symbioses during bleaching. Table 3 includes a list of cell signaling molecules and transcription factors differentially expressed in chapters 1 and 2 whose activities warrant further study in the pursuit of elucidating the cellular signaling mechanisms essential to coral bleaching. Interestingly, NF-κB subunits are included in Table 3, as they were up-regulated in bleached *A. palmata*. This is consistent with one of the early (if not only) hypothesized cellular signaling mechanisms leading to bleaching. Perez and Weis (2006) postulated that reactive oxygen species (ROS) generated by *Symbiodinium* during heat/light stress might

activate NF-κB, which can enter the nucleus and up-regulate inducible nitric oxide synthase (iNOS) (Mendes et al. 2003). NOS would then stimulate production of nitric oxide (NO), which reacts with ROS to produce peroxynitrite, which will stimulate cell death, i.e. bleaching.

This proposed mechanism is bolstered by the findings in *A. palmata* (chapter 2) describing: (1) the up-regulation of NF-κB subunits; (2) the up-regulation of a TNF receptor-associated factor (TRAF3) which activates NF-κB (Takeuchi et al. 1996); and (3) the down-regulation of NOS-interacting protein (NOSIP) a negative regulator of NOS (Dedio et al. 2001). The mechanism of Perez & Weis (2006) depends on the activity of iNOS, which so far has not been quantified via microarray or qPCR analyses. However, iNOS sequences are present in the *M. faveolata* and *Acropora millepora* EST libraries, and thus the activity of iNOS during stress and bleaching could easily be quantified using qPCR. Additionally, there is the assumption that NF-κB is activating the transcription of iNOS. A chromatin immunoprecipitation (ChIP) analysis could discern whether NF-κB binds to regulatory elements upstream of iNOS in corals.

Expecting a single signaling cascade to govern the bleaching process is overly optimistic, as cellular decisions include complex molecular interactions that adopt network architecture with pathways and proteins interacting with many others (e.g. Oda & Kitano 2006). As such, future investigation must extend beyond the NF-κB/NO story. Other transcription factors listed in Table 3 are worthy of discussion, but I will focus on Nrf3, ATF2, and ATF4. In particular, Nrf3 is an interesting transcription

factor given a probable role in oxidative stress-induced transcriptional regulation. For example, Nrf2, a transcription factor in the same protein family, binds to the antioxidant response element (ARE) (Kobayashi & Yamamoto 2006), which triggers the expression of numerous proteins that protect cells from oxidative stress (e.g. Sun et al. 2005). UniProt pages for Nrf3 (e.g. Q9Y4A8 – human Nrf3), however, state its function is to activate erythroid-specific globin gene expression. As this function is unlikely in corals, Nrf3 may be involved in iron homeostasis – indeed, Nrf2 elevation was correlated with raised iron absorption in mice (Raja et al. 1995). This is related to oxidative stress because excess iron is thought to generate oxidative stress (Puntarulo 2005), and metals such as iron react with hydrogen peroxide to produce ROS (Haber & Weiss 1934). As with NF-κB, a ChIP analysis with Nrf3 would be highly informative in the pursuit of genes activated by Nrf3.

Two other appealing transcription factors are members of the activating transcription factor (ATF) family: cAMP-dependent transcription factor ATF-2, and cAMP-dependent transcription factor ATF-4. Both of these transcription factors are activated by kinases which themselves are triggered by a cAMP-mediated signal arising from an activated cell surface receptor (Kageyama et al. 1991, Ameri & Harris 2008). Both ATF-2 and ATF-4 were up-regulated in *A. palmata* during thermal stress. Following activation, ATFs initiate transcription via binding to the cAMP-responsive element (CRE). ATF-2 binds to the CRE following homodimerization or heterodimerization with c-Jun (Hai & Curran 1991). Interestingly, ATF-2 is known to be responsive to genotoxic stress (i.e. DNA damage) (Ronai et al. 1998), and is

activated following signals from the MAPK and JNK signal transduction pathways (Gupta et al. 1995), which are prototypical stress-responsive pathways.

Likewise, ATF-4 is involved in stress-responsive signal transduction. For example, ATF-4 is activated following amino acid starvation and ER stress, which occurs when an over-abundance of unfolded proteins aggregate in the ER. This signaling pathway begins with the stress-induced activation of kinases that phosphorylate eukaryotic initiation factor 2 (eIF2α), which negatively regulates translation of most mRNAs but selectively up-regulates translation of ATF-4 (Harding et al. 2000). The activity of ATF-4 alleviates amino acid starvation and ER stress by activating the transcription of chaperones, antioxidant proteins, and amino acid metabolism proteins (reviewed in Rutkowski & Kaufman 2003). Consequently, cells lacking ATF-4 are more susceptible to ER stress, amino acid deficiency, and oxidative stress leading to increased cell death (Harding et al. 2003). Given the role of ATFs in model systems, their activity during coral bleaching certainly warrants further investigation.

Cell signaling: protein tyrosine phosphatases. There are four protein tyrosine phosphatases (PTPases) in Table 3, two of which are receptor-type PTPases. In general, PTPases are the opposite of kinases and thus *remove* phosphate groups from proteins that have phosphorylated tyrosine residues. While the function of these proteins cannot be deduced by BLAST homology, it is important to point out that PTPases are important components of signal transduction pathways, and that PTPases are differentially expressed in response to thermal stress in both coral species studied.

One PTPase that warrants further investigation is receptor-type tyrosine-protein phosphatase N2 (CAON819). This gene was down-regulated in *M. faveolata*, and it is interesting because its BLAST E-value is extremely low ($1e^{-128}$), which suggests that its function may be tightly associated with that of vertebrate homologs. In human neuroendocrine cells, this gene is involved in processes specific for neurosecretory granules, such as their biogenesis, trafficking or regulated exocytosis (Solimena et al. 1996). Elucidating the function of this receptor-type PTPase in corals is tempting given that secretory processes are likely involved in metabolite transfer, calcification, and exocytosis of algae.

Cell signaling: the Ca^{2+} signaling pathway. The results of chapters 1 and 2 culminated in the ability to form a molecular model of the events enacted by thermal stress that lead to the bleaching response. An early version of this model is present in chapter 1 (Figure 1). In expanding this objective, the focus turns to signal transduction pathways rather than cellular processes. Ultimately, I am aiming to form a molecular network that includes the following components: (1) an extracellular signal (e.g. heat, ROS, *Symbiodinium* signaling molecule), (2) receptor activation (e.g. receptor-type PTPases, GPCRs), (3) calcium or cAMP as a secondary messenger, (4) kinase activation (e.g. JNK and MAPK pathways), (5) activation of transcription factors (e.g. ATFs, NF-κB), and (6) mechanisms of cross-talk between different signaling pathways (i.e. places in a signaling cascade where a signal can bifurcate to involve another pathway and thereby another cellular response). In reaching these objectives, I

will focus on the calcium (Ca^{2+}) and mitogen-activated protein kinase (MAPK) signaling pathways.

Ca^{2+} signaling begs discussion because Ca^{2+} is a ubiquitous second messenger linking cellular homeostatic mechanisms to cell death and stress signaling pathways. Figure 1 is a simplified, stripped-down version of the Ca^{2+} signaling pathway compiled by KEGG (Kanehisa & Goto 2000). It is notable that many of the molecules present in the classic Ca^{2+} signaling pathway are present in our coral sequence libraries (Figure 1 - boxes in green, blue, or yellow – also see Table 4 for other Ca^{2+} signaling molecules present in corals). Most of these molecules have never been studied in the context of coral biology and bleaching; thus, investigating the activities/expression of ryanodine receptors (RYRs), Ca^{2+} transporters, the inositol 1,4,5-triphosphate receptor (IP_3R), and calcium/calmodulin-dependent protein kinases (CAMKs), for example, represent myriad topics of future study.

In studying how Ca^{2+} signaling may be involved in bleaching mechanisms, consider topics discussed above in the context of the transcription factor ATF-4. Recall that the unfolded protein response triggers ER stress, which leads to up-regulation of ATF-4, which activates transcription of, among other things, antioxidant proteins. How does this all connect to Ca^{2+} signaling and bleaching mechanisms? Consider the following notions: (1) the prevailing mechanism of coral bleaching involves the cytotoxic effects of oxidative stress (reviewed in Lesser 2006); (2) oxidative stress in general disrupts ER function; (3) protein folding in the ER also causes oxidative stress; (4) both ER stress and oxidative stress lead to an increase in

cytosolic Ca^{2+}; and (5) increased cytosolic Ca^{2+} increases ROS generation in the mitochondria (reviewed in Malhotra & Kaufman 2007). These responses inevitably lead to cell death (Li et al. 2006), which is a viable method by which corals bleach (Strychar et al. 2004). Thus, Ca^{2+} signaling, ER stress, and ATF-4 activity in the context of coral bleaching mechanisms represent prime areas of research. Further adding to this impetus is the fact that Ca^{2+} signaling links to many other cellular pathways – for example, in Figure 1, the beige-shaded box illustrates how PKA links Ca^{2+} signaling to MAPK signaling.

Cell signaling: the MAPK signaling pathway. The MAPK pathway is involved in various cellular functions, such as cell proliferation, differentiation, and cell death. Relevant to coral stress physiology, numerous extracellular stressors have been found to activate the MAPK pathway, including irradiation, heat shock, oxidative stress, and osmotic stress (Obata et al. 2000). MAPK signaling pathways are broken into 3 subgroups: the classical MAPK pathway, the JNK and p38 MAPK pathway, and the ERK5 pathway. Figure 2 is a simplified version of the entire MAPK signaling network compiled by KEGG (Kanehisa & Goto 2000). It is notable that many of the molecules present in the JNK, p38, and ERK5 MAPK pathways are present in our coral sequence libraries (Figure 2 - boxes in green and blue - also see Table 5 for other MAPK signaling molecules present in corals). Most of these molecules have never been studied in the context of coral biology and bleaching; thus, investigating the activities/expression of tumor necrosis factor receptors (TNFRs), TNFR-associated factors (TRAFs), nuclear factor kappa-B (NF-κB), nuclear factor of activated T-cells

(NFAT), and the numerous MAP kinases represent innumerable topics of future study. Similar to Ca^{2+} signaling, MAPK signaling also links to other pathways. For example, the beige-shaded box in Figure 2 illustrates a link between Ca^{2+} and MAPK signaling. Also, at the termini of the different MAPK pathways, it is evident that these signaling events connect to p53 and apoptotic signaling.

Many constituents of the different MAPK pathways can be investigated for their role in stress and bleaching. From chapter 2, we know that TRAF2 and NF-κB are differentially expressed upon thermal stress and bleaching. However, it remains unknown which molecules exist upstream and downstream of these targets. Using the scaffolds in Figure 2 and the abundant coral sequence resources, investigators will eventually be able to piece together complete molecular pathways. However, the ability to deduce signal transduction cascades and how they mechanistically alter cellular processes depends on a suite of molecular genetic and cellular tools that do not yet exist for corals. These tools include: the ability to establish transgenic lines of corals, perform gene knockdowns via RNAi, and access large antibody libraries. Since these tools are in the distant future, it is noteworthy that sequence resources alone allow investigators to study signal transduction using bioinformatics tools (Lindvall et al. 2003).

Using bioinformatics and rudimentary cellular tools, we might soon find direct evidence that stress indeed leads to the activation of MAPK signaling pathways in corals, which then results in the activation of transcription factors such as NF-κB and ATF-4. Of equal importance, though, is to find out what initially triggers the MAPK

pathway. One possibility is direct activation by the stressor itself. For example, ROS can directly activate both MAP3K5 and MAP3K1 and thereby activate the MAPK cascade (Droge 2002). Another possibility for an activator is a ligand-receptor interaction. TNFRs represent a start point for MAPK signaling cascades. TNFRs are activated by tumor necrosis factors (TNFs), which are cytokines involved in cell-cell communication. Our coral sequence libraries do indeed include homologs to TNFs, which opens the possibility that the bleaching response might be initiated by a precise molecular signal – or better yet, a signal from the algal endosymbionts.

The endpoint of MAPK signaling is also critical information in the context of coral bleaching. We know that MAPK pathways lead to the activation of NF-κB and ATF-4 for example, and we know that these transcription factors are indeed up-regulated in *A. palmata* during stress. However, discerning which genes are activated or repressed by these transcription factors, and how these downstream events lead to the breakdown of symbiosis, at this point, depends on literature searches based on different study systems. The NF-κB/NOS mechanism of bleaching posited by Perez & Weis (2006) was based on literature searches, and while it is supported by findings reported in this dissertation, further investigation is required to confirm the proposed mechanism.

The observed correlation between Symbiodinium genotype and host transcriptome

After performing experiments in chapters 1 and 2 and measuring marked transcriptomic responses to heat stress and bleaching in *A. palmata* and *M. faveolata*,

the results reported in chapter 3 were immensely surprising. At first it seemed unlikely that the resident *Symbiodinium* genotype could have a greater effect on the coral host transcriptome compared to experimental heat stress. However, a multitude of recent studies have documented coral host physiology being modulated by symbiont genotype (e.g. Little et al. 2004, Stat et al. 2008, Cantin et al. 2009, Mieog et al. 2009). Especially revealing are the results of Mieog *et al.* (2009); they found that *Symbiodinium* type was the most important predictor of holobiont fitness (as measured by growth, survival, and thermo-tolerance) among outplanted coral juveniles experimentally infected with different *Symbiodinium* genotypes.

Since it is clear that different *Symbiodinium* genotypes are more or less mutualistic to their coral hosts, it will be interesting to see specific genes differentially expressed between coral hosts housing different *Symbiodinium* genotypes. The results of the single host genotype experiment in chapter 3 offer an initial glimpse into what cellular processes are differentially regulated by different *Symbiodinium* genotypes. By comparing gene expression in top, middle, and bottom fragments, we found that pathways involved in protein translation, folding, and degradation were differentially expressed in clade B-containing top fragments compared to clade C-containing middle and bottom fragments. Lower expression of 13 ribosomal proteins and methionine aminopeptidase suggests less mRNA translation in top fragments, and lower expression of a subunit of mitochondrial ATP synthase suggests less respiration in top fragments. Furthermore, top fragments express galaxin, a protein of the extracellular organic matrix (Fukuda et al. 2003), less than middle and bottom fragments. These

results suggest that perhaps *M. faveolata* associated with clade B do not have the same energy budget as *M. faveolata* associated with clade C.

While these results are certainly promising in that they suggest that different *Symbiodinium* genotypes may modulate the host transcriptome by translocating differing amounts of metabolites, one must be cautious given that the experiment was performed with a single host colony. The ideal experiment will involve *Symbiodinium* genotyping of coral colonies prior to fragment collection. It will be imperative to collect fragments from multiple host colonies containing different *Symbiodinium* genotypes that receive similar amounts of sunlight. This design includes biological replication, and it controls for the effects of long-term acclimatization to different light fields. Furthermore, in order to discern whether there are true biological replicates, coral host genotyping with microsatellite markers will also be required. If able to satisfy these conditions, then the experiment will be quite simple, as thermal stress and bleaching do not even have to be part of the design. One could simply acclimate the fragments in a common tank for ~30 days to promote wound repair, and sample fragments for microarray analyses at the beginning, middle, and end of 30-day period.

Shaping the coral host transcriptome during experimental stress. Experimental fragments of *M. faveolata* used in the time course experiment of chapter 1 harbored different *Symbiodinium* genotypes, which begs the question: why was a symbiont-effect on host gene expression not revealed in this experiment? Based on the results of chapter 3, any experiment involving fragments with different *Symbiodinium* genotypes should retain a transcriptomic signature that correlates with *Symbiodinium* genotype.

To explain this inconsistency, one must consider the intensity of the stress regime, which is likely modulated by both experimental design factors (e.g. length of acclimation time, rate of temperature increase) and biological factors (e.g. species-specific sensitivities to stress).

Comparing chapters 2 and 3 offers an analysis of disparate experimental designs that illustrate my point. In the experiment described in chapter 2, the following conditions apply: a branching coral species in *A. palmata*; fragments containing only *Symbiodinium* clade A; an acclimation time of 4 days; and a rapid rate of temperature increase (1˚C/hr). In contrast, the multi-colony experiment in chapter 3 involved the following conditions: an encrusting coral species in *M. faveolata*; fragments containing different *Symbiodinium* genotypes; an acclimation time of nearly 30 days; and a slow rate of temperature increase (0.35˚C/hr). The first scenario (i.e. *A. palmata*, chapter 2) favored the detection of drastic changes in gene expression due to stress given that branching coral species are generally more sensitive than encrusting species (Loya et al. 2001), the coral fragments had little time to recover from fragmentation, and the temperature was increased rapidly. The second scenario (i.e. *M. faveolata*, chapter 3), however, favored the detection of gene expression due to partnering with different *Symbiodinium* genotypes because the stress intensity was low – the fragments were allowed to fully recover and the temperature was increased slowly.

The processes being discussed in this section are illustrated in Figure 3, which depicts the coral host transcriptome (as measured during experimental manipulation) being shaped by two competing 'effects' – those of stress and those of the resident

algal symbionts. The balance between these two competing effects is influenced by design factors such as acclimation time and thermal treatment, and by biological factors such as symbiont genotypes and host sensitivity to stress. The balance between stress and symbiont effects is tipped towards stress in experiments described in chapters 1 and 2, and the balance is tipped towards symbiont effects in experiments from chapter 3. As mentioned above, why was a symbiont effect on host gene expression not revealed in the experiment from chapter 1 where fragments of *M. faveolata* contained different clades of *Symbiodinium*? A likely explanation for this is that the short acclimation time and rapid thermal ramping outweighed the symbiont effects such that the balance remained tipped towards stress effects (however, it must be noted that any other of a multitude of factors not controlled in this comparison could have influenced the results).

Conclusions

In synthesizing the results of this dissertation, the shear complexity of the coral holobiont at the transcriptomic level and how aspects of experimental design modulate it truly stands out. The results of chapter 3 illustrate the enormous effect that the symbionts can have on their hosts. This effect must be considered in any experiment aiming to measure gene expression in corals. In straightforward experiments like those reported in chapters 1 and 2, many challenges arise in interpreting the expression of annotated genes; however, in the context of the conserved cellular stress response, the activities of some differentially expressed genes are clear. Discerning the identities of

non-annotated genes and their roles during stress and bleaching represents the true challenge for coral biologists. While a coral genome project can certainly aid in the annotation of genes, the identification and functional characterization of coral-specific genes will be slower to realize. The areas of bioinformatics, genomics, systems biology, and cell biology hold immense promise in the future as we strive to understand the coral-algal symbiosis at the level of a model system.

FIGURES

Figure 1. A schematic of the calcium (Ca^{2+}) signaling pathways based on the reference pathway in the KEGG database (Kanehisa & Goto 2000) found at http://www.genome.jp/kegg/pathway/hsa/hsa04020.html. Genes in green boxes are those for which homologous genes are present in sequence databases for *A. palmata* and/or *M. faveolata* (for Clone IDs see Table 4). Calmodulin (CaM), which is in a yellow box is both present in coral sequence databases and down-regulated upon thermal stress as detected using microarrays.

Figure 1.

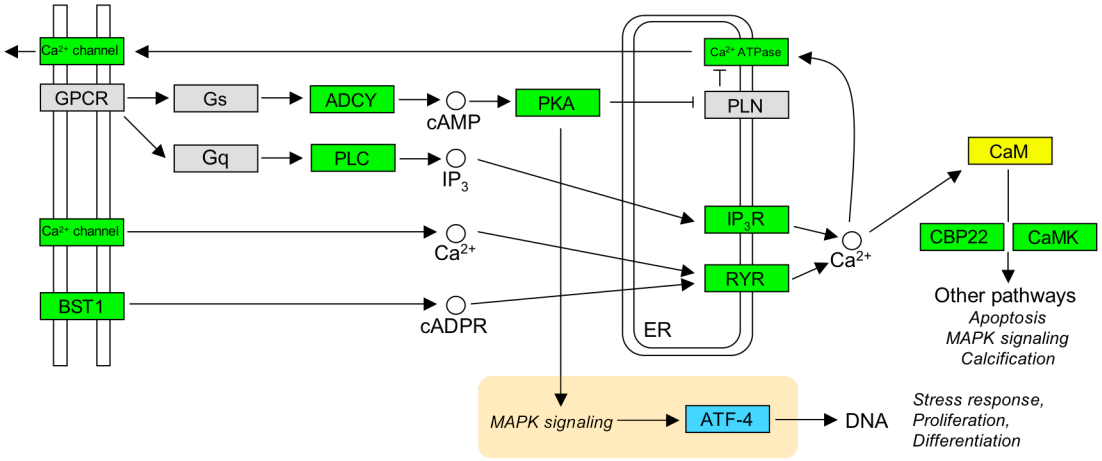
Ca2+ channel
GPCR
Gs
ADCY
cAMP
PKA
Ca2+ ATPase
PLN
Gq
PLC
IP3
CaM
Ca2+ channel
Ca2+
IP3R
CBP22
CaMK
BST1
cADPR
RYR
Ca2+
Other pathways
Apoptosis
MAPK signaling
Calcification
ER
MAPK signaling
ATF-4
DNA
Stress response,
Proliferation,
Differentiation

Figure 2. A schematic of the mitogen-activated protein kinase (MAPK) signaling pathways based on the reference pathway in the KEGG database (Kanehisa & Goto 2000) found at http://www.genome.jp/kegg/pathway/hsa/hsa04010.html. Genes in green boxes are those for which homologous genes are present in sequence databases for *A. palmata* and/or *M. faveolata* (for Clone IDs see Table 5). Genes in blue boxes are both present in coral sequence databases and up-regulated upon thermal stress as detected using microarrays.

Figure 2.

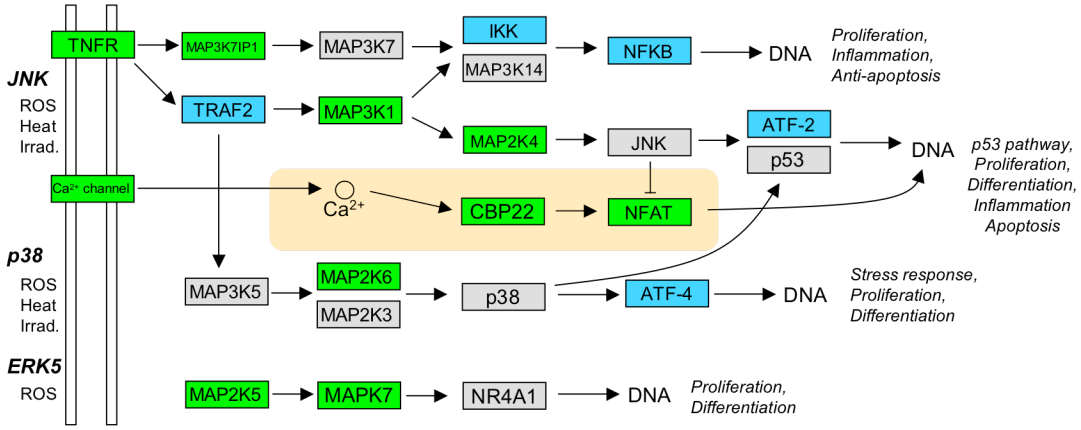
TNFR
MAP3K7IP1
MAP3K7
IKK
MAP3K14
NFKB
DNA
Proliferation,
Inflammation,
Anti-apoptosis
JNK
ROS
Heat
Irrad.
TRAF2
MAP3K1
MAP2K4
JNK
ATF-2
p53
DNA
p53 pathway,
Proliferation,
Differentiation,
Inflammation
Apoptosis
Ca2+ channel
Ca2+
CBP22
NFAT
p38
ROS
Heat
Irrad.
MAP3K5
MAP2K6
MAP2K3
p38
ATF-4
DNA
Stress response,
Proliferation,
Differentiation
ERK5
ROS
MAP2K5
MAPK7
NR4A1
DNA
Proliferation,
Differentiation

Figure 3. A 'see-saw' design illustrating the hypothesis that the coral host transcriptome is shaped by the competing effects of stress and their algal endosymbionts. Based on the microarray experiments described in this dissertation, it is supposed that symbiont effects are dominant in experiments using long acclimation times, slow thermal ramping, stress-resistant coral species, and coral species known to associate with multiple symbiont clades (i.e. similar to experiments in chapter 3). On the other hand, stress effects are dominant in experiments using short acclimation times, rapid thermal ramping, sensitive coral species, and species that associate with only one clade of symbiont (i.e. similar to experiments in chapter 2).

Figure 3.

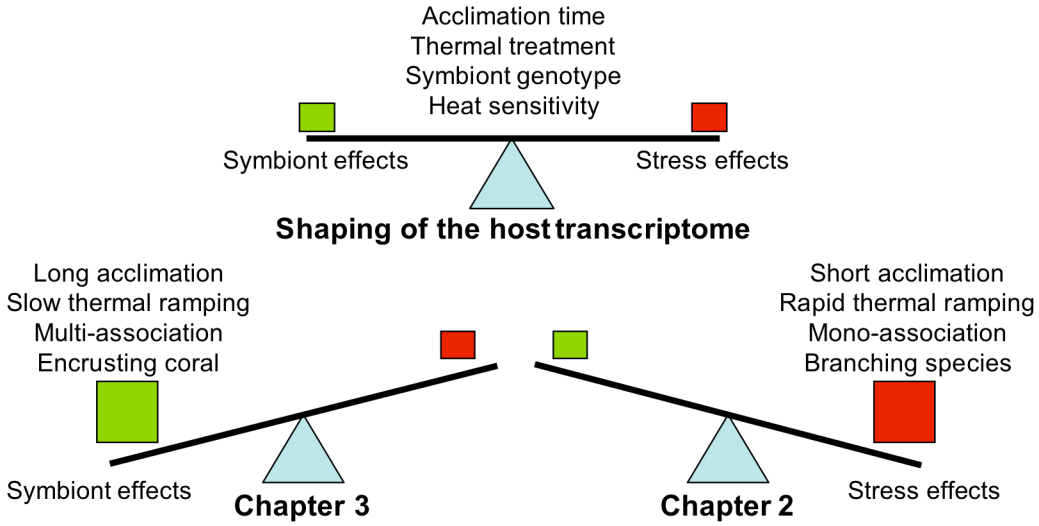
Acclimation time
Thermal treatment
Symbiont genotype
Heat sensitivity
Symbiont effects
Stress effects
Shaping of the host transcriptome
Long acclimation
Slow thermal ramping
Multi-association
Encrusting coral
Short acclimation
Rapid thermal ramping
Mono-association
Branching species
Symbiont effects
Chapter 3
Chapter 2
Stress effects

TABLES

Table 1. A list of differentially expressed cellular processes detected in microarray experiments in the corals *M. faveolata* and *A. palmata* (superscript 1 and 2 respectively). Letter superscripts denote the whether a process is part of the conserved cellular stress response (C), or possibly specific to symbiotic corals (S).

Table 1.

Cellular processes/components affected by thermal stress
Up-regulated
Antioxidant response [1,2,C]
Cell signaling and transcription factors [1,2,S]
Chaperone activity [1,2,C]
Glyoxylate cycle [2,S]
Nucleic acid stabilization and repair [2,C]
Removal of damaged macromolecules [2,C]
Vesicle/ion/macromolecule transport [1,2,S]
Down-regulated
Calcium homeostasis [1,2,C]
Cell cycle control [1,2,C]
Ribosomal proteins [1,2,C]
Modified (both up and down)
Actin cytoskeleton [1,2,C]
Cell death [1,2,C]
Extracellular matrix [1,2,S]
Metabolite transfer between host and symbiont [2,S]
Nitric oxide signaling [2,S]
Sensory perception [2,S]

Table 2. A list of differentially expressed genes overlapping between lists generated in microarray experiments of thermal stress in the corals *M. faveolata* and *A. palmata*. Clone IDs are searchable at: http://sequoia.ucmerced.edu/SymBioSys/index.php. A superscript O in the 'Clone ID' columns denote orthologous sequences.

Table 2.

Annotation	Clone ID *M. faveolata*	*A. palmata*	Cellular Component/Process
Actin	CAOO1104	CAOG395 CAOH739 CAOH820	Actin cytoskeleton
Ankyrin repeat domain-containing protein	CAOO1106	AOKG503	Cell signaling
Bromodomain-containing protein	CAON1597	AOKF837	Transcription regulation
Calmodulin	AOSF573	CAOG430	Calcium signaling
Collagen alpha-1(II) chain	AOSF1268˚	AOKF900˚	Extracellular matrix
Eukaryotic translation initiation factor subunit	AOSF620 AOSC681 CAON847	AOKF794	Translation regulation
Kunitz-type peptidase inhibitor	AOSF907˚	AOKF1161˚	Extracellular matrix
Gelsolin/Severin	AOSF1307˚ CAON1914	CAOG410˚	Actin cytoskeleton
Heat shock protein HSP 90-alpha	AOSC617	AOKF986	Chaperone activity
Histone H2A.V (Fragment)	AOSF622	AOKF1050	DNA binding
Myosin	CAON658˚ AOSF969	AOKF396˚ CAOH671	Actin cytoskeleton
Polyamine-modulated factor 1-binding prot. 1	CAOO2078	CAOH831	Actin cytoskeleton
Protein BTG1	AOSB1072	AOKF732	Cell cycle regulation
Selenoprotein	AOSF1308	AOKF908	Protein degradation
Transcription factor HES-1	AOSF533	CAOI984	Transcription regulation
Vitellogenin-2	AOSF1022˚	CAOH1099˚	Lipid metabolism

Table 3. A list of differentially expressed cell signaling molecules and transcription factors identified in microarray experiments in the corals *M. faveolata* and *A. palmata*. Clone IDs are searchable at: http://sequoia.ucmerced.edu/SymBioSys/index.php.

Table 3.

Clone ID	Common Name	E-value	Change
A. palmata			
AOKF1550	Nuclear factor erythroid 2-related factor 3 (Nrf3)	5.E-08	Up
AOKF1682	NF-κB p105 subunit (Death domain)	6.E-07	Up
AOKF1938	Receptor-type tyrosine-protein phosphatase α	6.E-45	Up
AOKF494	Serine/threonine-protein kinase 6	1.E-109	Down
AOKF654	Trxn init. factor TFIID subunit 13	5.E-21	Down
AOKF775	Protein sprint	5.E-06	Up
AOKF917	cAMP-dep. trxn factor ATF-2	8.E-31	Up
AOKF942	Nuclear factor erythroid 2-related factor 3 (Nrf3)	5.E-08	Up
AOKG1293	Trxnal repressor NF-X1	8.E-36	Up
CAOH485	NF-κB p105 subunit (Ankyrin repeat domain)	2.E-37	Up
CAOH623	cAMP-responsive element-binding protein-like 2	2.E-18	Up
CAOH936	cAMP-dependent trxn factor ATF-4	1.E-13	Up
CAOI879	Transmembrane emp24 domain-containing protein 1	2.E-25	Up
CCHX4259.b1	TNF receptor-associated factor 3 (TRAF3)	6.E-53	Up
CCHX9815	NF-κB p105 subunit (Rel homology domain)	1.E-38	Up
M. faveolata			
AOSB596	Nuclear hormone receptor family member nhr-6	4.E-23	Up
AOSB763	Protein tyrosine phosphatase type IVA	4.E-56	Up
AOSC957	Protein FEV	2.E-49	Down
AOSF1361	Adenosine receptor A1	2.E-07	Down
AOSF533	Trxn factor HES-1	3.E-22	Down
AOSF666	RING-box protein 2	5.E-49	Up
AOSF861	Tyrosine-protein phosphatase 1	4.E-20	Up
AOSF882	CCAAT/enhancer-binding protein γ	3.E-15	Down
CAON819	Receptor-type tyrosine-protein phosphatase N2	1.E-128	Down

Table 4. A list of genes identified in the sequences resources for the corals *A. palmata* and *M. faveolata* that are involved in calcium (Ca^{2+}) signaling. Clone IDs and contig numbers are searchable at: http://sequoia.ucmerced.edu/SymBioSys/index.php. Annotations are based on the best BLAST hit to the SwissProt database (OS=organism, GN=gene name, and Acc=Accession number).

Table 4.

Clone ID/Contig	Gene	SwissProt Annotation (best BLAST hit)
M. faveolata		
CCHW12760.b1_c_s	CAMK	Ca^{2+}/calmodulin-dep protein kinase type 1 OS=R. norvegicus GN=Camk1; Acc=KCC1A_RAT; E=7.0e-88
CCHW13802.b1_c_s	Ca^{2+} channel	Two pore calcium channel protein 1 OS=R. norvegicus GN=Tpcn1; Acc=TPC1_RAT; E=9.0e-28
Contig3371	CBP22	Calcium-binding protein p22 OS=R. norvegicus GN=Chp; Acc=CHP1_RAT; E=4.0e-60
CCHW12227.b1_c_s	IP_3R	Inositol 1,4,5-trisphosphate receptor OS=D. melanogaster GN=Itp-r83A; Acc=ITPR_DROME; E=2.0e-66
Contig2107	RYR	SPRY domain-containing SOCS box protein 3 OS=H. sapiens GN=SPSB3; Acc=SPSB3_HUMAN; E=8.0e-27
Contig3190	RYR	RING finger and SPRY containing protein 1 OS=P. abelii GN=RSPRY1; Acc=RSPRY_PONAB; E=1.0e-109
A. palmata		
CCHX6929.b1_c_s	Ca^{2+} channel	Extracellular Ca^{2+}-sensing receptor OS=M.musculus GN=Casr; Acc=CASR_MOUSE; E=1.0e-30
Contig2416	CBP22	Calcium-binding protein p22 OS=R. norvegicus GN=Chp; Acc=CHP1_RAT; E=2.0e-54
Contig2453	Ca^{2+} channel	Two pore calcium channel protein 1 OS=H. sapiens GN=TPCN1; Acc=TPC1_HUMAN; E=4.0e-29
Contig2876	CAMK	Calcium/calmodulin-dependent protein kinase OS=D. melanogaster GN=Caki; Acc=CAKI_DROME; E=3.0e-07
Contig3914	Ca^{2+} channel	Calcium-transporting ATPase type 2C member 1 OS=P. abelii GN=ATP2C1; Acc=AT2C1_PONAB; E=1.0e-08
Contig4585	Ca^{2+} channel	Plasma membrane Ca^{2+}-transporting ATPase 4 OS=R. norvegicus GN=Atp2b4; Acc=AT2B4_RAT; E=5.0e-69
CAFC486.g1_c_s	PLC	Inactive phospholipase C-like protein 2 OS=M.musculus GN=Plcl2; Acc=PLCL2_MOUSE; E=4.0e-80
CCHX8334.g1_c_s	PLC	Phosphoinositide phospholipase C 3 OS=A. thaliana GN=PLC3; Acc=PLCD3_ARATH; E=2.0e-06
CCHX9258.b1_c_s	IP_3R	Inositol 1,4,5-trisphosphate receptor type 2 OS=M. musculus GN=Itpr2; Acc=ITPR2_MOUSE; E=8.0e-73
CCHX12213.b1_c_s	BST1	ADP-ribosyl cyclase OS=A. kurodai; Acc=NADA_APLKU; E=1.0e-27
Contig2238	PKA	cAMP-dep protein kinase type II reg subunit OS=S. purpuratus PE=2 SV=1; Acc=KAPR_STRPU; E=1.0e-106
CAOI2411.b1_c_s	ADCY	Adenylate cyclase type 6 OS=R. norvegicus GN=Adcy6; Acc=ADCY6_RAT; E=3.0e-16
Contig6264	ADCY	Adenylate cyclase type 9 OS=M. musculus GN=Adcy9; Acc=ADCY9_MOUSE; E=3.0e-15
Contig1964	RYR	SPRY domain-containing SOCS box protein 3 OS=H. sapiens GN=SPSB3; Acc=SPSB3_HUMAN; E=2.0e-31

Table 5. A list of genes identified in the sequences resources for the corals *A. palmata* and *M. faveolata* that are involved in mitogen-activated protein kinase (MAPK) signaling. Clone IDs and contig numbers are searchable at: http://sequoia.ucmerced.edu/SymBioSys/index.php. Annotations are based on the best BLAST hit to the SwissProt database (OS=organism, GN=gene name, and Acc=Accession number).

Table 5.

Clone ID/Contig	Gene	SwissProt Annotation (best BLAST hit)
M. faveolata		
Contig3314	MAP2K4	Dual specificity MAP kinase kinase 4 OS=M. musculus GN=Map2k4; Acc=MP2K4_MOUSE; E=1.0e-101
CCHW9949.b1_c_s	MAP2K6	Dual specificity MAP kinase kinase 6 OS=M. musculus GN=Map2k6; Acc=MP2K6_MOUSE; E=8.0e-42
Contig3745	MAP3K1	MAP kinase kinase kinase 1 OS=R. norvegicus GN=Map3k1; Acc=M3K1_RAT; E=2.0e-08
Contig913	NFAT-5	Nuclear factor of activated T-cells 5 OS=M. musculus GN=Nfat5; Acc=NFAT5_MOUSE; E=9.0e-23
CCHW14552.b1_c_s	TNFR	TNF receptor superfamily member 16 OS=M. musculus GN=Ngfr; Acc=TNR16_MOUSE; E=2.0e-11
CCHW2966.b1_c_s	NFkB	Nuclear factor NF-kappa-B p105 subunit OS=G. gallus GN=NFKB1; Acc=NFKB1_CHICK; E=5.0e-40
Contig1270	NFkB	Nuclear factor NF-kappa-B p105 subunit OS=G. gallus GN=NFKB1; Acc=NFKB1_CHICK; E=1.0e-43
CCHW11334.b1_c_s	TRAF4	TNF receptor-associated factor 4 OS=H. sapiens GN=TRAF4; Acc=TRAF4_HUMAN; E=9.0e-35
CCHW13419.b1_c_s	TRAF1	TNF receptor-associated factor 1 OS=M. musculus GN=Traf1; Acc=TRAF1_MOUSE; E=1.0e-36
CCHW16073.b1_c_s	TRAF5	TNF receptor-associated factor 5 OS=H. sapiens GN=TRAF5; Acc=TRAF5_HUMAN; E=8.0e-07
CCHW8441.b1_c_s	TRAF6	TNF receptor-associated factor 6 OS=H. sapiens GN=TRAF6; Acc=TRAF6_HUMAN; E=1.0e-31
CCHW9787.b1_c_s	TRAF3	TNF receptor-associated factor 3 OS=M. musculus GN=Traf3; Acc=TRAF3_MOUSE; E=4.0e-48
AOSB596.b2_c_s	Nuclear receptor	Nuclear hormone receptor family member nhr-6 OS=C. elegans GN=nhr-6; Acc=NHR6_CAEEL; E=4.0e-23
Contig1070	Nuclear receptor	Nuclear receptor subfamily 2 group F member 1 OS=D. rerio GN=nr2f1; Acc=NR2F1_DANRE; E=1.0e-156
A. palmata		
AOKG2255.b2_c_s	MAP2K5	Dual specificity MAP kinase kinase 5 OS=R. norvegicus GN=Map2k5; Acc=MP2K5_RAT; E=6.0e-66
Contig6505	MAPK7	MAP kinase 7 OS=M. musculus GN=Mapk7; Acc=MK07_MOUSE; E=1.0e-116
CCHX10898.b1_c_s	MAP3K7IP1	MAP KKK 7-interacting protein 1 OS=H.sapiens GN=MAP3K7IP1; Acc=TAB1_HUMAN; E=8.0e-34
CCHX11092.b1_c_s	MAP3K1	MAP kinase kinase kinase 1 OS=M. musculus GN=Map3k1; Acc=M3K1_MOUSE; E=2.0e-17
CCHX8614.b1_c_s	TNFR	TNF receptor superfamily member 19 OS=H. sapiens GN=TNFRSF19; Acc=TNR19_HUMAN; E=1.0e-06
Contig3199	TNFR	TNF receptor superfamily member 14 OS=H. sapiens GN=TNFRSF14; Acc=TNR14_HUMAN; E=3.0e-09
Contig1488	NFkB	Nuclear factor NF-kappa-B p105 subunit OS=G. gallus GN=NFKB1; Acc=NFKB1_CHICK; E=2.0e-37
Contig1777	NFkB	Nuclear factor NF-kappa-B p105 subunit OS=M. musculus GN=Nfkb1; Acc=NFKB1_MOUSE; E=6e-07
Contig3207	NFkB	Nuclear factor NF-kappa-B p105 subunit OS=C. familiaris GN=NFKB1; Acc=NFKB1_CANFA; E=1e-38
Contig3687	IKK	Inhibitor of NF kappa-B kinase subunit alpha OS=X. laevis GN=chuk; Acc=IKKA_XENLA; E=5.0e-57
CCHX16355.b1_c_s	TRAF2	TNF receptor-associated factor 2 OS=M. musculus GN=Traf2; Acc=TRAF2_MOUSE; E=2.0e-12
CCHX4259.b1_c_s	TRAF3	TNF receptor-associated factor 3 OS=M. musculus GN=Traf3; Acc=TRAF3_MOUSE; E=6.0e-53
CCHX15459.b1_c_s	TRAF5	TNF receptor-associated factor 5 OS=M. musculus GN=Traf5; Acc=TRAF5_MOUSE; E=2.0e-27
CCHX3191.b1_c_s	TRAF6	TNF receptor-associated factor 6 OS=M. musculus GN=Traf6; Acc=TRAF6_MOUSE; E=1.0e-45
Contig4165	Nuclear receptor	Nuclear receptor subfam 2 grp C memb 2 OS=H. sapiens GN=NR2C2; Acc=NR2C2_HUMAN; E=1.0e-31

REFERENCES

Abele D, Heise K, Portner HO, Puntarulo S (2002) Temperature-dependence of mitochondrial function and production of reactive oxygen species in the intertidal mud clam *Mya arenaria*. Journal of Experimental Biology 205:1831-1841

Agrawal N, Kango M, Mishra A, Sinha P (1995) Neoplastic transformation and aberrant cell-cell interactions in genetic mosaics of lethal(2)giant larvae (lgl), a tumor suppressor gene of Drosophila. Developmental Biology 172:218-229

Allemand D, Ferrier-Pages C, Furla P, Houlbreque F, Puverel S, Reynaud S, Tambutte E, Tambutte S, Zoccola D (2004) Biomineralisation in reef-building corals: from molecular mechanisms to environmental control. Comptes Rendus Palevol 3:453-467

Allemand D, Tambutte E, Girard JP, Jaubert J (1998) Organic matrix synthesis in the scleractinian coral stylophora pistillata: role in biomineralization and potential target of the organotin tributyltin. Journal of Experimental Biology 201 (Pt 13):2001-2009

Ameri K, Harris AL (2008) Activating transcription factor 4. Int J Biochem Cell Biol 40:14-21

Baker AC (2003) Flexibility and specificity in coral-algal symbiosis: Diversity, ecology, and biogeography of *Symbiodinium*. Annu Rev Ecol Evol Syst 34:661-689

Baker AC, Rowan R, Knowlton N (1997) Symbiosis ecology of two Caribbean Acroporid corals. Proceedings of the 8th International Coral Reef Symposium 2:1295-1300

Baker AC, Starger CJ, McClanahan TR, Glynn PW (2004) Corals' adaptive response to climate change. Nature 430:741

Bay LK, Ulstrup KE, Nielsen HB, Jarmer H, Goffard N, Willis BL, Miller DJ, Van Oppen MJ (2009) Microarray analysis reveals transcriptional plasticity in the reef building coral Acropora millepora. Mol Ecol 18:3062-3075

Bell J, Neilson L, Pellegrini M (1988) Effect of heat shock on ribosome synthesis in Drosophila melanogaster. Molecular and Cellular Biology 8:91-95

Bentis CJ, Kaufman L, Golubic S (2000) Endolithic fungi in reef-building corals (Order : Scleractinia) are common, cosmopolitan, and potentially pathogenic. Biol Bull 198:254-260

Berkelmans R, Oliver JK (1999) Large-scale bleaching of corals on the Great Barrier Reef. Coral Reefs 18:55-60

Berkelmans R, van Oppen MJH (2006) The role of zooxanthellae in the thermal tolerance of corals: a 'nugget of hope' for coral reefs in an era of climate change. Proceedings of the Royal Society B-Biological Sciences 273:2305-2312

Bhagooli R, Hidaka M (2003) Comparison of stress susceptibility of in hospite and isolated zooxanthellae among five coral species. Journal of Experimental Marine Biology and Ecology 291:181-197

Black N, Voellmy R, Szmant A (1995) Heat shock protein induction in Montastraea faveolata and Aiptasia pallida exposed to elevated temperatures. Biological Bulletin 188:234-240

Boatright KM, Salvesen GS (2003) Mechanisms of caspase activation. Curr Opin Cell Biol 15:725-731

Bou-Abdallah F, Chasteen ND, Lesser MP (2006) Quenching of superoxide radicals by green fluorescent protein. Biochim Biophys Acta 1760:1690-1695

Brown B, Le Tissier M, Bythell J (1995) Mechanisms of bleaching deduced from histological studies of reef corals sampled during a natural bleaching event. Marine Biology 122:655–663

Brown BE (1997) Adaptations of reef corals to physical environmental stress. Advances in Marine Biology, Vol 31 31:221-299

Brown BE, Dunne RP, Goodson MS, Douglas AE (2002) Experience shapes the susceptibility of a reef coral to bleaching. Coral Reefs 21:119-126

Bruckner AW (2002) Proceedings of the Caribbean Acropora Workshop: Potential Applications of the U.S. Endangered Species Act as a Conservation Strategy. NMFS-OPR-24. NOAA Technical Memorandum, Silver Spring, Maryland

Brummelkamp TR, Nijman SM, Dirac AM, Bernards R (2003) Loss of the cylindromatosis tumour suppressor inhibits apoptosis by activating NF-kappaB. Nature 424:797-801

Brummendorf T, Kenwrick S, Rathjen FG (1998) Neural cell recognition molecule L1: from cell biology to human hereditary brain malformations. Current Opinion in Neurobiology 8:87-97

Bruno JF, Selig ER, Casey KS, Page CA, Willis BL, Harvell CD, Sweatman H, Melendy AM (2007) Thermal stress and coral cover as drivers of coral disease outbreaks. PLoS Biol 5:e124

Buckley BA, Gracey AY, Somero GN (2006) The cellular response to heat stress in the goby Gillichthys mirabilis: a cDNA microarray and protein-level analysis. Journal of Experimental Biology 209:2660-2677

Cadenas E, Davies KJ (2000) Mitochondrial free radical generation, oxidative stress, and aging. Free Radical Biology and Medicine 29:222-230

Cantin NE, van Oppen MJH, Willis BL, Mieog JC, Negri AP (2009) Juvenile corals can acquire more carbon from high-performance algal symbionts. Coral Reefs 28:405-414

Carpenter KE, Abrar M, Aeby G, Aronson RB, Banks S, Bruckner A, Chiriboga A, Cortes J, Delbeek JC, DeVantier L, Edgar GJ, Edwards AJ, Fenner D, Guzman HM, Hoeksema BW, Hodgson G, Johan O, Licuanan WY, Livingstone SR, Lovell ER, Moore JA, Obura DO, Ochavillo D, Polidoro BA, Precht WF, Quibilan MC, Reboton C, Richards ZT, Rogers AD, Sanciangco J, Sheppard A, Sheppard C, Smith J, Stuart S, Turak E, Veron JEN, Wallace C, Weil E, Wood E (2008) One-third of reef-building corals face elevated extinction risk from climate change and local impacts. Science 321:560-563

Chandra D, Choy G, Daniel PT, Tang DG (2005) Bax-dependent regulation of Bak by voltage-dependent anion channel 2. Journal of Biological Chemistry 280:19051-19061
Cheah KS, Lau ET, Au PK, Tam PP (1991) Expression of the mouse alpha 1(II) collagen gene is not restricted to cartilage during development. Development 111:945-953
Chen ZD, Dixon JE, Zalkin H (1990) Cloning of a chicken liver cDNA encoding 5-aminoimidazole ribonucleotide carboxylase and 5-aminoimidazole-4-N-succinocarboxamide ribonucleotide synthetase by functional complementation of Escherichia coli pur mutants. Proc Natl Acad Sci U S A 87:3097-3101
Cheng EH, Sheiko TV, Fisher JK, Craigen WJ, Korsmeyer SJ (2003) VDAC2 inhibits BAK activation and mitochondrial apoptosis. Science 301:513-517
Chowdhury S, Smith KW, Gustin MC (1992) Osmotic stress and the yeast cytoskeleton: phenotype-specific suppression of an actin mutation. J Cell Biol 118:561-571
Chun CK, Troll JV, Koroleva I, Brown B, Manzella L, Snir E, Almabrazi H, Scheetz TE, de Fatima Bonaldo M, Casavant TL, Soares MB, Ruby EG, McFall-Ngai MJ (2008) Effects of colonization, luminescence, and autoinducer on host transcription during development of the squid-vibrio association. Proceedings of the National Academy of Sciences of the United States of America 105:11323-11328
Clem RJ, Cheng EH, Karp CL, Kirsch DG, Ueno K, Takahashi A, Kastan MB, Griffin DE, Earnshaw WC, Veliuona MA, Hardwick JM (1998) Modulation of cell death by Bcl-XL through caspase interaction. Proc Natl Acad Sci U S A 95:554-559
Coakley WT (1987) Hyperthermia effects on the cytoskeleton and on cell morphology. Symp Soc Exp Biol 41:187-211
Coffroth MA, Santos SR (2005) Genetic diversity of symbiotic dinoflagellates in the genus Symbiodinium. Protist 156:19-34
Coles S, Jokiel P (1978) Synergistic effects of temperature, salinity and light on the hermatypic coral *Montipora verrucosa*. Marine Biology 49
Costanza R, dArge R, deGroot R, Farber S, Grasso M, Hannon B, Limburg K, Naeem S, ONeill RV, Paruelo J, Raskin RG, Sutton P, vandenBelt M (1997) The value of the world's ecosystem services and natural capital. Nature 387:253-260
Covarrubias MY, Khan RL, Vadigepalli R, Hoek JB, Schwaber JS (205) Chronic alcohol exposure alters transcription broadly in a key integrative brain nucleus for homeostasis: the nucleus tractus solitarus. Physiological Genomics 24:45-58
Cui X, Hwang JT, Qiu J, Blades NJ, Churchill GA (2005) Improved statistical tests for differential gene expression by shrinking variance components estimates. Biostatistics 6:59-75
Cuif JP, Dauphin Y, Freiwald A, Gautret P, Zibrowius H (1999) Biochemical markers of zoaxanthellae symbiosis in soluble matrices of skeleton of 24 Scleractinia

species. Comparative Biochemistry and Physiology A: Molecular and Integrative Physiology 123:269-278
Dallas PB, Gottardo NG, Firth MJ, Beesley AH, Hoffmann K, Terry PA, Freitas JR, Boag JM, Cummings AJ, Kees UR (2005) Gene expression levels assessed by oligonucleotide microarray analysis and quantitative real-time RT-PCR - how well do they correlate? BMC Genomics 6:59
Davidson JF, Schiestl RH (2001) Mitochondrial respiratory electron carriars are involved in oxidative stress during heat stress in *Saccaromyces cerevisiae.* Molecular and Cellular Biology 21:8483-8489
Davidson JF, Whyte B, Bissinger PH, Schiestl RH (1996) Oxidative stress is involved in heat-induced cell death in *Saccaromyces cerevisiae.* Proceedings of the National Academy of Sciences of the United States of America 93:5116-5121
de la Vega E, Degnan BM, Hall MR, Wilson KJ (2007) Differential expression of immune-related genes and transposable elements in black tiger shrimp (*Panaeus monodon*) exposed to a range of environmental stressors. Fish & Shellfish Immunology 23:1072-1088
Dedio J, Konig P, Wohlfart P, Schroeder C, Kummer W, Muller-Esterl W (2001) NOSIP, a novel modulator of endothelial nitric oxide synthase activity. Faseb J 15:79-89
Delon I, Brown NH (2007) Integrins and the actin cytoskeleton. Current Opinion in Cell Biology 19:43-50
DeSalvo MK, Sunagawa S, Fisher PL, Voolstra CR, Iglesias-Prieto R, Medina M (2010a) Coral host transcriptomic states are correlated with Symbiodinium genotypes. Molecular Ecology 19:1174-1186
DeSalvo MK, Sunagawa S, Voolstra CR, Medina M (2010b) Transcriptomic responses to heat stress and bleaching in the elkhorn coral *Acropora palmata*. Marine Ecology Progress Series 402:97-113
DeSalvo MK, Voolstra CR, Sunagawa S, Schwarz JA, Stillman JH, Coffroth MA, Szmant AM, Medina M (2008) Differential gene expression during thermal stress and bleaching in the Caribbean coral *Montastraea faveolata*. Mol Ecol 17:3952-3971
Domart-Coulon IJ, Elbert DC, Scully EP, Calimlim PS, Ostrander GK (2001) Aragonite crystallization in primary cell cultures of multicellular isolates from a hard coral, Pocillopora damicornis. Proc Natl Acad Sci U S A 98:11885-11890
Douglas AE (1998) Host benefit and the evolution of specialization in symbiosis. Heredity 81:599-603
Douglas AE (2003) Coral bleaching--how and why? Marine Pollution Bulletin 46:385-392
Douglass AD, Vale RD (2008) Single-molecule imaging of fluorescent proteins. Methods Cell Biol 85:113-125
Dove S, Carlos Ortiz J, Enriquez S, Fine M, Fisher P, Iglesias-Prieto R, Thornhill D, Hoegh-Guldberg O (2006) Response of the holosymbiont pigments from the

scleractinian coral *Montipora monasteriata* to short-term heat stress. Limnology and Oceanography 51:1149-1158
Downs CA, Fauth JE, Halas JC, Dustan P, Bemiss J, Woodley CM (2002) Oxidative Stress and Seasonal Coral Bleaching. Free Radical Biology & Medicine 33:533–543
Downs CA, Fauth JE, Robinson CE, Curry R, Lanzendorf B, Halas JC, Halas J, Woodley CM (2005) Cellular diagnostics and coral health: declining coral health in the Florida Keys. Mar Pollut Bull 51:558-569
Downs CA, Kramarsky-Winter E, Martinez J, Kushmaro A, Woodley CM, Loya Y, Ostrander GK (2009) Symbiophagy as a cellular mechanism for coral bleaching. Autophagy 5:211-216
Downs CA, Mueller E, Phillips S, Fauth JE, Woodley CM (2000) A molecular biomarker system for assessing the health of coral (Montastraea faveolata) during heat stress. Marine Biotechnology 2:533-544
Droge W (2002) Free radicals in the physiological control of cell function. Physiol Rev 82:47-95
Duchen MR (2000) Mitochondria and calcium: from cell signalling to cell death. Journal of Physiology 529 Pt 1:57-68
Dunn SR, Bythell JC, Le Tissier MDA, Burnett WJ, Thomason JC (2002) Programmed cell death and cell necrosis activity during hyperthermic stress-induced bleaching of the symbiotic sea anemone *Aiptasia* sp. Journal of Experimental Marine Biology and Ecology 272:29– 53
Dunn SR, Phillips WS, Spatafora JW, Green DR, Weis VM (2006) Highly conserved caspase and Bcl-2 homologues from the sea anemone *Aiptasia pallida*: lower metazoans as models for the study of apoptosis evolution. Journal of Molecular Evolution 63:95-107
Dunn SR, Schnitzler CE, Weis VM (2007) Apoptosis and autophagy as mechanisms of dinoflagellate symbiont release during cnidarian bleaching: every which way you lose. Proc Biol Sci 274:3079-3085
Dunn SR, Thomason JC, Le Tissier MD, Bythell JC (2004) Heat stress induces different forms of cell death in sea anemones and their endosymbiotic algae depending on temperature and duration. Cell Death Differ 11:1213-1222
Dykens JA, Shick JM, Benoit C, Buettner GR, Winston GW (1992) Oxygen Radical Production in the Sea-Anemone *Anthopleura Elegantissima* and Its Endosymbiotic Algae. Journal of Experimental Biology 168:219-241
Edge SE, Morgan MB, Gleason DF, Snell TW (2005) Development of a coral cDNA array to examine gene expression profiles in *Montastraea faveolata* exposed to environmental stress. Marine Pollution Bulletin 51:507-523
Edge SE, Morgan MB, Snell TW (2008) Temporal analysis of gene expression in a field population of the Scleractinian coral Montastraea faveolata. Journal of Experimental Marine Biology and Ecology 355:114-124
Etienne W, Meyer MH, Peppers J, Meyer RA (2004) Comparison of mRNA gene expression by RT-PCR and DNA microarray. Biotechniques 36:618-626

Fang LS, Huang SP, Lin KL (1997) High temperature induces the synthesis of heat-shock proteins and the elevation of intracellular calcium in the coral Acropora grandis. Coral Reefs 16:127-131
Fill M, Copello JA (2002) Ryanodine receptor calcium release channels. Physiological Reviews 82:893-922
Fitt WK, Warner ME (1995) Bleaching patterns of four species of Caribbean reef corals. Biological Bulletin 189:298-307
Frade PR, De Jongh F, Vermeulen F, Van Bleijswijk J, Bak RPM (2008) Variation in symbiont distribution between closely related coral species over large depth ranges. Molecular Ecology 17:691-703
Fukuda I, Ooki S, Fujita T, Murayama E, Nagasawa H, Isa Y, Watanabe T (2003) Molecular cloning of a cDNA encoding a soluble protein in the coral exoskeleton. Biochem Biophys Res Commun 304:11-17
Gateff E (1978) Malignant neoplasms of genetic origin in Drosophila melanogaster. Science 200:1448-1459
Gates RD, Baghdasarian G, Muscatine L (1992) Temperature stress causes host cell detachment in symbiotic cnidarians: implications for coral bleaching. Biol Bull 182:324-332
Gates RD, Edmunds PJ (1999) The Physiological Mechanisms of Acclimatization in Tropical Reef Corals. American Zoologist 39:30-43
Gavalas A, Dixon JE, Brayton KA, Zalkin H (1993) Coexpression of two closely linked avian genes for purine nucleotide synthesis from a bidirectional promoter. Mol Cell Biol 13:4784-4792
Gibson G (2002) Microarrays in ecology and evolution: a preview. Molecular Ecology 11:17-24
Gladfelter EH, Monahan RK, Gladfelter WB (1978) Growth rates of 5 reef-building corals in the northeast Caribbean. Bulletin of Marine Science 28:728-734
Gleason DF, Wellington GM (1993) Ultraviolet-Radiation and Coral Bleaching. Nature 365:836-838
Gleason MG (1993) Effects of Disturbance on Coral Communities - Bleaching in Moorea, French-Polynesia. Coral Reefs 12:193-201
Glynn PW (1988) El-Nino Southern Oscillation 1982-1983 - Nearshore Population, Community, and Ecosystem Responses. Annual Review of Ecology and Systematics 19:U309-&
Glynn PW (1993) Coral-Reef Bleaching - Ecological Perspectives. Coral Reefs 12:1-17
Glynn PW, Mate JL, Baker AC, Calderon MO (2001) Coral bleaching and mortality in Panama and Ecuador during the 1997-1998 El Nino-Southern Oscillation event: spatial/temporal patterns and comparisons with the 1982-1983 event. Bulletin of Marine Science 69:79-109
Glynn PW, Peters EC, Muscatine L (1985) Coral Tissue Microstructure and Necrosis - Relation to Catastrophic Coral Mortality in Panama. Diseases of Aquatic Organisms 1:29-37

Goreau T, McClanahan T, Hayes R, Strong A (2000) Conservation of coral reefs after the 1998 global bleaching event. Conservation Biology 14:5-15
Goulet TL (2006) Most corals may not change their symbionts. Marine Ecology-Progress Series 321:1-7
Goulet TL, Cook CB, Goulet D (2005) Effect of short-term exposure to elevated temperatures and light levels on photosynthesis of different host-symbiont combinations in the Aiptasia pallidal Symbiodinium symbiosis. Limnology and Oceanography 50:1490-1498
Gracey AY, Cossins AR (2003) Application of microarray technology in environmental and comparative physiology. Annual Review of Physiology 65:231-259
Gracey AY, Troll JV, Somero GN (2001) Hypoxia-induced gene expression profiling in the euryoxic fish Gillichthys mirabilis. Proceedings of the National Academy of Sciences of the United States of America 98:1993-1998
Grasso LC, Maindonald J, Rudd S, Hayward DC, Saint R, Miller DJ, Ball EE (2008) Microarray analysis identifies candidate genes for key roles in coral development. BMC Genomics 9:540
Gupta S, Campbell D, Derijard B, Davis RJ (1995) Transcription factor ATF2 regulation by the JNK signal transduction pathway. Science 267:389-393
Haber F, Weiss J (1934) The catalytic decomposition of H2O2 by iron salts. Proc R Soc Lond Ser A 147:332-351
Hai T, Curran T (1991) Cross-family dimerization of transcription factors Fos/Jun and ATF/CREB alters DNA binding specificity. Proc Natl Acad Sci U S A 88:3720-3724
Hajnoczky G, Davies E, Madesh M (2003) Calcium signaling and apoptosis. Biochemical and Biophysical Research Communications 304:445-454
Halbleib JM, Nelson WJ (2006) Cadherins in development: cell adhesion, sorting, and tissue morphogenesis. Genes and Development 20:3199-3214
Harding HP, Novoa I, Zhang Y, Zeng H, Wek R, Schapira M, Ron D (2000) Regulated translation initiation controls stress-induced gene expression in mammalian cells. Mol Cell 6:1099-1108
Harding HP, Zhang Y, Zeng H, Novoa I, Lu PD, Calfon M, Sadri N, Yun C, Popko B, Paules R, Stojdl DF, Bell JC, Hettmann T, Leiden JM, Ron D (2003) An integrated stress response regulates amino acid metabolism and resistance to oxidative stress. Mol Cell 11:619-633
Harel M, Ben-Dov E, Rasoulouniriana D, Siboni N, Kramarsky-Winter E, Loya Y, Barak Z, Wiesman Z, Kushmaro A (2008) A new Thraustochytrid, strain Fng1, isolated from the surface mucus of the hermatypic coral Fungia granulosa. FEMS Microbiol Ecol 64:378-387
Harriott VJ (1985) Mortality-Rates of Scleractinian Corals before and during a Mass Bleaching Event. Marine Ecology-Progress Series 21:81-88
Harvell CD, Kim K, Burkholder JM, Colwell RR, Epstein PR, Grimes DJ, Hofmann EE, Lipp EK, Osterhaus AD, Overstreet RM, Porter JW, Smith GW, Vasta GR

(1999) Emerging marine diseases--climate links and anthropogenic factors. Science 285:1505-1510
Harvell D, Jordán-Dahlgren E, Merkel S, Rosenberg E, Raymundo L, Smith G, Weil E, Willis B (2007) Coral disease, environmental drivers, and the balance between coral and microbial associates. Oceanography 20:172-195
Hawkins RD, Bashiardes S, Powder KE, Sajan SA, Bhonagiri V, Alvarado DM, Speck J, Warchol ME, Lovett M (2007) Large scale gene expression profiles of regenerating inner ear sensory epithelia. PLoS ONE 2:e525
Hayes JD, McLellan LI (1999) Glutathione and glutathione-dependent enzymes represent a co-ordinately regulated defence against oxidative stress. Free Radical Research 31:273-300
Hayes RL, King CM (1995) Induction of 70-kD heat shock protein in scleractinian corals by elevated temperature: significance for coral bleaching. Molecular Marine Biology and Biotechnology 4:36-42
Helman Y, Natale F, Sherrell RM, Lavigne M, Starovoytov V, Gorbunov MY, Falkowski PG (2008) Extracellular matrix production and calcium carbonate precipitation by coral cells in vitro. Proc Natl Acad Sci U S A 105:54-58
Herruer MH, Mager WH, Raue HA, Vreken P, Wilms E, Planta RJ (1988) Mild temperature shock affects transcription of yeast ribosomal protein genes as well as the stability of their mRNAs. Nucleic Acids Research 16:7917-7929
Hidalgo C (2005) Cross talk between Ca2+ and redox signalling cascades in muscle and neurons through the combined activation of ryanodine receptors/Ca2+ release channels. Philosophical Transactions of the Royal Society of London B: Biological Sciences 360:2237-2246
Hockenbery D, Nunez G, Milliman C, Schreiber RD, Korsmeyer SJ (1990) Bcl-2 is an inner mitochondrial membrane protein that blocks programmed cell death. Nature 348:334-336
Hoegh-Guldberg O (1999) Climate change, coral bleaching and the future of the world's coral reefs. Mar Freshw Res 50:839-866
Hoegh-Guldberg O, Mumby PJ, Hooten AJ, Steneck RS, Greenfield P, Gomez E, Harvell CD, Sale PF, Edwards AJ, Caldeira K, Knowlton N, Eakin CM, Iglesias-Prieto R, Muthiga N, Bradbury RH, Dubi A, Hatziolos ME (2007) Coral reefs under rapid climate change and ocean acidification. Science 318:1737-1742
Hoegh-Guldberg O, Salvat B (1995) Periodic Mass-Bleaching and Elevated Sea Temperatures - Bleaching of Outer Reef Slope Communities in Moorea, French-Polynesia. Marine Ecology-Progress Series 121:181-190
Hoegh-Guldberg O, Smith GJ (1989) The effect of sudden changes in temperature, irradiance and salinity on the population density and export of zooxanthellae from the reef corals *Stylophora pistillata* (Esper 1797) and *Seriatopora hystrix* (Dana 1846). Journal of Experimental Marine Biology and Ecology 129:279-303

Hoeksema BW (1991) Control of Bleaching in Mushroom Coral Populations (Scleractinia, Fungiidae) in the Java Sea - Stress Tolerance and Interference by Life-History Strategy. Marine Ecology-Progress Series 74:225-237
Hofmann GE, Burnaford JL, Fielman KT (2005) Genomics-fueled approaches to current challenges in marine ecology. Trends in Ecology and Evolution 20:305-311
Holmgren A (1985) Thioredoxin. Annual Review of Biochemistry 54:237-271
Hooper LV, Wong MH, Thelin A, Hansson L, Falk PG, Gordon JI (2001) Molecular analysis of commensal host-microbial relationships in the intestine. Science 291:881-884.
Huang SP, Lin KL, Fang LS (1998) The involvement of calcium in heat-induced coral bleaching. Zoological Studies 37:89-94
Hudson JH (1981) Growth-Rates in Montastraea-Annularis - a Record of Environmental-Change in Key-Largo-Coral-Reef-Marine-Sanctuary, Florida. Bulletin of Marine Science 31:444-459
Hughes TP (1994) Catastrophes, Phase Shifts, and Large-Scale Degradation of a Caribbean Coral Reef. Science 265:1547-1551
Hughes TP, Baird AH, Bellwood DR, Card M, Connolly SR, Folke C, Grosberg R, Hoegh-Guldberg O, Jackson JB, Kleypas J, Lough JM, Marshall P, Nystrom M, Palumbi SR, Pandolfi JM, Rosen B, Roughgarden J (2003) Climate change, human impacts, and the resilience of coral reefs. Science 301:929-933
Hughes TP, Tanner JE (2000) Recruitment failure, life histories, and long-term decline of Caribbean corals. Ecology 81:2250-2264
Huot J, Houle F, Marceau F, Landry J (1997) Oxidative stress-induced actin reorganization mediated by the p38 mitogen-activated protein kinase/heat shock protein 27 pathway in vascular endothelial cells. Circ Res 80:383-392
Iglesias-Prieto R, Beltran VH, LaJeunesse TC, Reyes-Bonilla H, Thome PE (2004) Different algal symbionts explain the vertical distribution of dominant reef corals in the eastern Pacific. Proc Biol Sci 271:1757-1763
Iglesias-Prieto R, Matta JL, Robins WA, Trench RK (1992) Photosynthetic response to elevated temperature in the symbiotic dinoflagellate Symbiodinium microadriaticum in culture. Proceedings of the National Academy of Sciences of the United States of America 89:10302-10305
Jackson JB, Kirby MX, Berger WH, Bjorndal KA, Botsford LW, Bourque BJ, Bradbury RH, Cooke R, Erlandson J, Estes JA, Hughes TP, Kidwell S, Lange CB, Lenihan HS, Pandolfi JM, Peterson CH, Steneck RS, Tegner MJ, Warner RR (2001) Historical overfishing and the recent collapse of coastal ecosystems. Science 293:629-637
Janmey PA, Stossel TP (1987) Modulation of gelsolin function by phosphatidylinositol 4,5-bisphosphate. Nature 325:362-364
Jimbo M, Yanohara T, Koike K, Koike K, Sakai R, Muramoto K, Kamiya H (2000) The D-galactose-binding lectin of the octocoral Sinularia lochmodes: characterization and possible relationship to the symbiotic dinoflagellates.

Comparative Biochemistry and Physiology - Part B: Biochemistry and Molecular Biology 125:227-236
Jokiel PL, Coles SL (1977) Effects of temperature on the mortality and growth of Hawaiian reef corals. Marine Biology 1977:201-208
Jones AM, Berkelmans R, van Oppen MJH, Mieog JC, Sinclair W (2008) A community change in the algal endosymbionts of a scleractinian coral following a natural bleaching event: field evidence of acclimatization. Proceedings of the Royal Society B-Biological Sciences 275:1359-1365
Jones R (2005) The ecotoxicological effects of Photosystem II herbicides on corals. Marine Pollution Bulletin 51:495-506
Jones RJ, Hoegh-Guldberg O, Larkum AWD, Schreiber U (1998) Temperature-induced bleaching of corals begins with impairment of the CO_2 fixation mechanism in zooxanthellae. Plant Cell Environ 21:1219
Kageyama R, Sasai Y, Nakanishi S (1991) Molecular characterization of transcription factors that bind to the cAMP responsive region of the substance P precursor gene. cDNA cloning of a novel C/EBP-related factor. J Biol Chem 266:15525-15531
Kalmykova AI, Klenov MS, Gvozdev VA (2005) Argonaute protein PIWI controls mobilization of retrotransposons in the Drosophila male germline. Nucleic Acids Research 33:2052-2059
Kanehisa M, Goto S (2000) KEGG: kyoto encyclopedia of genes and genomes. Nucleic Acids Res 28:27-30
Kasri NN, Parys JB, Callewaert G, Missiaen L, De Smedt H (2004) Calmodulin and calcium-release channels. Biological Research 37:577-582
Kassahn KS, Caley MJ, Ward AC, Connolly AR, Stone G, Crozier RH (2007) Heterologous microarray experiments used to identify the early gene response to heat stress in a coral reef fish. Molecular Ecology 16:1749-1763
Katzenellenbogen RA, Egelkrout EM, Vliet-Gregg P, Gewin LC, Gafken PR, Galloway DA (2007) NFX1-123 and poly(A) binding proteins synergistically augment activation of telomerase in human papillomavirus type 16 E6-expressing cells. J Virol 81:3786-3796
Kellogg CA (2004) Tropical Archaea: diversity associated with the surface microlayer of corals. Marine Ecology Progress Series 273:81-88
Kerr MK (2003) Design considerations for efficient and effective microarray studies. Biometrics 59:822-828
Khalesi MK (2008) Cell cultures from the symbiotic soft coral Sinularia flexibilis. In Vitro Cell Dev Biol Anim
Kimura RH, Choudary PV, Stone KK, Schmid CW (2001) Stress induction of Bm1 RNA in silkworm larvae: SINEs, an unusual class of stress genes. Cell Stress Chaperones 6:263-272
Kinzie RA, Chee GS (1979) Effect of Different Zooxanthellae on the Growth of Experimentally Re-Infected Hosts. Biological Bulletin 156:315-327
Kitano H, Oda K (2006) Self-extending symbiosis: a mechanism for increasing robustness through evolution. Biologial Theory 1:61-66

Kobayashi M, Yamamoto M (2006) Nrf2-Keap1 regulation of cellular defense mechanisms against electrophiles and reactive oxygen species. Adv Enzyme Regul 46:113-140
Koike K, Jimbo M, Sakai R, Kaeriyama M, Muramoto K, Ogata T, Maruyama T, Kamiya H (2004) Octocoral chemical signaling selects and controls dinoflagellate symbionts. Biological Bulletin 207:80-86
Kondrashov FA, Koonin EV, Morgunov IG, Finogenova TV, Kondrashova MN (2006) Evolution of glyoxylate cycle enzymes in Metazoa: evidence of multiple horizontal transfer events and pseudogene formation. Biol Direct 1:31
Kopecky EJ, Ostrander GK (1999) Isolation and primary culture of viable multicellular endothelial isolates from hard corals. In Vitro Cell Dev Biol Anim 35:616-624
Kornberg HL, Madsen NB (1958) The metabolism of C2 compounds in microorganisms. 3. Synthesis of malate from acetate via the glyoxylate cycle. Biochem J 68:549-557
Kovalenko A, Chable-Bessia C, Cantarella G, Israel A, Wallach D, Courtois G (2003) The tumour suppressor CYLD negatively regulates NF-kappaB signalling by deubiquitination. Nature 424:801-805
Kozmik Z, Ruzickova J, Jonasova K, Matsumoto Y, Vopalensky P, Kozmikova I, Strnad H, Kawamura S, Piatigorsky J, Paces V, Vlcek C (2008) Assembly of the cnidarian camera-type eye from vertebrate-like components. Proceedings of the National Academy of Sciences of the United States of America 105:8989-8993
Kultz D (2003) Evolution of the cellular stress proteome: from monophyletic origin to ubiquitous function. J Exp Biol 206:3119-3124
Kultz D (2005) Molecular and evolutionary basis of the cellular stress response. Annual Review of Physiology 67:225-257
Kultz D, Madhany S, Burg MB (1998) Hyperosmolality causes growth arrest of murine kidney cells - Induction of GADD45 and GADD153 by osmosensing via stress-activated protein kinase. Journal of Biological Chemistry 273:13645-13651
Kushmaro A, Loya Y, Fine M, Rosenberg E (1996) Bacterial infection and coral bleaching. Nature 380:396
LaJeunesse TC, Reyes-Bonilla H, Warner ME (2007) Spring "bleaching" among *Pocillopora* in the Sea of Cortez, Eastern Pacific. Coral Reefs 26:265-270
LaJeunesse TC, Trench RK (2000) Biogeography of two species of *Symbiodinium* (Freudenthal) inhabiting the intertidal sea anemone *Anthopleura elegantissima* (Brandt). Biological Bulletin 199:126-134
Lasker HR, Peters EC, Coffroth MA (1984) Bleaching of Reef Coelenterates in the San-Blas Islands, Panama. Coral Reefs 3:183-190
Lees-Miller JP, Helfman DM (1991) The molecular basis for tropomyosin isoform diversity. Bioessays 13:429-437

Lesser MP (1996) Elevated temperatures and ultraviolet radiation cause oxidative stress and inhibit photosynthesis in symbiotic dinoflagellates. Limnol Oceanogr 41:271-283
Lesser MP (1997) Oxidative stress causes coral bleaching during exposure to elevated temperatures. Coral Reefs 16::187–192
Lesser MP (2004) Experimental biology of coral reef ecosystems. Journal of Experimental Marine Biology and Ecology 300:217-252
Lesser MP (2006) Oxidative stress in marine environments: biochemistry and physiological ecology. Annu Rev Physiol 68:253-278
Lesser MP, Farrell JH (2004) Exposure to solar radiation increases damage to both host tissues and algal symbionts of corals during thermal stress. Coral Reefs 23:367-377
Lesser MP, Stochaj WR, Tapley DW, Shick JM (1990) Bleaching in Coral-Reef Anthozoans - Effects of Irradiance, Ultraviolet-Radiation, and Temperature on the Activities of Protective Enzymens against Active Oxygen. Coral Reefs 8:225-232
Levitan DR, Fukami H, Jara J, Kline D, McGovern TM, McGhee KE, Swanson CA, Knowlton N (2004) Mechanisms of reproductive isolation among sympatric broadcast-spawning corals of the Montastrea annularis species complex. Evolution 58:308-323
Li J, Lee B, Lee AS (2006) Endoplasmic reticulum stress-induced apoptosis: multiple pathways and activation of p53-up-regulated modulator of apoptosis (PUMA) and NOXA by p53. J Biol Chem 281:7260-7270
Li SW, Prockop DJ, Helminen H, Fassler R, Lapvetelainen T, Kiraly K, Peltarri A, Arokoski J, Lui H, Arita M, et al. (1995) Transgenic mice with targeted inactivation of the Col2 alpha 1 gene for collagen II develop a skeleton with membranous and periosteal bone but no endochondral bone. Genes Dev 9:2821-2830
Li T, Spearow J, Rubin CM, Schmid CW (1999) Physiological stresses increase mouse short interspersed element (SINE) RNA expression in vivo. Gene 239:367-372
Lindquist S (1986) The heat-shock response. Annual Review of Biochemistry 55:1151-1191
Lindvall JM, Blomberg KE, Smith CI (2003) In silico tools for signal transduction research. Brief Bioinform 4:315-324
Lirman D (1999) Reef fish communities associated with Acropora palmata: relationships to benthic attributes. Bulletin of Marine Science 65:235-252
Litjens SH, de Pereda JM, Sonnenberg A (2006) Current insights into the formation and breakdown of hemidesmosomes. Trends in Cell Biology 16:376-383
Little AF, van Oppen MJ, Willis BL (2004) Flexibility in algal endosymbioses shapes growth in reef corals. Science 304:1492-1494
Livak KJ, Schmittgen TD (2001) Analysis of relative gene expression data using real-time quantitative PCR and the 2(-Delta Delta C(T)) Method. Methods 25:402-408

Lohr J, Munn CB, Wilson WH (2007) Characterization of a latent virus-like infection of symbiotic zooxanthellae. Applied and Environmental Microbiology 73:2976-2981
Loram JE, Trapido-Rosenthal HG, Douglas AE (2007) Functional significance of genetically different symbiotic algae *Symbiodinium* in a coral reef symbiosis. Molecular Ecology 16:4849-4857
Loven DP (1988) A role for reduced oxygen species in heat induced cell killing and the induction of thermotolerance. Medical Hypotheses 26:39-50
Loya Y, Sakai K, Yamazato K, Nakano Y, Sambali H, van Woesik R (2001) Coral bleaching: the winners and the losers. Ecology Letters 4:122-131
Malhotra JD, Kaufman RJ (2007) The endoplasmic reticulum and the unfolded protein response. Semin Cell Dev Biol 18:716-731
Marhaver KL, Edwards RA, Rohwer F (2008) Viral communities associated with healthy and bleaching corals. Environmental Microbiology On-line first
Marshall PA, Baird AH (2000) Bleaching of corals on the Great Barrier Reef: differential susceptibilities among taxa. Coral Reefs 19:155-163
Martzen MR, McMullen BA, Smith NE, Fujikawa K, Peanasky RJ (1990) Primary structure of the major pepsin inhibitor from the intestinal parasitic nematode Ascaris suum. Biochemistry 29:7366-7372
Mayfield AB, Gates RD (2007) Osmoregulation in anthozoan-dinoflagellate symbiosis. Comparative Biochemistry and Physiology A: Molecular and Integrative Physiology 147:1-10
McClintock B (1950) The origin and behavior of mutable loci in maize. Proceedings of the National Academy of Sciences of the United States of America 36:344-355
McClintock B (1984) The significance of responses of the genome to challenge. Science 226:792-801
Medina M, Collins AG, Takaoka TL, Kuehl JV, Boore JL (2006) Naked corals: Skeleton loss in Scleractinia. Proceedings of the National Academy of Sciences of the United States of America 103:9096-9100
Meints RH, Pardy RL (1980) Quantitative demonstration of cell surface involvement in a plant-animal symbiosis: lectin inhibition of reassociation. . Journal of Cell Science 43
Mendes AF, Caramona MM, Carvalho AP, Lopes MC (2003) Differential roles of hydrogen peroxide and superoxide in mediating IL-1-induced NF-kappa B activation and iNOS expression in bovine articular chondrocytes. J Cell Biochem 88:783-793
Meyer E, Aglyamova GV, Wang S, Buchanan-Carter J, Abrego D, Colbourne JK, Willis BL, Matz MV (2009) Sequencing and de novo analysis of a coral larval transcriptome using 454 GS-Flx. BMC Genomics 10:219
Middlebrook R, Hoegh-Guldberg O, Leggat W (2008) The effect of thermal history on the susceptibility of reef-building corals to thermal stress. J Exp Biol 211:1050-1056

Mieog JC, Olsen JL, Berkelmans R, Bleuler-Martinez SA, Willis BL, van Oppen MJ (2009) The roles and interactions of symbiont, host and environment in defining coral fitness. PLoS One 4:e6364
Mieog JC, van Oppen MJH, Cantin NE, Stam WT, Olsen JL (2007) Real-time PCR reveals a high incidence of Symbiodinium clade D at low levels in four scleractinian corals across the Great Barrier Reef: implications for symbiont shuffling. Coral Reefs 26:449-457
Mizushima N, Sugita H, Yoshimori T, Ohsumi Y (1998) A new protein conjugation system in human. The counterpart of the yeast Apg12p conjugation system essential for autophagy. J Biol Chem 273:33889-33892
Morgan MB, Edge SE, Snell TW (2005) Profiling differential gene expression of corals along a transect of waters adjacent to the Bermuda municipal dump. Mar Pollut Bull 51:524-533
Muller J, Menzel D, Samaj J (2007) Cell-type specific disruption and recovery of the cytoskeleton in *Arabidopsis thaliana* epidermal root cells upon heat shock stress. Protoplasma 230:231-242
Muscatine L (1967) Glycerol Excretion by Symbiotic Algae from Corals and Tridacna and Its Control by Host. Science 156:516-519
Muscatine L (1990) The role of symbiotic algae in carbon and energy flux in reef corals. In: Dubinsky Z (ed) Ecosystems of the world 25: Coral Reefs. Elsevier, Amsterdam, p 75-87
Muscatine L, Pool RR (1979) Regulation of numbers of intracellular algae. Proc R Soc Lond B Biol Sci 204:131-139
Nakamura T, van Woesik R (2001) Water-flow rates and passive diffusion partially explain differential survival of corals during the 1998 bleaching event. Marine Ecology-Progress Series 212:301-304
Nakamura T, Yamasaki H, van Woesik R (2003) Water flow facilitates recovery from bleaching in the coral Stylophora pistillata. Marine Ecology-Progress Series 256:287-291
Nicotera P, Leist M, Ferrando-May E (1998) Intracellular ATP, a switch in the decision between apoptosis and necrosis. Toxicology Letters 102-103:139-142
Nii CM, Muscatine L (1997) Oxidative stress in the symbiotic sea anemone *Aiptasia pulchella* (Carlgren, 1943): Contribution of the animal to superoxide ion production at elevated temperature. Biol Bull 192:444-456
Nijman SM, Luna-Vargas MP, Velds A, Brummelkamp TR, Dirac AM, Sixma TK, Bernards R (2005) A genomic and functional inventory of deubiquitinating enzymes. Cell 123:773-786
Obata T, Brown GE, Yaffe MB (2000) MAP kinase pathways activated by stress: the p38 MAPK pathway. Crit Care Med 28:N67-77
Oda K, Kitano H (2006) A comprehensive map of the toll-like receptor signaling network. Mol Syst Biol 2:2006 0015
Orrenius S, Burkitt MJ, Kass GE, Dypbukt JM, Nicotera P (1992) Calcium ions and oxidative cell injury. Annals of Neurology 32 Suppl:S33-42

Orrenius S, Zhivotovsky B, Nicotera P (2003) Regulation of cell death: the calcium-apoptosis link. Nature Reviews Molecular Cell Biology 4:552-565
Pandolfi JM, Bradbury RH, Sala E, Hughes TP, Bjorndal KA, Cooke RG, McArdle D, McClenachan L, Newman MJ, Paredes G, Warner RR, Jackson JB (2003) Global trajectories of the long-term decline of coral reef ecosystems. Science 301:955-958
Pandolfi JM, Jackson JB (2006) Ecological persistence interrupted in Caribbean coral reefs. Ecol Lett 9:818-826
Papina M, Meziane T, van Woesik R (2003) Symbiotic zooxanthellae provide the host-coral Montipora digitata with polyunsaturated fatty acids. Comparative Biochemistry and Physiology B-Biochemistry & Molecular Biology 135:533-537
Park WR, Nakamura Y (2005) p53CSV, a novel p53-inducible gene involved in the p53-dependent cell-survival pathway. Cancer Res 65:1197-1206
Patten NL, Harrison PL, Mitchell JG (2008) Prevalence of virus-like particles within a staghorn scleractinian coral (*Acropora muricata*) from the Great Barrier Reef. Coral Reefs On-line first
Patton JS, Abraham S, Benson AA (1977) Lipogenesis in the intact coral Pocillopora capitata and its isolated zooxanthellae: evidence for a light-driven carbon cycle between symbiont and host Marine Biology 44:235-247
Pereira SG, Oakley F (2008) Nuclear factor-kappaB1: regulation and function. Int J Biochem Cell Biol 40:1425-1430
Perez S, Weis V (2006) Nitric oxide and cnidarian bleaching: an eviction notice mediates breakdown of a symbiosis. J Exp Biol 209:2804-2810
Perkins ND (2007) Integrating cell-signalling pathways with NF-kappaB and IKK function. Nat Rev Mol Cell Biol 8:49-62
Place SP, O'Donnell MJ, Hofmann GE (2008) Gene expression in the intertidal mussel *Mytilus californianus*: physiological response to environmental factors on a biogeographic scale. Marine Ecology-Progress Series 356:1-14
Pochon X, Montoya-Burgos JI, Stadelmann B, Pawlowski J (2006) Molecular phylogeny, evolutionary rates, and divergence timing of the symbiotic dinoflagellate genus Symbiodinium. Molecular Phylogenetics and Evolution 38:20-30
Popov VN, Moskalev EA, Shevchenko M, Eprintsev AT (2005) [Comparative analysis of the glyoxylate cycle clue enzyme isocitrate lyases from organisms of different systemic groups]. Zh Evol Biokhim Fiziol 41:507-513
Prives C, Hall PA (1999) The p53 pathway. J Pathol 187:112-126
Puntarulo S (2005) Iron, oxidative stress and human health. Mol Aspects Med 26:299-312
Putnam NH, Srivastava M, Hellsten U, Dirks B, Chapman J, Salamov A, Terry A, Shapiro H, Lindquist E, Kapitonov VV, Jurka J, Genikhovich G, Grigoriev IV, Lucas SM, Steele RE, Finnerty JR, Technau U, Martindale MQ, Rokhsar DS (2007) Sea anemone genome reveals ancestral eumetazoan gene repertoire and genomic organization. Science 317:86-94

Puverel S, Tambutte E, Pereira-Mouries L, Zoccola D, Allemand D, Tambutte S (2005) Soluble organic matrix of two Scleractinian corals: partial and comparative analysis. Comp Biochem Physiol B Biochem Mol Biol 141:480-487

Raja KB, Gerard B, McKie AT, Simpson RJ, Peters TJ, Grandchamp B, Beaumont C (1995) Duodenal expression of NF-E2 in mouse models of altered iron metabolism. Br J Haematol 91:483-489

Rajeevan MS, Vernon SD, Taysavang N, Unger ER (2001) Validation of array-based gene expression profiles by real-time (kinetic) RT-PCR. Journal of Molecular Diagnostics 3:26-31

Ratner VA, Zabanov SA, Kolesnikova OV, Vasilyeva LA (1992) Induction of the mobile genetic element Dm-412 transpositions in the Drosophila genome by heat shock treatment. Proceedings of the National Academy of Sciences of the United States of America 89:5650-5654

Rawlings ND, Tolle DP, Barrett AJ (2004) Evolutionary families of peptidase inhibitors. Biochem J 378:705-716

Reyes-Bermudez A, DeSalvo MK, Voolstra CR, Sunagawa S, Szmant AM, Iglesias-Prieto R, Medina M (2009) Gene expression microarray analysis encompassing metamorphosis and the onset of calcification in the scleractinian coral *Montastraea faveolata*. Marine Genomics 2:149-159

Reyes-Bermudez A, Miller DJ (2009) In vitro culture of cells derived from larvae of the staghorn coral Acropora millepora. Coral Reefs 28:859-864

Richier S, Rodriguez-Lanetty M, Schnitzler CE, Weis VM (2008) Response of the symbiotic cnidarian *Anthopleura elegantissima* transcriptome to temperature and UV increase. Comp Biochem Physiol D: Genomics Proteomics 3:283-289

Richier S, Sabourault C, Courtiade J, Zucchini N, Allemand D, Furla P (2006) Oxidative stress and apoptotic events during thermal stress in the symbiotic sea anemone, *Anemonia viridis*. Febs J 273:4186-4198

Richter C (1998) Nitric oxide and its congeners in mitochondria: implications for apoptosis. Environmental Health Perspectives 106 Suppl 5:1125-1130

Ridley AJ (2006) Rho GTPases and actin dynamics in membrane protrusions and vesicle trafficking. Trends Cell Biol 16:522-529

Riobo NA, Clementi E, Melani M, Boveris A, Cadenas E, Moncada S, Poderoso JJ (2001) Nitric oxide inhibits mitochondrial NADH:ubiquinone reductase activity through peroxynitrite formation. Biochemical Journal 359:139-145

Rodriguez-Lanetty M, Phillips WS, Dove S, Hoegh-Guldberg O, Weis VM (2008) Analytical approach for selecting normalizing genes from a cDNA microarray platform to be used in q-RT-PCR assays: a cnidarian case study. J Biochem Biophys Methods 70:985-991

Rodriguez-Lanetty M, Phillips WS, Weis VM (2006) Transcriptome analysis of a cnidarian-dinoflagellate mutualism reveals complex modulation of host gene expression. BMC Genomics 7:23

Rodriguez-Roman A, Hernandez-Pech X, Thome PE, Enriquez S, Iglesias-Prieto R (2006) Photosynthesis and light utilization in the Caribbean coral Montastraea

faveolata recovering from a bleaching event. Limnology and Oceanography 51:2702-2710
Rohwer F, Seguritan V, Azam F, Knowlton N (2002) Diversity and distribution of coral-associated bacteria. Mar Ecol Prog Ser 243:1-10
Ronai Z, Yang YM, Fuchs SY, Adler V, Sardana M, Herlyn M (1998) ATF2 confers radiation resistance to human melanoma cells. Oncogene 16:523-531
Rosenberg E, Koren O, Reshef L, Efrony R, Zilber-Rosenberg I (2007) The role of microorganisms in coral health, disease and evolution. Nat Rev Microbiol 5:355-362
Ross AC (1993) Cellular-Metabolism and Activation of Retinoids - Roles of Cellular Retinoid-Binding Proteins. Faseb Journal 7:317-327
Rowan R (2004) Coral bleaching: thermal adaptation in reef coral symbionts. Nature 430:742
Rowan R, Knowlton N (1995) Intraspecific diversity and ecological zonation in coral-algal symbiosis. Proc Natl Acad Sci U S A 92:2850-2853
Rowan R, Knowlton N, Baker AC, Jara J (1997) Landscape ecology of algal symbiont communities explains variation in episodes of coral bleaching. Nature 388:265-269
Rowan R, Powers DA (1991) Molecular genetic identification of symbiotic dinoflagellates (zooxanthellae). Marine Ecology Progress Series 71:65-73
Rutkowski DT, Kaufman RJ (2003) All roads lead to ATF4. Dev Cell 4:442-444
Saeed AI, Sharov V, White J, Li J, Liang W, Bhagabati N, Braisted J, Klapa M, Currier T, Thiagarajan M, Sturn A, Snuffin M, Rezantsev A, Popov D, Ryltsov A, Kostukovich E, Borisovsky I, Liu Z, Vinsavich A, Trush V, Quackenbush J (2003) TM4: a free, open-source system for microarray data management and analysis. Biotechniques 34:374-378
Salih A, Larkum A, Cox G, Kuhl M, Hoegh-Guldberg O (2000) Fluorescent pigments in corals are photoprotective. Nature 408:850-853
Salm RV, Coles SL, (eds.) (2001) Coral Bleaching and Marine Protected Areas. Proceedings of the Workshop on Mitigating Coral Bleaching Impact Through MPA Design, Bishop Museum, Honolulu, Hawaii, 29-31 May 2001. Asia Pacific Coastal Marine Program, The Nature Conservancy, Honolulu, Hawaii, USA:118 pp.
Sampayo EM, Ridgway T, Bongaerts P, Hoegh-Guldberg O (2008) Bleaching susceptibility and mortality of corals are determined by fine-scale differences in symbiont type. Proc Natl Acad Sci U S A 105:10444-10449
Santillo S, Orlando P, De Petrocellis L, Cristino L, Guglielmotti V, Musio C (2006) Evolving visual pigments: Hints from the opsin-based proteins in a phylogenetically old "eyeless" invertebrate. Biosystems 86:3-17
Schallreuter KU, Gibbons NC, Zothner C, Abou Elloof MM, Wood JM (2007) Hydrogen peroxide-mediated oxidative stress disrupts calcium binding on calmodulin: more evidence for oxidative stress in vitiligo. Biochemical and Biophysical Research Communications 360:70-75

Schwarz JA, Brokstein PB, Voolstra C, Terry AY, Miller DJ, Szmant AM, Coffroth MA, Medina M (2008) Coral Life History and Symbiosis: functional genomic resources for two reef building Caribbean corals, *Acropora palmata* and *Montastraea faveolata*. BMC Genomics 9:97

Scott IC, Blitz IL, Pappano WN, Imamura Y, Clark TG, Steiglitz BM, Thomas CL, Maas SA, Takahara K, Cho KW, Greenspan DS (1999) Mammalian BMP-1/Tolloid-related metalloproteinases, including novel family member mammalian Tolloid-like 2, have differential enzymatic activities and distributions of expression relevant to patterning and skeletogenesis. Dev Biol 213:283-300

Severance EG, Szmant AM, Karl SA (2004) Microsatellite loci isolated from the Caribbean coral, *Montastraea annularis*. Molecular Ecology Notes 4:74-76

Shapiro SD (1998) Matrix metalloproteinase degradation of extracellular matrix: biological consequences. Current Opinion in Cell Biology 10:602-608

Sharp VA, Brown BE, Miller D (1997) Heat Shock Protein (Hsp 70) Expression in the tropical reef coral *Goniopora Djiboutiensis*. Journal of Thermal Biology 22:11-19

Shashar N, Stambler N (1992) Endolithic algae within corals - life in an extreme environment. Journal of Experimental Marine Biology and Ecology 163:277-286

Shimizu S, Eguchi Y, Kamiike W, Matsuda H, Tsujimoto Y (1996) Bcl-2 expression prevents activation of the ICE protease cascade. Oncogene 12:2251-2257

Shin MH, Moon YJ, Seo J-E, Lee Y, Kim KH, Chung JH (2008) Reactive oxygen species produced by NADPH oxidase, xanthine oxidase, and mitochondrial electron transport system mediate heat shock-induced MMP-1 and MMP-9 expression. Free Radical Biology and Medicine 44:635-645

Shyy TT, Asch BB, Asch HL (1989) Concurrent collapse of keratin filaments, aggregation of organelles, and inhibition of protein synthesis during the heat shock response in mammary epithelial cells. J Cell Biol 108:997-1008

Simonson SJ, Wu ZH, Miyamoto S (2007) CYLD: a DUB with many talents. Developmental Cell 13:601-603

Singh SP, Coronella JA, Benes H, Cochrane BJ, Zimniak P (2001) Catalytic function of Drosophila melanogaster glutathione S-transferase DmGSTS1-1 (GST-2) in conjugation of lipid peroxidation end products. Europeaon Journal of Biochemistry 268:2912-2923

Smith DJ, Suggett DJ, Baker NR (2005) Is photoinhibition of zooxanthellae photosynthesis the primary cause of thermal bleaching in corals? Global Change Biology 11:1-11

Smith-Keune C, Dove S (2007) Gene Expression of a Green Fluorescent Protein Homolog as a Host-Specific Biomarker of Heat Stress Within a Reef-Building Coral. Marine Biotechnology (NY)

Solimena M, Dirkx R, Jr., Hermel JM, Pleasic-Williams S, Shapiro JA, Caron L, Rabin DU (1996) ICA 512, an autoantigen of type I diabetes, is an intrinsic membrane protein of neurosecretory granules. Embo J 15:2102-2114

Sonawane M, Carpio Y, Geisler R, Schwarz H, Maischein HM, Nuesslein-Volhard C (2005) Zebrafish penner/lethal giant larvae 2 functions in hemidesmosome formation, maintenance of cellular morphology and growth regulation in the developing basal epidermis. Development 132:3255-3265

Spurgeon JPG (1992) The Economic Valuation of Coral Reefs. Marine Pollution Bulletin 24:529-536

Stanley GD (1981) The early history of scleractinian corals and its geologic consequences. Geology 9:507-511

Stanley GD, van de Schootbrugge B (2009) The Evolution of the Coral-Algal Symbiosis. In: van Oppen MJH, Lough JM (eds) Coral Bleaching: Patterns, Processes, Causes and Consequences, Vol 205. Spinger-Verlag, Berlin Heidelberg

Stat M, Carter D, Hoegh-Guldberg O (2006) The evolutionary history of Symbiodinium and scleractinian hosts - Symbiosis, diversity, and the effect of climate change. Perspectives in Plant Ecology Evolution and Systematics 8:23-43

Stat M, Morris E, Gates RD (2008) Functional diversity in coral-dinoflagellate symbiosis. Proc Natl Acad Sci U S A 105:9256-9261

Steen RG, Muscatine L (1987) Low-Temperature Evokes Rapid Exocytosis of Symbiotic Algae by a Sea-Anemone. Biological Bulletin 172:246-263

Stillman JH, Tagmount A (2009) Seasonal and latitudinal acclimatization of cardiac transcriptome responses to thermal stress in porcelain crabs, Petrolisthes cinctipes. Mol Ecol 18:4206-4226

Strand D, Raska I, Mechler BM (1994) The Drosophila lethal(2)giant larvae tumor suppressor protein is a component of the cytoskeleton. Journal of Cell Biology 127:1345-1360

Strychar KB, Coates M, Sammarco PW, Piva TJ (2004) Bleaching as a pathogenic response in scleractinian corals, evidenced by high concentrations of apoptotic and necrotic zooxanthellae. Journal of Experimental Marine Biology and Ecology 304:99-121

Sullivan JC, Kalaitzidis D, Gilmore TD, Finnerty JR (2007) Rel homology domain-containing transcription factors in the cnidarian Nematostella vectensis. Dev Genes Evol 217:63-72

Sun X, Erb H, Murphy TH (2005) Coordinate regulation of glutathione metabolism in astrocytes by Nrf2. Biochem Biophys Res Commun 326:371-377

Sunagawa S, DeSalvo MK, Voolstra CR, Reyes-Bermudez A, Medina M (2009a) Identification and Gene Expression Analysis of a Taxonomically Restricted Cysteine-Rich Protein Family in Reef-Building Corals. PLoS ONE 4:e4865

Sunagawa S, Desantis TZ, Piceno YM, Brodie EL, Desalvo MK, Voolstra CR, Weil E, Andersen GL, Medina M (2009b) Bacterial diversity and White Plague Disease-associated community changes in the Caribbean coral *Montastraea faveolata*. Isme J 3:512-521

Sunagawa S, Wilson EC, Thaler M, Smith ML, Caruso C, Pringle JR, Weis VM, Medina M, Schwarz JA (2009c) Generation and analysis of transcriptomic

resources for a model system on the rise: the sea anemone Aiptasia pallida and its dinoflagellate endosymbiont. BMC Genomics 10:258
Suzuki R, Shimodaira H (2006) Pvclust: an R package for assessing the uncertainty in hierarchical clustering. Bioinformatics 22:1540-1542
Szmant AM, Gassman NJ (1990) The effects of prolonged "bleaching" on the tissue biomass and reproduction of the reef coral *Montastrea annularis*. Coral Reefs 8:217-224
Takeuchi M, Rothe M, Goeddel DV (1996) Anatomy of TRAF2. Distinct domains for nuclear factor-kappaB activation and association with tumor necrosis factor signaling proteins. J Biol Chem 271:19935-19942
Tambutte E, Allemand D, Mueller E, Jaubert J (1996) A compartmental approach to the mechanism of calcification in hermatypic corals. Journal of Experimental Biology 199:1029-1041
Tchernov D, Gorbunov MY, de Vargas C, Yadav SN, Milligan AJ, Haggblom M, Falkowski PG (2004) Membrane lipids of symbiotic algae are diagnostic of sensitivity to thermal bleaching in corals. Proceedings of the National Academy of Sciences of the United States of America 101:13531-13535
Teranishi KS, Stillman JH (2007) A cDNA microarray analysis of the response to heat stress in hepatopancreas tissue of the porcelain crab Petrolisthes cinctipes. Comparative Biochemistry and Physiology D-Genomics & Proteomics 2:53-62
The_UniProt_Consortium (2008) The Universal Protein Resource (UniProt). Nucleic Acids Res 36:D190-D195
Thornhill DJ, Lajeunesse TC, Kemp DW, Fitt WK, Schmidt GW (2006) Multi-year, seasonal genotypic surveys of coral-algal symbioses reveal prevalent stability or post-bleaching reversion. Mar Biol 148:711-722
Tibshirani R, Hastie T, Narasimhan B, Chu G (2002) Diagnosis of multiple cancer types by shunken centroids of gene expression. Proceedings of the National Academy of Sciences of the United States of America 99:6567-6572.
Titlyanov EA, Titlyanova TV, Leletkin VA, Tsukahara J, van Woesik R, Yamazato K (1996) Degradation of zooxanthellae and regulation of their density in hermatypic corals Marine Ecology Progress Series 139:167-178
Tiwari BS, Belenghi B, Levine A (2002) Oxidative stress increased respiration and generation of reactive oxygen species, resulting in ATP depletion, opening of mitochondrial permeability transition, and programmed cell death. Plant Physiology 128:1271-1281
Toller WW, Rowan R, Knowlton N (2001a) Repopulation of Zooxanthellae in the Caribbean Corals *Montastraea annularis* and *M. faveolata* following Experimental and Disease-Associated Bleaching. The Biological Bulletin 201:360–373
Toller WW, Rowan R, Knowlton N (2001b) Zooxanthellae of the Montastraea annularis species complex: patterns of distribution of four taxa of Symbiodinium on different reefs and across depths. Biol Bull 201:348-359

Townsend JP, Hartl DL (2002) Bayesian analysis of gene expression levels: statistical quantification of relative mRNA level across multiple strains or treatments. Genome Biol 3:RESEARCH0071

Trapido-Rosenthal H, Zielke S, Owen R, Buxton L, Boeing B, Bhagooli R, Archer J (2005) Increased zooxanthellae nitric oxide synthase activity is associated with coral bleaching. Biological Bulletin 208:3-6

Trench RK (1979) The cell biology of plant-animal symbiosis. Annual Review of Plant Physiology 30:485-453

Vagin VV, Sigova A, Li C, Seitz H, Gvozdev V, Zamore PD (2006) A distinct small RNA pathway silences selfish genetic elements in the germline. Science 313:320-324

van Oppen MJ, Gates RD (2006) Conservation genetics and the resilience of reef-building corals. Molecular Ecology 15:3863-3883

Vandesompele J, De Preter K, Pattyn F, Poppe B, Van Roy N, De Paepe A, Speleman F (2002) Accurate normalization of real-time quantitative RT-PCR data by geometric averaging of multiple internal control genes. Genome Biology 3:1-11

Vargas MR, Pehar M, Cassina P, Beckman JS, Barbeito L (2006) Increased glutathione biosynthesis by Nrf2 activation in astrocytes prevents p75NTR-dependent motor neuron apoptosis. J Neurochem 97:687-696

Voolstra CR, Schwarz JA, Schnetzer J, Sunagawa S, Desalvo MK, Szmant AM, Coffroth MA, Medina M (2009) The host transcriptome remains unaltered during the establishment of coral-algal symbioses. Mol Ecol 18:1823-1833

Wang T, Barbacioru C, Hyland F, Xiao W, Hunkapiller KL, Blake J, Chan F, Gonzalez C, Zhang L, Samaha RR (2006) Large scale real-time PCR validation on gene expression measurements from two commercial long-oligonucleotide microarrays. 7:59

Ward S, Harrison P, Hoegh-Guldberg O (2002) Coral bleaching reduces reproduction of scleractinian corals and increases susceptibility to future stress. Proceedings of the Ninth International Coral Reef Symposium 2

Warner ME, Fitt WK, Schmidt GW (1996) The effects of elevated temperature on the photosynthetic efficiency of zooxanthellae in hospite from four different species of reef coral: a novel approach. Plant, Cell and Environment 19:291-299

Warner ME, Fitt WK, Schmidt GW (1999) Damage to photosystem II in symbiotic dinoflagellates: A determinant of coral bleaching. Proc Natl Acad Sci U S A 96:8007-8012

Warner ME, LaJeunesse TC, Robison JD, Thur RM (2006) The ecological distribution and comparative photobiology of symbiotic dinoflagellates from reef corals in Belize: Potential implications for coral bleaching. Limnology and Oceanography 51:1887-1897

Wegley L, Yu YN, Breitbart M, Casas V, Kline DI, Rohwer F (2004) Coral-associated archaea. Mar Ecol Prog Ser 273:89-96

Weil E, Smith G, Gil-Agudelo DL (2006) Status and progress in coral reef disease research. Dis Aquat Organ 69:1-7
Weis VM (2008) Cellular mechanisms of Cnidarian bleaching: stress causes the collapse of symbiosis. J Exp Biol 211:3059-3066
Weis VM, Davy SK, Hoegh-Guldberg O, Rodriguez-Lanetty M, Pringle JR (2008) Cell biology in model systems as the key to understanding corals. Trends Ecol Evol 23:369-376
Wessler SR (1996) Turned on by stress. Plant retrotransposons. Current Biology 6:959-961
Westfall PH, Young SS (1993) On adjusting P-values for multiplicity. Biometrics 49:941-945
Wilson WH, Dale AL, Davy JE, Davy SK (2005) An enemy within? Observations of virus-like particles in reef corals. Coral Reefs 24:145-148
Wilson WH, Francis I, Ryan K, Davy SK (2001) Temperature induction of viruses in symbiotic dinoflagellates. Aquatic Microbial Ecology 25:99-102
Wood-Charlson EM, Hollingsworth LL, Krupp DA, Weis VM (2006) Lectin/glycan interactions play a role in recognition in a coral/dinoflagellate symbiosis. Cell Microbiol 8:1985-1993
Wu H, Churchill GA (2005) J/MAANOVA User Manual
Wu H, Kerr MK, Cui X, Churchill GA (2003) MAANOVA: A Software Package for the Analysis of Spotted cDNA Microarray Experiments. In: Giovanni Parmigiani ESG, Rafael A. Irizarry and Scott L. Zeger (ed) The Analysis of Gene Expression Data Methods and Software. Springer-Verlag, New York, p 313-341
Xue L, Igaki T, Kuranaga E, Kanda H, Miura M, Xu T (2007) Tumor suppressor CYLD regulates JNK-induced cell death in Drosophila. Developmental Cell 13:446-454
Yamada K, Strahler JR, Andrews PC, Matthews RG (2005) Regulation of human methylenetetrahydrofolate reductase by phosphorylation. Proc Natl Acad Sci U S A 102:10454-10459
Yoshida M, Xia Y (2003) Heat shock protein 90 as an endogenous protein enhancer of inducible nitric-oxide synthase. J Biol Chem 278:36953-36958
Yu L, Kelly U, Ebright JN, Malek G, Saloupis P, Rickman DW, McKay BS, Arshavsky VY, Bowes Rickman C (2007) Oxidative stress-induced expression and modulation of Phosphatase of Regenerating Liver-1 (PRL-1) in mammalian retina. Biochimica et Biophysica Acta 1773:1473-1482
Yuen T, Wurmbach E, Pfeffer RL, Ebersole BJ, Sealfon SC (2002) Accuracy and calibration of commercial oligonucleotide and custom cDNA microarrays. Nucleic Acids Research 30:e48
Zheng Q, Wang XJ (2008) GOEAST: a web-based software toolkit for Gene Ontology enrichment analysis. Nucleic Acids Res 36:W358-363